

HEAT TRANSFER COEFFICIENTS FOR
FINNED TUBED COIL IMMERSSED
IN AGITATED VESSEL

by

Fatma KIZILÇEÇ

B.S. in Ch.E., Istanbul Technical University, 1982

Bogazici University Library



14

39001100314155

Submitted to the Institute for Graduate Studies in
Science and Engineering in partial fulfillment of
the requirements for the degree of
Master of Science

in

Chemical Engineering

Boğaziçi University

1980

KEY WORDS

HEAT TRANSFER COEFFICIENTS
FINNED COIL HEAT TRANSFER PERFORMANCE
HEAT TRANSFER
(in mixing vessels)

ACKNOWLEDGEMENTS

I would like to express my thanks to my thesis supervisors, Doç.Dr.Fahir Borak and Doç.Dr.Z.İlsen Önsan, for their tolerance, understanding, and guidance throughout this work.

ABSTRACT

Heat transfer coefficients for agitated liquids in a flat bottomed vessel equipped with finned tube helical coil were determined over the 125-500r.p.m range of agitator speeds by using a flat paddle turbine impeller in order to examine the effect of finned coil geometry.

The heat transfer experiments have been carried out in two sets using three finned coils with different spacing. In the first set heat transfer coefficients were calculated for each coil using the Wilson graphical method by changing the hot stream flow rate and the temperature at constant agitator speed. In the second set only agitator speed was varied while hot and cold stream flow rates and temperatures were maintained constant. The overall conductance was determined from the heat transfer rate and log mean temperature difference by calculating the tube side heat transfer coefficient from the Sieder-Tate correlation, the outside heat transfer coefficient was found.

In addition to these experiments, the heat transfer coefficients in one type of finned coiled agitated vessel were also observed under unsteady state conditions.

The experimental data were compared with smooth tubes. As a result of this investigation the finned coils were found to be more heat transfer effective than the smooth coils. The values of the mixing coefficients were in agreement with previously published data. Unsteady state experiments showed that the correlation derived to find outside heat transfer coefficients under steady state conditions could be used also for unsteady state conditions.

Higher heat transfer coefficients were obtained at higher agitator speeds.

ÖZET

Kanatlı serpantin geometrisinin etkisini incelemek amacıyla, düz bıçaklı türbin karıştırıcılı, kanatlı serpantinle donatılmış düz tabanlı tankta, karıştırıcı hızı 125-500dev/dak sınırlarında değiştirilerek karıştırılan sıvılar için ısı transfer katsayıları ölçülmüştür.

Isı transfer deneyleri, üç farklı kanat aralığı olan serpantinler kullanılarak iki grupta gerçekleştirilmiştir. İlk deney grubunda sabit karıştırıcı hızı kullanılmış, sıcak sıvı debisi ve sıcaklığı değiştirilerek Wilson grafik yöntemi ile üç farklı serpantin sisteminde ısı transfer katsayıları hesaplanmıştır.

İkinci deney grubunda sıcak ve soğuk akış hızları ve sıcaklıkları sabit tutularak sadece karıştırıcı hızı değiştirilmiştir. Bileşik ısı transfer katsayısı, ısı transfer hızı ve logaritmik ortalamalı sıcaklık düşüsünden elde edilmiş ve boru tarafı ısı transfer katsayısı Sieder-Tate eşitliğinden hesaplanarak dış ısı transfer katsayısı bulunmuştur.

Bu deneylere ilave olarak, tek tip kanatlı serpantinli karıştırıcılı tankta kararsız hal şartlarında ısı transfer

katsayıları gözlenmiştir.

Deneysel sonuçlar kanatsız boru sonuçları ile karşılaştırılmıştır. Bu çalışmanın sonucu olarak, kanatlı serpantinlerin, kanatsız serpantinlerden ısı transfer bakımından daha etkili olduğu gözlenmiştir. Karıştırıcı tarafı ısı transfer katsayısı değerleri literatürdeki daha önce yayımlanmış değerlerle uyum sağlamıştır.

Kararsız hal deneyleri sonucunda kararlı hal şartlarında dış taraf ısı transfer katsayısını bulmak için kullanılan eşitliğin, kararsız hal durumundada kullanılabileceği gösterilmiştir.

Ayrıca yüksek karıştırıcı hızlarında, yüksek ısı transfer katsayıları elde edilmiştir.

TABLE OF CONTENTS

	<u>Page</u>
KEYWORDS	iii
ACKNOWLEDGEMENT	iv
ABSTRACT	v
ÖZET	vii
LIST OF TABLES	xii
LIST OF FIGURES	xiii
LIST OF SYMBOLS	xv
I. INTRODUCTION	1
I.A. Augmentative Heat Transfer	3
I.A.1 Extended Surface Heat Transfer	4
I.A.2 Classification of Extended Surface	6
I.B. Fin Efficiency	8
I.B.1 Fin Efficiency for Radial Fins with Rectangular Profile	9
I.B.2 Manufacture of Transverse Finned Tubes	14
I.C. Mechanical Aid in Heat Transfer	15

	I.C.1	The Factors that Effects Heat Transfer in Agitated Vessels.	20
II.		ANALYSIS OF FINNED COIL (IMMERSED IN AGITATED VESSEL) HEAT TRANSFER PERFORMANCE	24
	2.A	Determination of Heat Transfer Coefficients	25
	2.B	Correlation for Individual Heat Transfer Film Coefficients	29
	2.B.1	Inside Film Coefficients (in coil)	29
	2.B.2	Outside Film Coefficients (in vessel)	31
III.		EXPERIMENTAL SET UP	36
	3.A	Experimental Equipment	36
	3.A.1	The Vessel	37
	3.A.2	Coils	39
	3.A.3	The Stirrer	39
	3.A.4	Thermocouples	41
	3.A.5	Digital Thermometer	43
	3.A.6	Hot Water Reservoir	43
	3.A.7	Cold Water Reservoir	43
	3.A.8	Rotary Pumps	44
	3.B	Experimental Arrangement and Procedure	44
	3.B.1	Steady-State Experiments	45
	3.B.2	Unsteady-State Experiments	47
IV.		RESULTS	51
	4.A.	Evaluation of Experimental Data	52
	4.A.1	Steady-State Results	52

4.A.1.a	Calculation of Inside Film Coefficients	53
4.A.1.b	Calculation of Outside Film Coefficients	59
4.A.2	Unsteady-State Results	62
V.	DISCUSSION	68
5.A	Discussion of Results with Bare Coil Performance	68
5.B	Comparison with Literature	75
	REFERENCES	78
	APPENDICES	82
	APPENDIX I EXPERIMENTAL DATA	83
	APPENDIX II PHYSICAL PROPERTIES OF WATER	95

LIST OF TABLES

		<u>Page</u>
TABLE 1.1	Impeller types and usage range	17
TABLE 2.1	Correlations for convective heat transfer coefficients for the case of smooth tube helical coil	33
TABLE 2.2	Finned coil heat transfer correlations	35
TABLE 3.1	Range of parameters covered	36
TABLE 3.2	Finned tube dimensions	39
TABLE 3.3	Comparison of geometry of vessel and auxiliary equipment	42
TABLE 3.4	Range of parameters for set I (Agitator speed variable)	48
TABLE 3.5	Range of parameters for set II (Hot water conditions variable)	49
TABLE 4.1	Reynolds number exponent and geometry factors	61
TABLE 4.2	Unsteady-state results of high finned coil	64
TABLE 4.3	Unsteady-state results of high finned coil	65
TABLE 4.4	Unsteady-state results of high finned coil	66
TABLE 5.1	Comparison of bare and finned coil heat transfer performance	69
TABLE A.I.1	Efficiencies of radial fin of rectangular profile	84
TABLE A.I.2	Experimental data of set I (Agitator speed as variable)	86
TABLE A.I.3	Experimental data of set II (Hot stream conditions as variable)	88
TABLE A.I.4	Experimental results of set II from Wilson plot	90

LIST OF FIGURES

		<u>Page</u>
FIGURE 1.1	Types of coil systems in stirred vessels	2
FIGURE 1.2	Types of transverse fin tubing	7
FIGURE 1.3	Radial fin with rectangular profile	12
FIGURE 1.4	Types of impellers for Newtonian fluids	18
FIGURE 1.5	Types of agitators for viscous fluids	19
FIGURE 1.6	Comparison of flow patterns for radial (flat bladed) and axial (propeller) agitators	20
FIGURE 3.1	Vessel and auxiliary equipment	38
FIGURE 3.2	Finned tube dimensions	40
FIGURE 3.3	Experimental arrangement	46
FIGURE 4.1	Wilson plot for run 41-46	54
FIGURE 4.2	Wilson plot for run 47-52	54
FIGURE 4.3	Wilson plot for run 53-57	55
FIGURE 4.4	Wilson plot for run 58-63	55
FIGURE 4.5	Wilson plot for run 64-69	56
FIGURE 4.6	Wilson plot for run 70-75	56
FIGURE 4.7	Wilson plot for run 76-81	57
FIGURE 4.8	Wilson plot for run 82-86	57
FIGURE 4.9	Wilson plot for run 87-91	58
FIGURE 4.10	Wilson plot for run 92-96	58
FIGURE 4.11	Unsteady state results for three different agitator speed for high finned coil	63
FIGURE 5.1	Conductance ratio of finned coil to bare coil	71

FIGURE 5.2	Effect of fin space and agitator speed on H_o	72
FIGURE 5.3	Effect of fin space and agitator speed on H_o	72
FIGURE 5.4	Effect of fin space and agitator speed on H_o	73
FIGURE 5.5	Comparison of present study with previous correlations	76
FIGURE A.I.1	Temperature-time data (for high finned coil)	92
FIGURE A.I.2	Temperature-time data (for high finned coil)	93
FIGURE A.I.3	Temperature-time data (for high finned coil)	94

LIST OF SYMBOLS

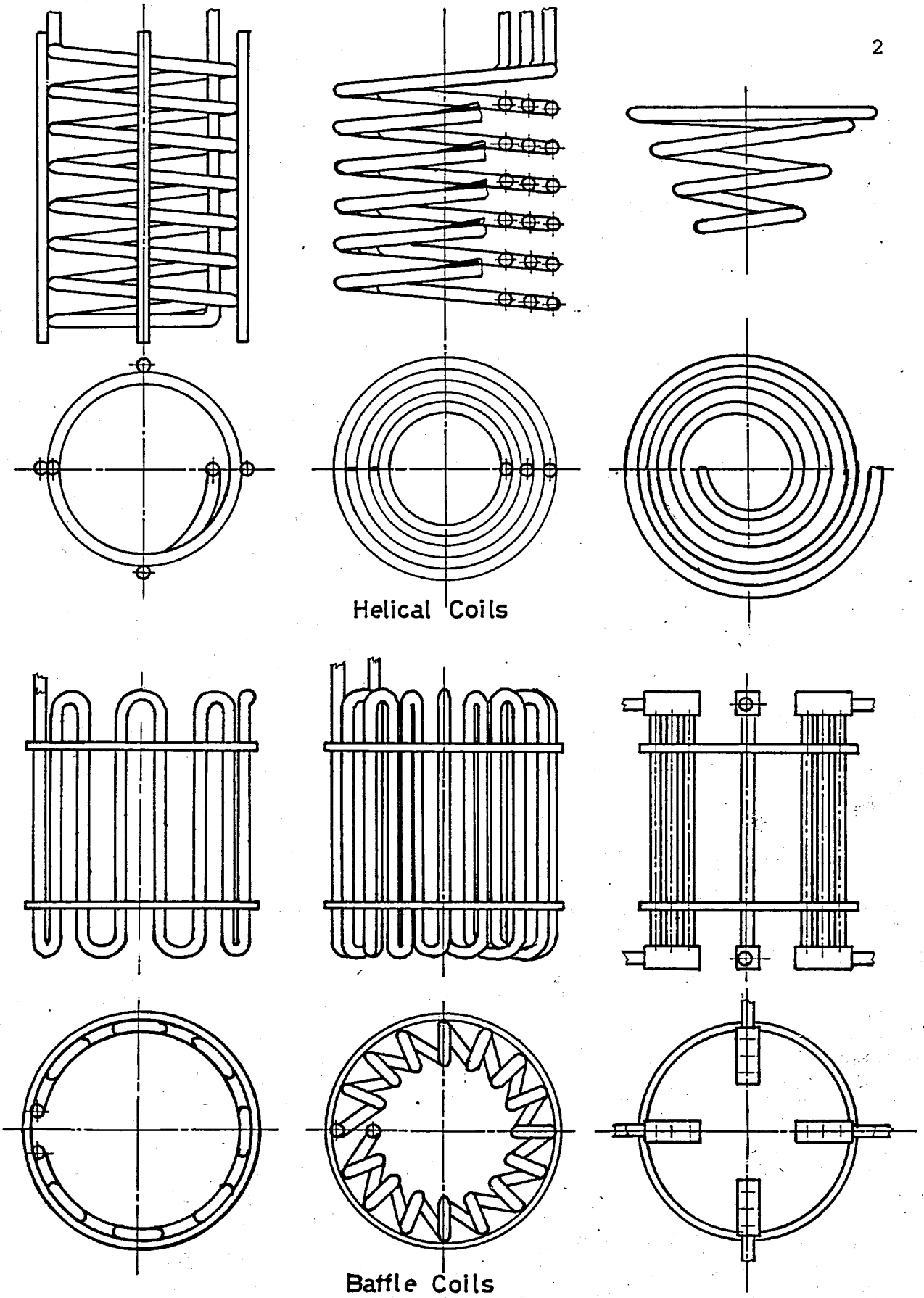
- $A_o, A_{eff}, A_f, A_i, A_u, A_T, A_p$: Primary, effective, fin, inside average, total, profile heat transfer areas respectively (m^2)
- C_1, C_2 : First and second order Bessel functions
- C_h : Specific heat of hot water ($J/kg^\circ C$)
- C_w : Specific heat of cold water ($J/kg^\circ C$)
- D_A : Agitator diameter (m)
- D_H : Diameter of coil tubing (m)
- D_C : Diameter of coil (m)
- D_F : Diameter of fin (m)
- D_T : Diameter of tank (m)
- ff_i, ff_{ci} : Fouling factors inside vessel and inside coil respectively ($m^2 \text{ }^\circ C/W$)
- H_i : Film heat transfer coefficient inside the coil ($W/m^2 \text{ }^\circ C$)
- H_o : Film heat transfer coefficient inside the vessel ($W/m^2 \text{ }^\circ C$)
- H_s : Fin space (m)

H_F	: Fin thickness (m)
H_L	: Liquid height inside the vessel (m)
H_A	: Agitator height from the bottom of vessel (m)
H_C	: Coil height from the bottom of vessel (m)
H_H	: Fin height (m)
I_0, I_1	: Zero and first order Bessel functions
k	: Thermal conductivity of water ($W/m^{\circ}C$)
k_w	: Thermal conductivity of coil wall ($W/m^{\circ}C$)
K_0, K_1	: Zero and first order Bessel function
L_C	: Length of coil (m)
M	: Cold water flow rate (m^3/sec)
N	: Agitator speed (rpm)
N_{Nu}	: Nusselt number, hD/k
N_{Re}	: Reynold number, $D_A^2 N\rho/\mu$
N_{Pr}	: Prandtl number, $C_p \mu/k$
S_C	: Space between coils (m)
Q, q	: Heat transfer rate (Cal/hr)
T_1, TH_1	: Inlet temperature of hot stream ($^{\circ}C$)
T_2, TH_2	: Exit temperature of hot stream ($^{\circ}C$)
t_o, TCO	: Inlet temperature of cold stream ($^{\circ}C$)

$t_{1,TC1}$: Exit temperature of cold stream ($^{\circ}\text{C}$)
T_o	: Temperature at the base of fin ($^{\circ}\text{C}$)
t_w	: Coil wall temperature ($^{\circ}\text{C}$)
U	: Overall heat transfer coefficient ($\text{W}/\text{m}^2\text{ }^{\circ}\text{C}$)
V_H	: Velocity of hot stream (m/sec)
W	: Hot water flow rate (m^3/sec)
W_{ib}	: Impeller blade width (m)
x	: Thickness of coil tube wall (m)
ϕ	: Dimensionless term for fin efficiency $(r_F - r_H)^{3/2} \left(\frac{2H}{kA_p} \right)^{1/2}$
η	: Fin efficiency
Ω	: Dimensionless term for fin efficiency $\frac{r_H}{r_F}$
μ	: Viscosity (kg/m sec)
ρ	: Density (kg/m^3)
θ	: Time (sec)
δ_o	: Fin thickness (m)
ΔT_{lm}	: Logarithmic mean temperature difference ($^{\circ}\text{C}$)

I. INTRODUCTION

A stirred vessel fitted with a heating coil or a heating jacket is a common piece of chemical process equipment, used for blending of miscible liquids, stage-wise solvent extraction in liquid-liquid and liquid-solid systems and carrying out liquid phase chemical reactions in either batch-wise or continuous operation. In these systems heat transfer from a coil or jacket to vessel contents (a heating operation) or heat transfer from vessel contents to a jacket or a coil (a cooling operation) is aimed. Although jacketed vessels have much less area than coiled vessels (so much less heat transfer), in the case of heat transfer to high consistency materials, they are preferred to coiled vessels which have open impellers such as the marine propeller, the various turbine designs and paddles that require higher power input to attain reasonable heat transfer rates. Coiled vessels have lower manufacturing cost and, because of the increased turbulence, it is to be expected that the tube side coefficients for a coiled tube will be greater for a given flow rate than that for a jacket or for a straight tube. Some examples of coils immersed in vessel are shown in Figure (1.1).



Figure(1.1). Types of coil systems in stirred vessel.

The performance of coiled tubes as in the case of heat exchangers can be substantially improved by a number of augmentative techniques. In addition to mechanical aid, heat transfer area can be increased.

The aim of this investigation is to determine the heat transfer coefficients in the coil and outside the coil to which fins have been attached. Water has been used as the fluid flowing in the coil and around the coil inside the vessel.

The theory of extended surfaces is given in this chapter. In Chapter 2, calculation of heat transfer coefficients and a literature survey are presented. The experimental apparatus used in this investigation and the experimental procedure are summarized in Chapter 3. The results of the experimental work and discussion and comparison of these results with values found in literature are given in Chapters 4 and 5 respectively.

I.A AUGMENTATIVE HEAT TRANSFER

There are various techniques of augmenting heat transfer resulting in an increase in the convective heat transfer coefficient. Enhancement techniques can be classified as passive methods, which require no direct application of external power, and as active schemes which require external power.

The passive techniques can be classified as follows:[1]

Treated surfaces	Swirl flow devices
Rough surfaces	Surface tension devices
Displaced enhancement devices	Fluid additives.

The active techniques include:

Mechanical aids	Electrostatic fields
Surface vibration	Injection
Fluid vibration	Suction

Two or more of these techniques may be utilized simultaneously (compound augmentation). Compound techniques are a slowly emerging area of enhancement which hold promise for practical applications since the heat transfer coefficients can usually be increased above each of the several techniques acting alone.

In this investigation, compound augmentation with an extended surface tube and mechanical aid, i.e. an agitator, have been used to increase the heat transfer coefficient.

I.A.1. Extended Surface Heat Transfer

Roughness on the coil surface produced by finning, threading or knurling will minimize the amount of coil by increasing the heat transfer rate per unit length of coil

Finned tubes also have an additional advantage in heating duties that their ratio of external to internal surface is large giving rise to lower tube wall temperatures than on plain tubes, which reduces the risk of polymerization, cracking, cooking and other ill effects of local heat transfer in reactors.

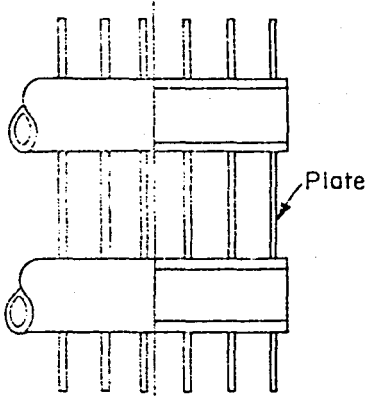
Extended surface heat transfer is the study of high-performance heat transfer components with respect to smaller weights, volumes, costs, accommodating shapes. Typical components are found in air-land-space vehicles and their power sources; chemical, refrigeration and cryogenic processes; electric and electronic circuitry; conventional furnaces and gas turbines; process heat dissipators and waste-heat boilers; nuclear-fuel modules, direct energy conversion.

In the design and construction of various types of heat transfer equipment, simple shapes such as cylinders, bars and plates are used to implement the flow of heat between a source and a sink. They provide heat absorbing or heat-rejecting surfaces and each is known as a prime surface. When a prime surface is extended by appendages intimately connected with it, such as metal tapes and spines on the tubes, the additional surface is known as an extended surface [2].

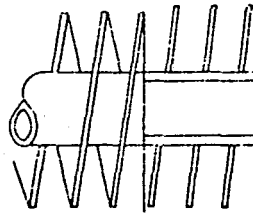
I.A.2. Classification of Extended Surfaces

There are mainly three kinds of extended surfaces [3]. Longitudinal fins consist of long metal strips or channels attached to the outside of the pipes or tubes. The strips are attached either by grooving and peening the tube or by welding continuously along the base. When channels are attached, they are integrally welded to the tube. Longitudinal fins are most commonly employed in problems involving gases and viscous liquids or when one of a pair of heat transfer streams causes streamline flow. The Longitudinal fins are the simplest fin from the standpoint of manufacture as well as mathematics.

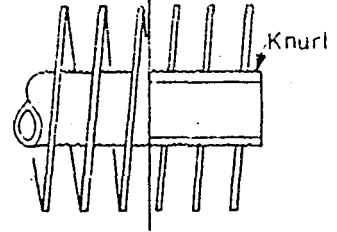
Transverse fins are made in a variety of types and are employed primarily for the cooling and heating of gases in crossflow. Transverse fins can be classified as radial fins, helical fins, disc type fins, and discontinuous fins. These type of fins are placed around the tube or pipe surface diameter with certain spacin. Transverse fin exchangers in crossflow are used only when the film coefficients of the fluids passing over them are low. This applies particularly to gases and air at low and moderate pressures. The most interesting applications of transverse fins are found in the larger gas cooling and heating services such as on furnaces, tempering coils for air conditioning, air-cooled steem condensers for turbine and, engine work. Types of transverse fin tubing, are illustrated in Figure (1.2).



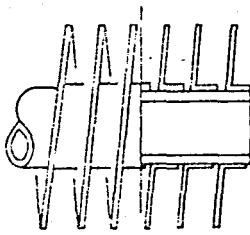
(a) Round tube and plate



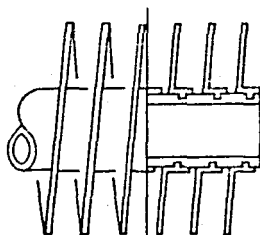
(b) Tension-wound



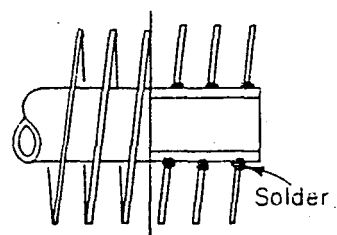
(c) Tension-wound on knurled-tube surface



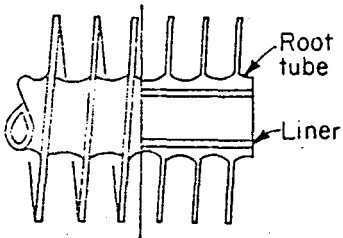
(d) L-footed, tension-wound



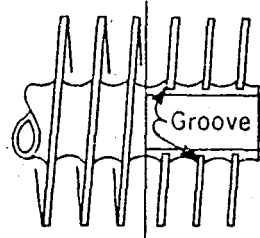
(e) L-footed, embedded, tension-wound



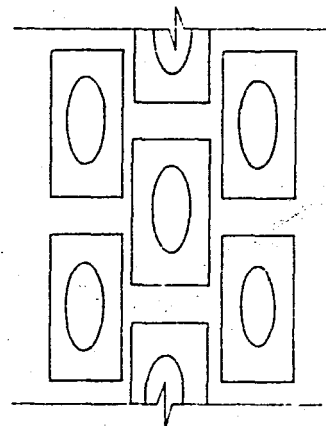
(f) Tension-wound and bonded



(g) Integral tin extruded from tube



(h) Grooved tube, tension-wound fin, peened



(i) Elliptical tube with rectangular fins

Figure (1.2) Types of transverse fin tubing

Spine or peg type fins employ cones, pyramids or cylinders which extend from the pipe surface so that they are usable for either longitudinal flow or crossflow. When two flowing fluids are separated by a metal wall and the surface extended into both fluids by means of spines or pegs whose bases are superimposed, this surface is called as double extended surface. Per unit wall area it should be possible to add as much surface as desired as long as there are no restrictions along the axes of the spines. Such an arrangement will be called for only when the coefficients from both fluids to their respective fins are small.

I.B. FIN EFFICIENCY

The problem of how to increase the heat transfer between a structure and its surroundings confronts the engineer and scientist in almost all most of technological development. When fins are attached to prime surfaces the heat transfer area increases by an amount equal to the surface area of the fins. However these fins also increase the resistance to heat flow. Thus the effective increase in heat transfer area is less than the actual increase in area. The ratio of the apparent area to actual area is a measure of the fin efficiency [2]. In other words, the fin efficiency is defined as the ratio of the actual heat dissipation of a fin to its ideal heat dissipation if the entire fin surface were at the same temperature as its base. The overall heat transfer coefficient U based on total

area (i.e. bare tube area + surface area of fins) is less than of the bare tube at the same temperature. If the increase in surface area is proportionally more than the decrease in heat transfer coefficient, the total heat transfer rate will increase compared to a bare tube. Thus it is very important to investigate the effect of fin spacing on the efficiency of extended surface.

I.B.1 Fin Efficiency for Radial Fins with Rectangular Profile

Each type of finned tube has its own characteristics and effectiveness for the transfer of heat between the fin and the fluid inside the tube. In the calculation of fin effectiveness for the different fin geometries, it is important to make an analysis of the constraints or assumptions which are employed to define and limit the problem and often to simplify its solution [2]. These limiting assumptions which are generally used in solutions are explained as follows.

1. The heat flow in the fin and its temperatures remain constant with time.
2. The fin material is homogeneous its thermal conductivity is the same in all directions, and remains constant.
3. The heat transfer coefficient to the fin is constant and uniform over the entire surface of the fin.
4. The temperature of the medium surrounding the fin is uniform.
5. The fin thickness is so small compared with its height that temperature gradients across the fin thickness may be neglected.

6. The temperature at the base of the fin is uniform.
7. There is no contact resistance where the base of the fin points the prime surface.
8. There are no heat sources within the fin itself.
9. The heat transferred through the outer most edge of the fin is negligible compared with that leaving the fin through its lateral surface.
10. Heat transfer to or from the fin is proportional to temperature excess between the fin and the surrounding medium.

For the radial fin shown in Figure(1.3) profile is confined by two symmetrical curves $y = \frac{\delta_0}{2}$, $y = -\frac{\delta_0}{2}$. From the difference in heat conducted into differential element at (r) and that leaving the element at $(r + dr)$, the heat balance equation can be obtained.

$$q = -kA \cdot \frac{dT}{dr} \quad (1.1)$$

$$\frac{dq}{dr} = -k \frac{d}{dr} \cdot \left(A \frac{dT}{dr} \right) \quad A = 2\pi r \delta_0 \quad (1.2)$$

$$dq = k \frac{d}{dr} \left(2\pi r \cdot 2 \left(\frac{\delta_0}{2} \right) \cdot \frac{dT}{dr} \right) dr$$

This is the equation for a steady state system and can be equated to the heat leaving the element (dr) by convection. Then if h is the convection coefficient,

$$dq = 2H (2\pi r dr)T \quad (1.3)$$

And the heat balance

$$4\pi H T r dr = 2\pi k \frac{d}{dr} (r \delta_0 \frac{dT}{dr}) dr \quad (1.4)$$

will simplify to

$$r \frac{d^2 T}{dr^2} + \frac{dT}{dr} - \frac{2H}{k\delta_0} r T = 0 \quad (1.5)$$

Multiplying both sides of the above equation by r and equating $(\frac{2H}{k\delta_0})^{1/2} = m$, one would obtain

$$r^2 \frac{d^2 T}{dr^2} + \frac{dT}{dr} - m^2 r^2 T = 0 \quad (1.6)$$

The resulting equation is the modified Bessel's equation.

General solution of this equation is [2],

$$T = C_1 I_0 (mr) + C_2 K_0 (mr) \quad (1.7)$$

where I_0 and K_0 are the zero order Bessel functions. For the solution which assumes no heat flow by convection through the edge of fin, the two boundary conditions applied are

$$\begin{aligned} \text{at } r = r_H \quad T &= T_0 \\ r = r_F \quad \frac{dT}{dr} \Big|_{r=r_F} &= 0 \end{aligned}$$

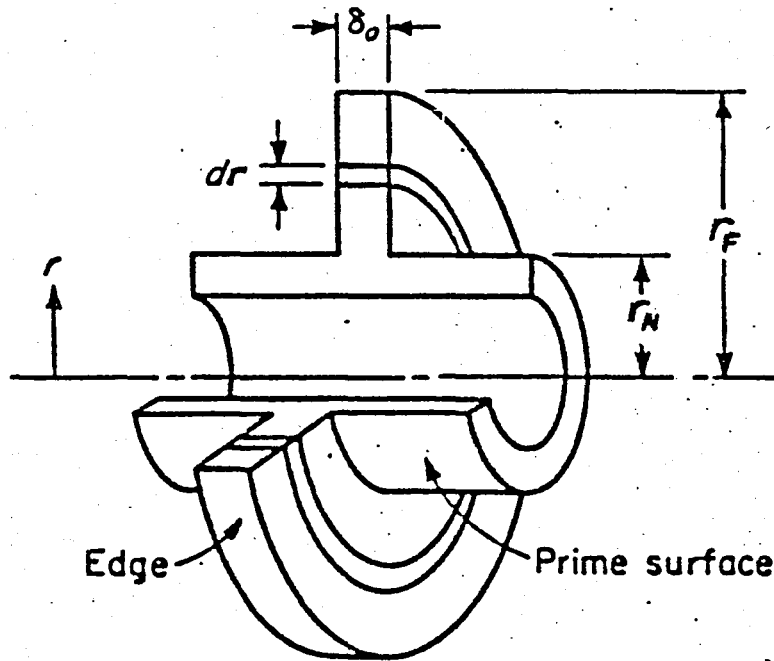


Figure (1.3) Radial fin with rectangular profile.

In order to determine the constants C_1 and C_2 these boundary conditions are inserted in equation (1.7).

$$T_0 = C_1 I_0(mr_H) + C_2 K_0(mr_H) \quad (1.8)$$

$$0 = C_1 I_1(mr_F) - C_2 K_1(mr_F) \quad (1.9)$$

to yield

$$T = \frac{T_0 \left[K_1(mr_F) I_0(mr) + I_1(mr_F) K_0(mr) \right]}{I_0(mr_H) K_1(mr_F) + I_1(mr_F) K_0(mr_H)} \quad (1.10)$$

Heat flow through the base of the fin is determined from the general relationship

$$q_0 = 2\pi k r_H \delta_0 \left. \frac{dT}{dr} \right|_{r=r_H} \quad (1.11)$$

By differentiating equation (1.10) at $r = r_H$ and substituting into Equation (1.11), Equation (1.12) is obtained.

$$q_o = 2\pi r_H \delta_o km T_o \left| \frac{I_1(mr_H) K_1(mr_H) - K_1(mr_F) I_1(mr_H)}{I_0(mr_H) K_1(mr_F) + I_1(mr_F) K_0(mr_H)} \right| \quad (1.12)$$

The "ideal" heat flow is given by the expression

$$q_{id} = 2\pi(r_F^2 - r_H^2) HT_o \quad (1.13)$$

Using the fin efficiency definition (the ratio of actual heat dissipation to ideal heat dissipation) the following expression is obtained for

$$\eta = \frac{2r_o}{m(r_F^2 - r_H^2)} \left| \frac{I_1(mr_F) K_1(mr_H) - K_1(mr_F) I_1(mr_H)}{I_0(mr_H) K_1(mr_F) + I_1(mr_F) K_0(mr_H)} \right| \quad (1.14)$$

By defining dimensionless terms,

$$\Omega = \frac{r_H}{r_F}$$

and

$$\phi = (r_F - r_H)^{3/2} \left(\frac{2H}{kA_p} \right)^{1/2}$$

where

$$A_p = \delta_o (r_F - r_H)$$

Values of the fin efficiency can be obtained as a function of the parameter ϕ and the radius ratio Ω . These values exist in tabular form Table(A.I.1) or in graphical representation [2].

1.B.2 Manufacture of Transverse Finned Tubes

In one method of manufacturing finned tubes, a metal ribbon similar in composition to the tube is helically wound and continuously arc-welded to the tube. The higher and thicker the fins, the fewer the maximum number of fins per unit length of tube which can be arc-welded since the fin spacing must also accommodate the welding electrode. High temperature high fin tubes on closer spacing are made by electrically resistance welding the fins tube. High-fin tubes can also be extruded directly from the tube wall metal as in the case of the integral low fin tubing. Whether fins are attached by arc-welding or resistance welding, the fin-to-tube attachment for all practical design considerations introduces a negligible bond or contact resistance [2].

In air-fin cooler design generally disk type fins are welded to the tube or shrunk to it. In order to shrink a fin onto a tube a disc, with inside diameter slightly less than the outside diameter of the tube, is heated until its inside diameter exceeds the outside diameter of the tube. It is slipped onto the tube, and upon cooling the disc shrinks to the tube and forms a band with it.

Also in some types, a metal ribbon is wound in tension around a tube. These types are not metallurgically bonded and rely entirely upon the tension in the ribbon to provide contact.

In this study, first a copper sheet of certain thickness was used to prepare discs with predetermined inside and outside diameters. Then for the attachment of the copper tube and the discs (of the same material as tube), tin-lead soldering was used. In order to avoid the bond resistance, the space between the outer surface of tube and inner edge of the discs was kept as small as possible.

1.C. MECHANICAL AID IN HEAT TRANSFER

It was noted that mechanically aided heat transfer is included in the active techniques of augmentative heat transfer. Agitators as a mixing equipment are the prime contributor to heat transfer. The classification of agitators generally depends on the liquid being mixed. Open impellers such as marine propellers, turbines, paddles are used for heat transfer to fluids with viscosities not greater than ten poises because of higher power requirement. With close clearance impellers such as horseshoe, scraper agitators, helical ribbon agitators, helicone mixers, and porcupine processors, clearance between blade and the vessel wall is effectively zero that is, the wall is essentially scraped clean with each passage of the scraper. Several means are used to force the scraper blades toward the vessel wall; springs, flexible blades, hydrodynamic action (blades or hinges) or a combination of the last two means. Close clearance agitators are mainly used for high viscosity pseudo plastic materials which have a "flow behaviour

index", m , of a few lengths, and for materials which tend to foul or deposit on the heat transfer surface as a result of crystallization of chemical reaction such as polymerization or thermal degradation [4].

Open and Close clearance agitators are listed in Table (1.1) with the viscosity range of use . In Figure (1.4) and Figure (1.5) types of agitators for newtonian and viscous fluids are illustrated. Agitators can also be classified according to the main flow direction. Agitators such as propellers, pitched blade turbines produce axial flow patterns parallel to the agitator. Flat bladed and curved bladed impellers produce radial flow patterns across the tube bank. Figure (1.6) illustrates radial and axial flow patterns produced by turbine and marine propellers.

Liquid motion in agitated vessels are described by the ratio of inertial to viscous forces per unit volume of liquid; namely by the modified Reynolds number of the impellers.

Representative velocity (v) of liquid in an agitated vessel will be proportional to the tip velocity of impeller

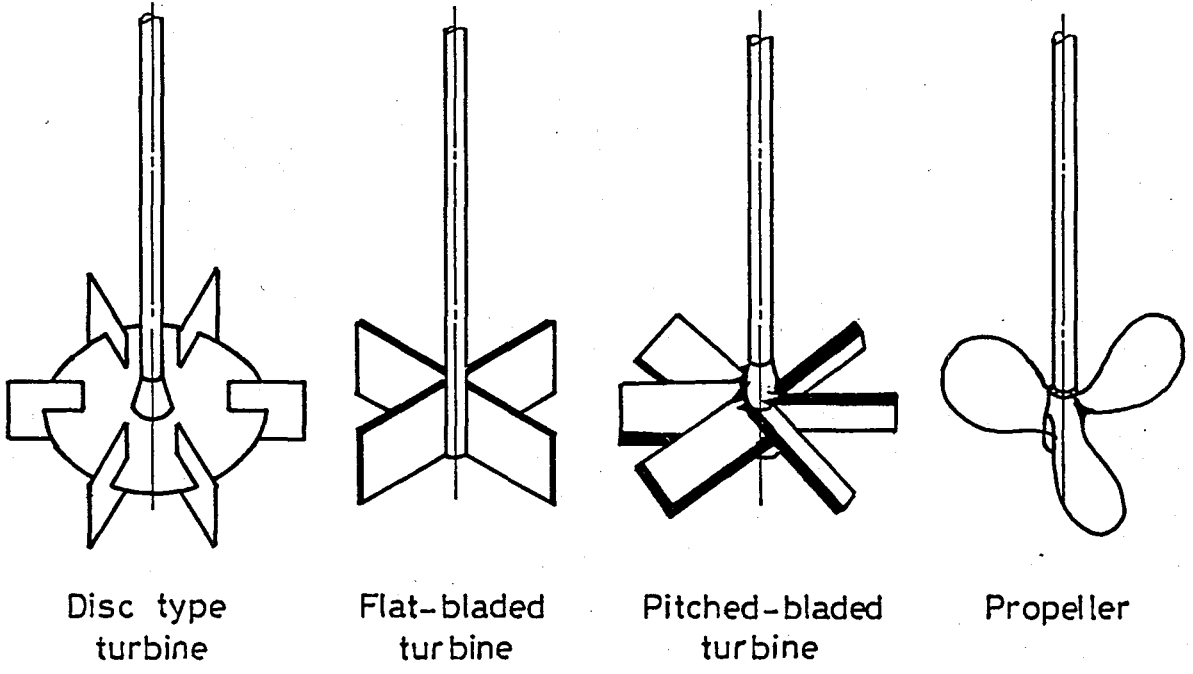
$$v \sim ND_A \quad (1.15)$$

Therefore Reynold Number is defined by [5]

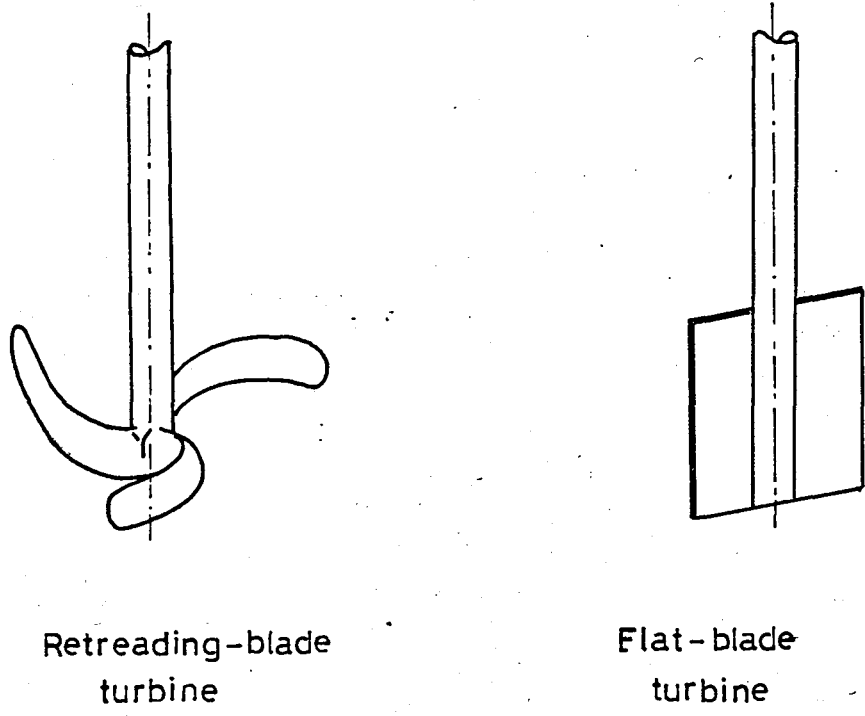
$$\frac{\text{Inertial Force}}{\text{Viscous Force}} = \frac{\rho N^2 D_A}{\mu \frac{N}{D_A}} = \frac{ND_A^2 \rho}{\mu} \quad (1.16)$$

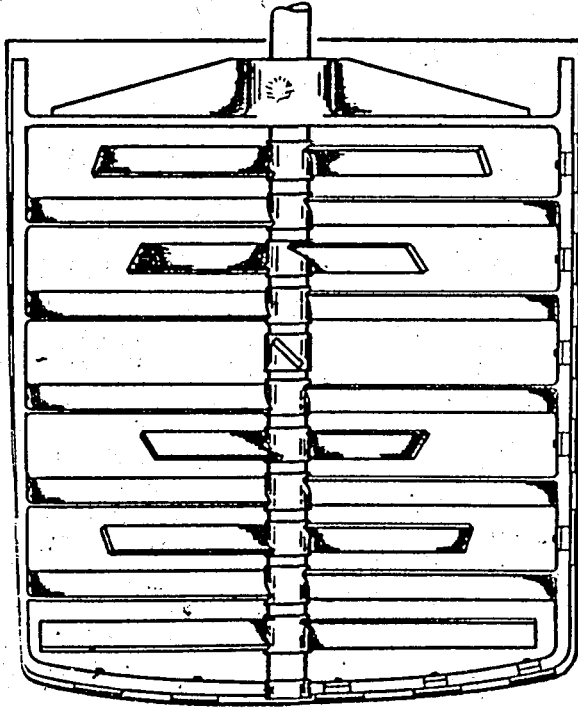
Table (1.1) Impeller types and usage range

<u>Impellers</u>	<u>Comment</u>	<u>Viscosity range (cps)</u>
Paddles	unbaffled paddles produce vortexing with low viscosity liquids.	$\sim 10^2 - 5 \cdot 10^4$
Propellers	generally used with low-moderate viscosity liquids	up to 10^4
Turbines	these agitators are generally be mounted one impeller diameter from the bottom	up to $6 \cdot 10^4$
Simple Anchor	with no baffle or cross blades, with vertical baffle or tiers of horizontal pitched blades	up to 10^4 $10^4 - 10^5$
Helical Ribbon	useful over widest range	$10^5 - 10^7$
Double motion scraper	demanding blending service such as grease manufacture	$> 10^5$
Dual shaft (helicone mixer)	various design with intermeshing blades Includes sigma blades for demanding service such as polymer reactions.	$> 10^5$

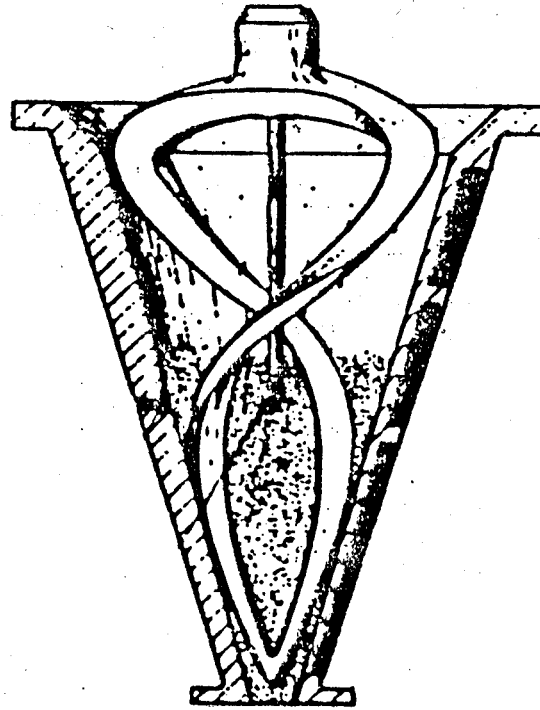


Figure(1.4). Types of impeller for Newtonian fluids.

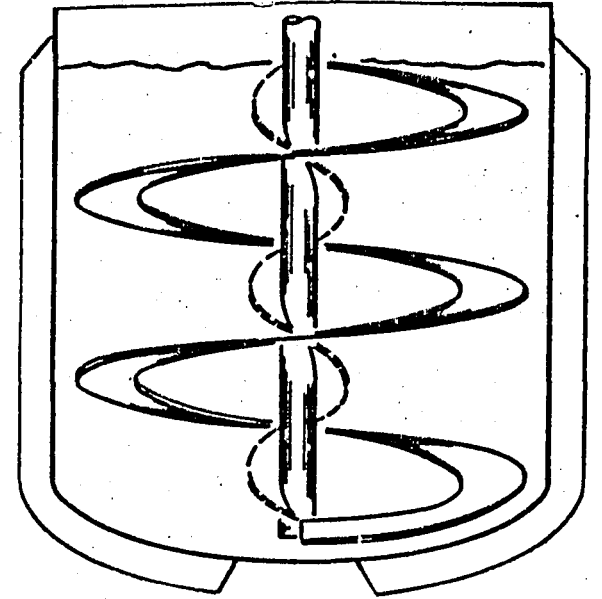




Double-motion scraper agitator.



Helicone mixer.



Helical ribbon agitator with single helix.

Figure (1.5). Types of agitator for viscous liquids.

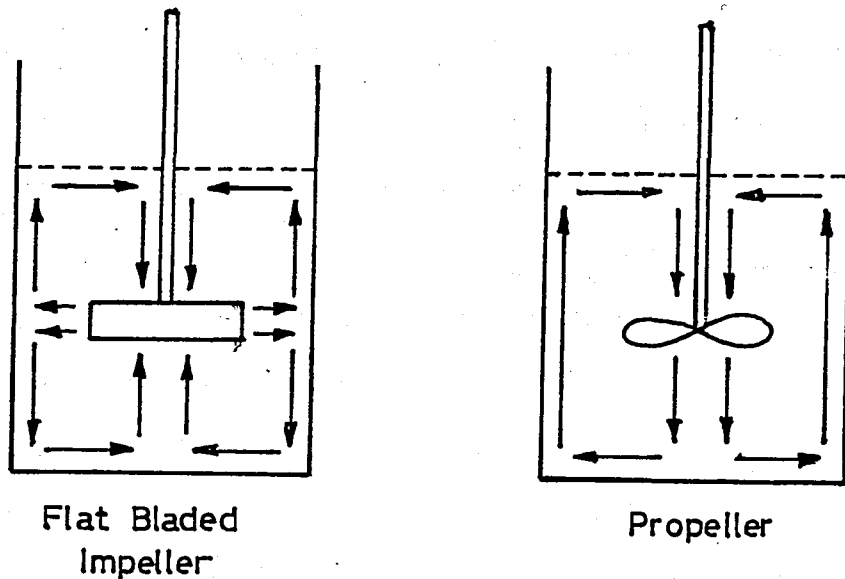


Figure (1.6). Comparison of flow patterns for radial (flatbladed) and axial (propeller) agitators.

In other words Reynolds Number is the ratio of the applied to the applied to the opposing viscous forces in a system.

I.C.1 The Factors That Effects Heat Transfer in Agitated Vessel.

The heat transfer in an agitated vessel depends on a number of physical geometrical and operational factors.

a) Effect of impeller clearance from bottom and from wall: In the turbulent region, for the radial flow 90° turbine the heat transfer coefficients decrease as the impeller distance from the vessel bottom decreases while for the propeller and 45° turbine heat transfer coefficients increase as impeller clearance decreases [6]. This indicates that the axial flow impellers generate greater fluid velocity at heat transfer

surface when they are moved closer to bottom. In the investigation of Rushton [7], the highest heat transfer coefficients were obtained when the turbine was placed at one-half of the liquid height. When the impeller was placed higher, vortexing increased and the coefficients decreased.

In the study of the influence of the clearance between a horseshoe agitator and the vessel wall, Uhl and Voznick [8] showed that as the clearance between the agitator and the vessel wall increase horse power requirement and heat transfer coefficients decrease.

b) Effect of impeller type :

Although in Cumming and West's [9] study for testing the use of retreading-blade turbine, e.i., radial flow type agitator, gave the same film coefficients as the use of two retreading blade turbines, when the pitched-blade turbine was used the coefficients were on the order of 10 per cent lower than the coefficients obtained for the retreading blade turbine. When pitched blade turbine, which produces radial flow with an axial flow component, is used there is no change in the film coefficient. Askew and Beckman [6] shown that as the fluid circulation pattern in the vessel changes from radial in the case of a turbine to axial in the case of a propeller the heat transfer coefficient decreases. The reason for this decrease in heat transfer coefficient is that the main flow direction is parallel to the agitator in the case of a propeller. Therefore, for a helical coil the flow around the upper tubes is obstructed by the lower tubes [10]. In another study

Rushton, et al [7] found that with a 12 in diameter 45° , 6 blade fan - blade turbine having a blade width of 3 in and placed 10 in above the vessel bottom, the film coefficients were approximately 10 per cent lower than with the curved blade.

Some work was done using a second curved blade turbine positioned $1.0D_A$ above the bottom of the turbine. This arrangement did not give higher film transfer coefficients than the single impeller, although Ackley [11] predicted that higher coefficients would result with multiple turbines in larger vessels.

From the comparison of helical screw agitator and anchor agitator, a conclusion can be drawn that the helical screw in a positive straight forward way provides sufficient turnover with attendant adequate mixing of the liquid bulk [8]. This serves to adequately mix the charge for high viscosities in the order of 10^4 or 10^5 poises, while it inhibits the intense mixing possible with the generated turbulence resulting in higher transfer coefficients by the anchor at higher values of N_{Re} .

c) Effect of Impeller Size:

With the radial flow 90° turbine heat transfer coefficients decrease as impeller size decreases while the primarily axial flow propeller and 45° turbine yield higher coefficients at a constant Reynolds number [6].

d) Effect of Viscosity:

For most practical applications using a high viscosity fluid,

a scraper or anchor type impeller which causes a more uniform velocity at the vessel wall would be used. The influence of increases in agitator speed on heat transfer becomes less at higher viscosities. The dissipation of energy between impeller and coil is larger for a more viscous fluid and the relative changes in fluid velocity near the coil caused by increases in impeller speed became less at higher viscosities [4].

II. ANALYSIS OF FINNED COIL (IMMERSED IN AGITATED VESSEL)

HEAT TRANSFER PERFORMANCE

The overall heat transfer coefficient in an agitated vessel with heating coil is expressed as the sum of individual resistance.

$$\frac{1}{U_o} = \frac{1}{H_o} + ff_i + \frac{x}{k_w} \frac{A_o}{A_m} + \frac{1}{H_i} \frac{A_o}{A_i} + ff_{ci} \quad (2.1)$$

The term H_o represents the convective heat transfer coefficient on the process side i.e., outside wall of a coil, the terms ff_i and ff_{ci} show fouling factors outside and inside the coil, the third term represents metal resistance of the fin and tube, and H_i represents the convective heat transfer coefficient inside the heating coil. Because the inner and outer heat-transfer surfaces are not equal, in the case of finned coils, the overall coefficient U must be referred to inner or outer coil surface. In the above equation the overall heat transfer coefficient has been based on outside surface of the bare tube. Assuming no fouling on either side of the finned coil wall equation (2.1) becomes

$$\frac{1}{U_o} = \frac{1}{H_o} \frac{A_o}{A_{eff}} + \frac{x}{k_w} \frac{A_o}{A_m} + \frac{1}{H_i} \frac{A_o}{A_i} \quad (2.2)$$

A_{eff} is the effective area as opposed to geometric external surface area which is obtained from the following equation.

$$A_{eff} = A_o + \eta A_f \quad (2.3)$$

2 .A DETERMINATION OF HEAT TRANSFER COEFFICIENTS

The heat transfer coefficient is not a characteristics of the fluid medium. On the contrary it depends in a complicated way on a number of variables [12].

The inside film coefficient H_i depends on :

- a) Fluid properties, such as thermal conductivity viscosity, density, and specific heat
- b) Coil geometry, as coil tube diameter, coil helix diameter and pitch.
- c) Flow velocity, dictating flow regime; streamline double helical, transition or fully developed turbulent flow, and
- d) Driving force ΔT and temperature distribution.

Similarly, the outside film coefficient H_o depends on :

- a) Fluid properties.
- b) Coil geometry
- c) Vessel geometry, baffle width, number of baffles and impeller dimensions.
- d) Degree of mixing, and

e) Driving force ΔT and temperature distribution.

In order to determine heat transfer coefficients from experimental data, there are three methods :

1. Measurement of the temperature of the heat transfer barrier by imbedded thermocouples [13,14,15].
2. Measurement of mechanical energy losses and use of momentum and heat transport analogies [16].
3. By the use of Wilson Plot [17,9,5] .

In this section, Wilson plot and the method which is used to calculate the film heat transfer resistance of a fluid moving in forced convection is discussed.

If the velocity of one of the fluids is permitted to vary while all of the other elements of the heat transfer system are held constant then it is apparent that the overall resistance will vary according to the variation of resistance of the fluid film whose velocity is being changed. The Wilson plot depends on this approach [18].

Case 1. Determination of the inside film coefficient, H_i

The heat flux is directly proportional to the driving force provided by the temperature difference ΔT and inversely proportional to the resistance in the system, or

$$\text{flux} \sim \frac{\text{Potential}}{\text{Resistance}}$$

The resistance is given by $1/U$ conductance. Then the above equation becomes,

$$\frac{Q}{A} = \frac{\Delta T}{1/U} \quad (2.4)$$

If the overall conductance is determined for a series of experiments at variable fluid velocity inside the coil and fixed agitator speed fixed fluid velocity inside the vessel and fixed temperature, equation (2.2) reduces to :

$$\frac{1}{U_o} = \gamma + \frac{1}{H_i} \frac{A_o}{A_i} \quad (2.5)$$

From a large number of tests with water flowing through the coils, the following equation has been determined [19].

$$\frac{1}{H_i} = \frac{1}{(1 + 0.011 T_w) V^{0.8}} \quad (2.6)$$

Therefore the heat transfer coefficient inside the coil can be equated to

$$H_i = K' V^{0.8}$$

Thus, if the overall resistance determined from experimental data is plotted with $1/U_o$ as the ordinate and $1/V^{0.8}$ as the abscissa, the points will fall on a straight line whose slope will be $A_o/A_i K'$ and intercept will be γ

$$\gamma = \frac{1}{H_o} \frac{A_o}{A_{eff}} + \frac{x}{k_w} \frac{A_o}{A_m} \quad (2.7)$$

H_i and H_o can be obtained from equations (2.6) and (2.7).

Case 2. Determination of the outside film coefficient H_o

The outside film coefficient is determined from experiments in which a series of agitator speeds resulting in changing liquid velocity on the vessel side is used, while all other factors including the fluid velocity and temperature inside the coil are kept constant. The overall conductance is determined from the heat transfer rate and log-mean temperature difference as in the first case. Using the heat transfer coefficient value inside the tube from the Sieder-Tate [20] correlation for coiled tubes, and the known tube wall thermal resistance, the outside film coefficient H_o can be calculated from the following equation.

$$\frac{A_o}{A_{\text{eff.}} H_o} = \frac{1}{U_o} - \frac{x}{k_w} \frac{A_o}{A_m} - \frac{1}{H_i} \frac{A_o}{A_i} \quad (2.8)$$

$$H_o = \frac{1}{(A_o + 2A_f) \left(\frac{1}{U_o A_o} - \frac{x}{k_w} \frac{1}{A_m} - \frac{1}{H_i A_i} \right)} \quad (2.9)$$

Since the fin efficiency (η) and the outside heat transfer coefficient are mutually dependent an iterative procedure is employed.

The particular procedure that is used in the calculated of the outside heat transfer coefficient in the present study, is discussed in detail in Chapter IV.

2.B CORRELATIONS FOR INDIVIDUAL HEAT TRANSFER FILM COEFFICIENTS

2.B.1. Inside Film Coefficient (in coil)

There are numerous relationships predicting heat transfer coefficient for different ranges of Reynolds numbers.

For the turbulent flow region i.e $10\,000 < N_{Re} < 12\,000$ and $0.7 < N_{pr} < 700$, Jeschke [21] found the correlation for air in curved tubes on the exterior of which the temperature was approximately uniform.

$$\frac{h_i D_H}{k_b} = 0.023 \left(\frac{D_H V_H \rho}{\mu_b} \right)^{0.8} \left(\frac{C_p \mu_b}{k} \right)^{0.4} \left(1 + 3.5 \frac{D_H}{D_C} \right) \quad (2.10)$$

The Sieder-Tate equation [20] for fluids flowing in coiled tubes is,

$$\frac{h_i D_H}{k_b} = 0.023 \left(\frac{D_H V_H \rho}{\mu_b} \right)^{0.8} \left(\frac{C_p \mu_b}{k_b} \right)^{0.33} \left(\frac{\mu_b}{\mu_w} \right)^{0.14} \left(1 + 3.5 \frac{D_H}{D_C} \right) \quad (2.11)$$

Pratt's [22] equation is valid for the fully developed turbulent flow region; and this condition may not be realized unless the Reynolds number is at least 15 000.

$$\frac{h_i d_H}{k_b} = 0.0225 \left(\frac{D_H V_H \rho}{\mu_b} \right)^{0.8} \left(\frac{C_p \mu_b}{k_b} \right)^{0.4} \left(1 + 3.4 \frac{D_H}{D_C} \right) \quad (2.12)$$

The Dittus and Boelter [23] equation does not include the viscosity correction ratio.

$$\frac{h_i D_H}{k_b} = 0.023 \left(\frac{D_H V_H \rho}{\mu_b} \right)^{0.8} \left(\frac{C_p \mu_b}{k_b} \right)^{0.4} \quad (2.13)$$

The transition region range is between 2100 and 10 000 for the N_{Re} Hausen's equation [24] describes this region as well as the laminar and the fully turbulent region.

$$\frac{h_i D_H}{k_b} = 0.116 \left| \left(\frac{D_H V_H \rho}{\mu_b} \right)^{2/3} - 125 \right| \cdot \left(\frac{C_p \mu_b}{k_b} \right)^{1/3} \cdot \left[1 + \left(\frac{D_H}{L} \right)^{2/3} \right] \left(\frac{\mu_b}{\mu_w} \right)^{0.14} \quad (2.14)$$

For laminar flow i.e $N_{Re} < 2100$, the modified Graetz [20] theoretical equation is,

$$\frac{h_i D_H}{k_b} = 0.0116 \cdot f_c \cdot \left(\frac{D_H V_H \rho}{\mu_b} \right)^{4/3} \cdot \left(\frac{C_p \mu_b}{k_b} \right)^{1/3} \cdot \left(\frac{D_c}{L} \right)^{1/3} \cdot \left(\frac{\mu_b}{\mu_w} \right)^{0.14} \quad (2.15)$$

where f_c = friction factor for coiled tubes.

The equation used in the calculation of the inside heat transfer coefficient in the study is the Sieder and Tate equation [20].

2.B.2 Outside film coefficient (in vessel)

Using dimensional analysis, one may obtain the following general dimensionless equation for the outside heat transfer coefficient and the variables mentioned in Chapter 2.A For geometrically similar systems the equation derived from dimensional analysis reduces to,

$$\phi(N_{Re}, N_{Nu}, N_{Pr}, V_{is}) = 0 \quad \text{or}$$

$$N_{Nu} = C \cdot N_{Re}^A \cdot N_{Pr}^B \cdot V_{is}^E \quad (2.16)$$

The dimensionless numbers in equation (2.16) are defined as follows.

$$N_{Nu} = \frac{H_o D_H}{k}$$

The Nusselt number (the ratio of the resistance to heat transfer occurring by conduction only, to the actual resistance to heat transfer).

$$N_{Re} = \frac{D_A^2 N \rho}{\mu}$$

The Modified Reynolds number (the ratio of the inertial forces to the opposing viscous force in a system)

$$N_{Pr} = \frac{C_p \mu}{k}$$

The Prandtl number (the ratio of the heat transferred by bulk transport to the heat transferred by conduction)

$$V_{is} = \frac{\mu_b}{\mu_w}$$

The Viscosity Correction Factor (the ratio of the process-liquid viscosities at bulk temperatures and at wall temperatures)

Heat transfer with smooth coil surfaces has been examined frequently in the literature and results have been correlated in terms of variables obtained from dimensional analysis.

Oldshue and Gretton [15], Cumming and West [9], Chilton, Drew and Jebens [13], Pratt [22], E. DE Maerteleire [25] have investigated the flat-bladed impeller with a helical coil. Ackley [11] and Skelland-Blake-Dabrovsky [26], Ülkü-Çakaloğlu [27] performed similar experiments using a propeller. Dunlap and Rushton [14], Rushton-Litcman-Mahoney [7], Gentry [28], presented data for heat transfer with baffle coil systems. In some cases it may be advantageous to use a baffle coil arrangement in which the heating tubes are positioned vertically in the vessel to act as baffles rather than the more common helical coils. This choice generally depends on costs in construction. In Table (2.1) correlations for smooth tubed helical coil are listed.

Although heat transfer with smooth coil surfaces have received much attention as in the case of surface roughness and its influence on mass and heat transfer in pipe flow, limited data are available for roughness with agitated liquids. In the past Appleton and Brennan [10] have reported heat transfer results for bare and low finned helical and baffle coils with separate correlating curves for each surface geometry and test fluid. According to Appleton and Brennan, the use of a single correlation for the entire Prandtl number range ignores the fact that the relation between the film coefficient and impeller speed depends on the fluid viscosity. Also, in their calculations, the Prandtl number was evaluated at the mean film temperature which was the mean of the average coil temperature and the bulk fluid temperature, thereby

Table (2.1) Correlations for convective heat transfer coefficients for the case of smooth tube helical coil

INVESTIGATORS		CORRELATIONS	N_{Re} RANGE												
E.DE MAERTELERIE	[25]	$\frac{H_o D_T}{k_b} = 1.379 (N_{Re})^{0.534} (N_{Pr})^{0.295} \left(\frac{\mu}{\mu_w}\right)^{0.192}$	$1.67 \cdot 10^2 - 245 \cdot 10^5$												
ULKU-ÇAKALOZ	[27]	$\frac{H_o D_H}{k_b} = E (N_{Re})^a (N_{Pr})^{0.36} \left(\frac{\mu}{\mu_w}\right)^{0.14} \left(\frac{D_H}{D_C}\right)^{1.069} \left(\frac{D_C}{D_A}\right)^{0.295} \left(\frac{S_C}{D_H}\right)^{0.388}$	<table border="0"> <tr> <td>E</td> <td>a</td> <td>$0.9 \cdot 10^5 - 1.65 \cdot 10^5$</td> </tr> <tr> <td>1.21</td> <td>0.488</td> <td>$1.9 \cdot 10^4 - 9.4 \cdot 10^5$</td> </tr> <tr> <td>0.27</td> <td>0.605</td> <td>$4 \cdot 10^3 - 9.3 \cdot 10^5$</td> </tr> <tr> <td>1.217</td> <td>0.468</td> <td></td> </tr> </table>	E	a	$0.9 \cdot 10^5 - 1.65 \cdot 10^5$	1.21	0.488	$1.9 \cdot 10^4 - 9.4 \cdot 10^5$	0.27	0.605	$4 \cdot 10^3 - 9.3 \cdot 10^5$	1.217	0.468	
E	a	$0.9 \cdot 10^5 - 1.65 \cdot 10^5$													
1.21	0.488	$1.9 \cdot 10^4 - 9.4 \cdot 10^5$													
0.27	0.605	$4 \cdot 10^3 - 9.3 \cdot 10^5$													
1.217	0.468														
APPLETON	[10]	$\frac{H_o D_H}{k_b} = 0.0376 (N_{Re})^{0.7} (N_{Pr})^{0.33} \left(\frac{D_A}{D_T}\right)^{0.1} \left(\frac{D_H}{D_T}\right)^{0.5}$	$10^3 - 10^5$												
ACKLEY	[11]	$\frac{H_o D_T}{k_b} = 1.40 (N_{Re})^{0.62} (N_{Pr})^{0.33} \left(\frac{\mu}{\mu_w}\right)^{0.14}$	$2 \cdot 10^3 - 7 \cdot 10^5$												
CHILTON ET-al	[13]	$\frac{H_o D_T}{k_b} = 0.87 (N_{Re})^{0.62} (N_{Pr})^{0.33} \left(\frac{\mu}{\mu_w}\right)^{0.14}$	$3 \cdot 10^2 - 4 \cdot 10^5$												
FRATT	[22]	$\frac{H_o D_T}{k_b} = 34 (N_{Re})^{0.5} (N_{Pr})^{0.3} \left(\frac{S_C}{H_C}\right)^{0.8} \left(\frac{W_{1b}}{D_C}\right)^{0.25} \left(\frac{D_A D_T}{D_H^3}\right)^{0.1}$	$2 \cdot 10^4 - 5 \cdot 10^5$												
CUMMING - WEST	[9]	$\frac{H_o D_T}{k_b} = 1.01 (N_{Re})^{0.62} (N_{Pr})^{0.32} \left(\frac{\mu}{\mu_w}\right)^{0.14}$	$2 \cdot 10^3 - 7 \cdot 10^5$												
OLDSHUE - GREYTON	[15]	$\frac{H_o D_H}{k_b} = 0.17 (N_{Re})^{0.67} (N_{Pr})^{0.37} \left(\frac{D_A}{D_T}\right)^{0.1} \left(\frac{D_H}{D_T}\right)^{0.5}$	$4 \cdot 10^2 - 1.5 \cdot 10^6$												
SKELLAND - DABROWSKY	[26]	$\frac{H_o D_H}{k_b} = 0.345 (N_{Re})^{0.62} \left(\frac{D_T}{H_C}\right)^{0.27}$	$2.5 \cdot 10^5 - 10^6$												
JHA and RAO	[29]	$\frac{H_o D_T}{k_b} = 0.18 (N_{Re})^{0.67} (N_{Pr})^{0.33} \left(\frac{D_H}{D_T}\right)^{-0.48} \left(\frac{D_C}{D_T}\right)^{-0.27} \left(\frac{H_C}{D_T}\right)^{0.14}$	$1 - 2.5 \cdot 10^5$												

eliminating the need of the Sieder-Tate viscosity ratio. These tests indicated that fins produce larger gains in transfer rate with the helical coil geometry than with the baffle arrangement but the smooth surface coefficients for the two are about the same at similar Reynolds numbers.

Another finned coil heat transfer investigation in agitated vessels was performed by Gentry [28]. Although Gentry used a vessel having a height-to-diameter ratio of two, his results are in good agreement with Appleton's. His tests indicated that baffles having large fin spacing, gave higher heat transfer coefficients than, baffles having low fin spacing.

Although heat transfer occurs from coil surface to agitated fluids, some investigators have used the tank diameter in the Nusselt number description. In this investigation the coil tube diameter was used in calculating the Nusselt number by taking into consideration Oldshue and Skelland's [15, 26] warning about the definitions of the Nusselt number. Correlations for finned coils are listed in Table (2.2).

Table (2.2) Finned Coil Heat Transfer Correlations

INVESTIGATORS	IMPELLER	COIL TYPE	CORRELATIONS	N_{Re} RANGE
GENTRY	[28] Dual-impeller six flat blade	Baffle	$\frac{H_o D_H}{k_b} = 0.00379 (N_{Re})^{0.778} \cdot (N_{Pr})^{0.4} \left(\frac{\mu_b}{\mu_w}\right)^{0.288} \left(\frac{H_S}{H_F}\right)^{0.145}$	$55 - 2.10^5$
APPLETON-BRENNAN [10]	Flat-blade	Helical	$\frac{H_o D_H}{k_b} = 0.00209 (N_{Re})^{0.89} \cdot (N_{Pr})^{0.5} \left(\frac{D_H}{D_T}\right)^{0.5} \left(\frac{D_A}{D_T}\right)^{0.1}$	$2.10^4 - 10^5$
	Flat-blade	Helical	$\frac{H_o D_H}{k_b} = 0.00846 (N_{Re})^{0.7} \cdot (N_{Pr})^{0.5} \left(\frac{D_A}{D_T}\right)^{0.33}$	$2.10^4 - 2.10^5$
	Ritched blade	Helical	$\frac{H_o D_H}{k_b} = 0.00107 (N_{Re})^{0.92} \cdot (N_{Pr})^{0.5} \left(\frac{D_H}{D_T}\right)^{0.5} \left(\frac{D_A}{D_T}\right)^{0.1}$	$2.10^4 - 2.10^5$

III. EXPERIMENTAL SET UP

The equipment and the experimental procedure used in the present work are described in the following sections.

3.A EXPERIMENTAL EQUIPMENT

The vessel and auxiliary equipment dimensions used in this investigation as shown in Figure (3.1) are described below in Table (3.1) together with the ranges of parameters covered.

Table (3.1) Range of Parameters Covered

<u>Parameters</u>	<u>Range</u>
N (agitator speed)	125 - 500 rev/min
N_{Re} (Reynolds number for agitated side)	20 000 - 100 000
N_{Re} (Reynolds number for coil side)	3600 - 14 000
$\frac{H_L}{D_T}$ (ratio of liquid height to tank diameter)	0.85
$\frac{D_A}{D_T}$ (ratio of the agitator diameter to the tank diameter)	0.4
$\frac{H_A}{D_T}$ (ratio of impeller height from the bottom to tank diameter)	0.3

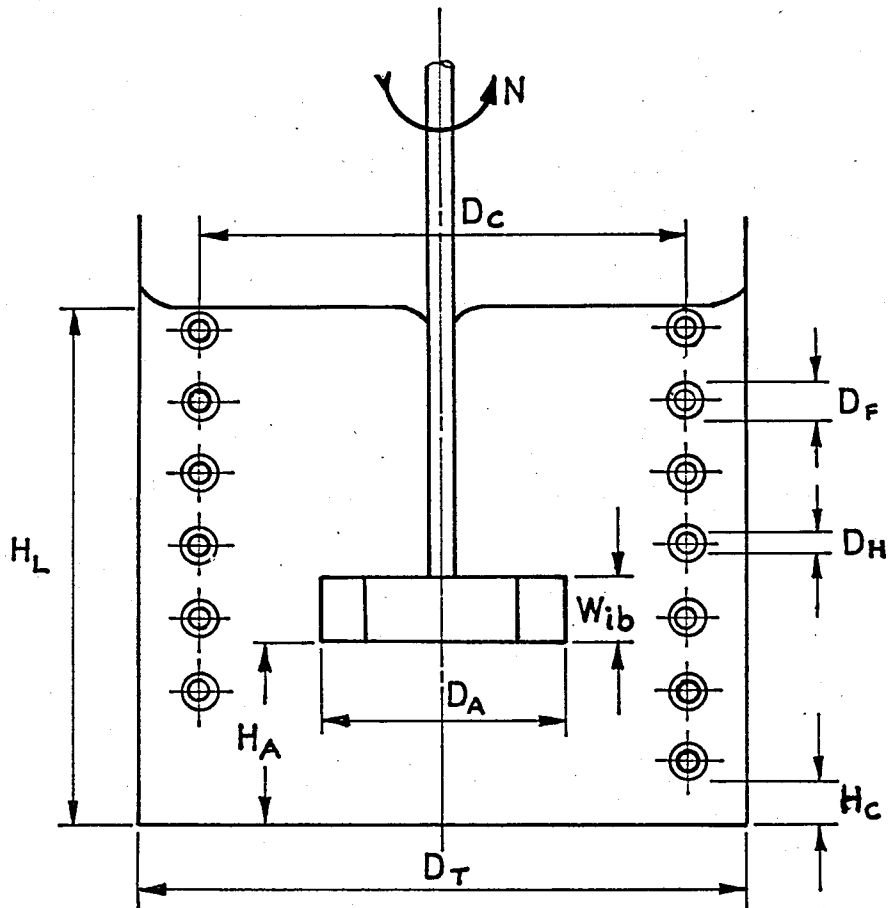
Table (3.1) Continued

$\frac{W_{ib}}{D_A}$	(ratio of impeller blade width to impeller diameter)	0.20
$\frac{D_C}{D_T}$	(ratio of coil diameter to tank diameter)	0.8
$\frac{L_C}{D_T}$	(ratio of coil length in tank to tank diameter)	0.7
$\frac{D_H}{D_C}$	(ratio of coil tube diameter to coil diameter)	0.04
$\frac{S_C}{D_H}$	(ratio of the space between coils to coil tube diameter)	1.0
$\frac{H_C}{D_T}$	(ratio of coil height from vessel bottom to vessel diameter)	0.10
$\frac{H_S}{H_F}$	(ratio of fin space to fin thickness)	25-35-55

The experimental set up consisted of a helical finned coil serving as a heating loop, immersed in the vessel, a stirrer, a number of thermocouples, a digital thermometer, pumps, a hot and cold water reservoir and heaters.

3.A.1 The vessel

The mixing, shown in Figure (3.1) was constructed of galvanized tin, and it was flat bottomed, having 20.0 ± 0.1 cm (7.9 in) inside diameter. The vessel had a glass liquid level indicator pipe. All equipment including vessel were insulated with glass wool.



$D_T: 200 \pm 0.1$ cm

$H_L: 17.0 \pm$ cm

$D_A: 7.99 \pm 0.01$ cm

$H_A: 6.0 \pm 0.2$ cm

$D_C: 16 \pm 0.2$ cm

$H_C: 20 \pm 0.1$ cm

$D_F: 0.12 \pm 0.001$ cm

$W_{ib}: 1.92 \pm 0.001$ cm

$D_H: 0.635 \pm 0.001$ cm

$N: 125 - 500$ r.p.m

Figure(3.1) Vessel and auxiliary equipment

3.A.2 Coils

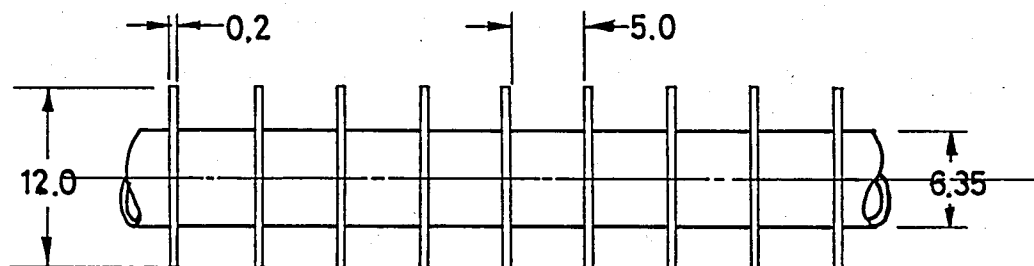
The coils were constructed of clean finned copper tubings having an inside diameter of 0.470 ± 0.1 cm (0.185 in) and an outside diameter of 0.635 ± 0.1 cm (0.250 in) and an one-tube diameter spacing. The helical finned tubings had fin space ranging from $0.5 \pm (0.1)$ cm to $1.1 \pm (0.1)$ cm. Dimensions for the copper finned-tube coils are provided in Figure (3.2) and Table (3.2). The coil length in the vessel was 300 cm (118 in) and the number of turns were 7.

Table (3.2) Finned Tube Dimensions

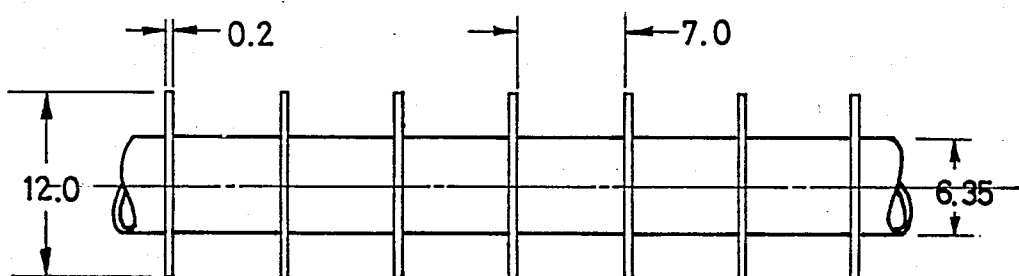
<u>PARAMETER</u>	<u>LOW FINS</u>		<u>MEDIUM FINS</u>		<u>HIGH FINS</u>	
Fin diameter D_F , cm(in)	1.200	(0.472)	1.200	(0.472)	1.200	(0.472)
Root diameter D_H , cm(in)	0.635	(0.250)	0.635	(0.250)	0.635	(0.250)
Fin Density	1.82	(4.62)	1.49	(3.78)	0.86	(2.18)
Fin thickness H_F , cm(in)	0.02	(0.0079)	0.02	(0.0079)	0.02	(0.0079)
Fin height H_H , cm (in)	0.565	(0.222)	0.565	(0.222)	0.565	(0.222)
Fin space H_S , cm (in)	0.5	(0.197)	0.7	(0.276)	1.1	(0.433)
Fin area A_F , m^2 (ft^2)	0.0932	(1.003)	0.0761	(0.819)	0.0438	(0.471)
Primary surface A_O , m^2 (ft^2) area.	0.0577	(0.621)	0.0581	(0.625)	0.0588	(0.633)
Total area A_T , m^2 (ft^2)	0.151	(1.625)	0.134	(1.442)	0.103	(1.109)

3.A.3 The Stirrer

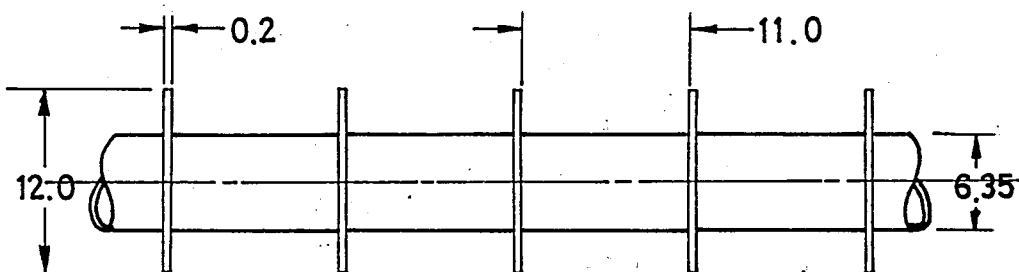
In all runs, a flat blade turbine impeller, also 7.99 ± 0.01 cm (3.15 in) diameter was used. It contained six



LOW FINNED TUBE



MEDIUM FINNED TUBE



HIGH FINNED TUBE

(Dimensions in mm)

Figure (3.2). Finned tube dimensions.

blades each 1.99 ± 0.01 cm (0.82 in) in actual width. The impeller was also placed 6.0 ± 0.2 cm (2.4 in) from the bottom of the vessel.

By changing the arrangement of pulley on the agitator drive, it was possible to obtain shaft speeds of 125, 200, 300, 400, and 500 r.p.m

A hasler speed indicator (tachometer) was used to measure the impeller speed.

The comparison of geometry of this study's with literature is given in Table (3.3)

3.A.4 Thermocouples

Hot and cold stream inlet and outlet temperature as well as bulk fluid temperatures were measured using 0.10 cm sheath diameter, iron-constantan thermocouples calibrated to $\pm 0.1^\circ\text{C}$. The first thermoelement name shows positive(+) point and the second thermoelement name shows negative(-) point in a circuit connection. Their temperature range of operation is -200 to $+700^\circ\text{C}$. This upper limit can be increased to $+900^\circ\text{C}$ in short time measurements. In order to prevent thermoelements from the corrosive effect of water, after cleaning the junction points they are coated with nail lacquer.

Table (3.3) Comparison of geometry of vessel and auxiliary equipment

INVESTIGATOR	IMPELLER				COIL				VESSEL		
	D_A (cm)	W_{ib}/D_A	H_c/D_A	Type	Material	D_H	S_c	D_c	D_T	H_1/D_T	Bottom type
Gentry 28	15.2	-	-	dual impeller six flat bladed	-	1.27	-	-	45.7	2	flat
Appleton-Brennan 10	15.24	0.25	-	six flat bladed	Copper	1.9	5.08	30.48	45.72	1.22	flat
Present Study	7.99	0.24	2	six flat bladed turbine	Copper	0.635	0.635	16	20	0.85	flat

3.A.5 Digital Thermometer

Temperature measurement were made with a digital thermometer by means of iron-constantan thermocouples. Some technical specifications of this instruments are given below.

Type	: D192M12
Line voltage	: 220 V AC \pm % 15, 48-52 Hz
Measurement Sensitivity	: \pm % 0.1 (full scale)
Input impedance	: min 1 M Ω
Operating Temperature	: - 10 ^o C to +50 ^o C

3.A.6 Hot Water Reservoir

The hot water reservoir was an insulated galvanized tank approximately capable of holding $62.5 \cdot 10^3 \text{ cm}^3$. Two electrical heating coils were placed inside the reservoir in order to supply the hot water running inside the coil. The desired temperature was controlled by an immersed thermocouple.

3.A.7 Cold Water Reservoir

A 50 lt container was used as cold water source. In order to prevent variation of the heat of pump connected to this container, liquid level in the container was kept constant throughout the experiment.

3.A.8 Rotary Pumps

The pumps connected to the hot stream feed line and the cold stream feed and exit line were two rotary pumps whose capacity was 50 W, 200 U/min and 90 W, 200 U/min respectively.

3.B EXPERIMENTAL ARRANGEMENT and PROCEDURE

Since an objection may be raised to use of a mercury thermometer for recording temperatures in heat transfer rate process owing to the large heat capacity and resulting time lag of the instrument, in all runs six iron-constantan thermocouples which were calibrated against one another in water at room temperature and or different temperatures, were used. After calibrating all thermocouples one was inserted into the vessel for measuring bulk liquid temperatures, the others were placed in the hot stream inlet, hot stream outlet, the cold stream inlet, and cold stream outlet. And one thermocouple, as mentioned earlier, was inserted into the hot water reservoir. After putting thermocouples in drilled connection pipes, the small connection holes were sealed by liquid joint and wrapped by teflon band.

The vessel was insulated with glass wool and then wrapped by nylon sheets as were all connection pipes. The finned helical coil and the stirrer were fitted inside the vessel with their axes coincident with the axes of the vessel and coil ends were mounted to the vessel lid with corks, to

keep the coil in the same position.

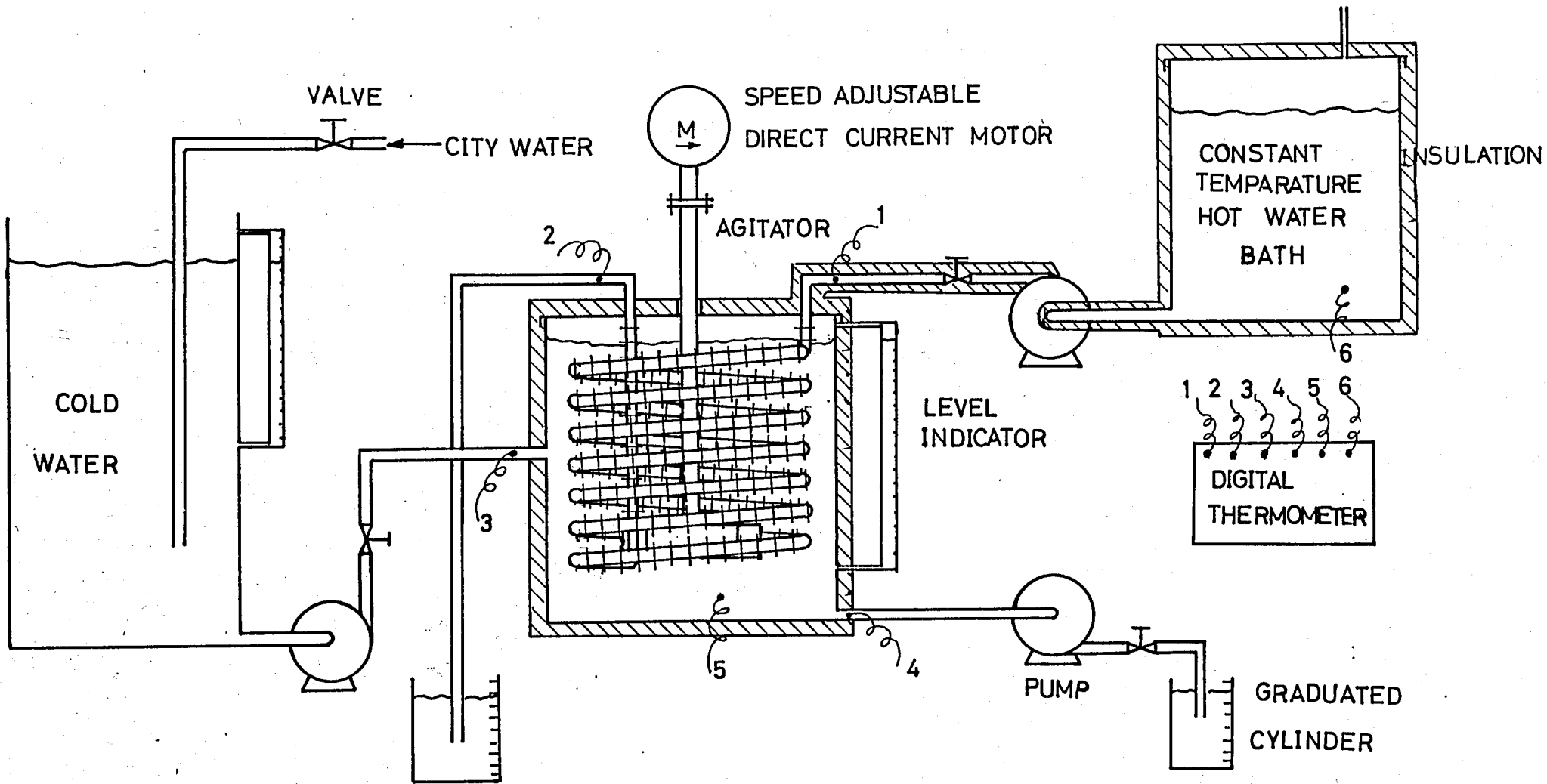
The hot and cold stream rates were measured by collecting water in a graduated cylinder for periods of one or two minutes. Two streams were flowing countercurrently, and the liquid depth in the vessel was maintained at 17.0 ± 0.1 cm (6.7 in) by manipulating the value on the cold stream exit line. The experimental arrangement is shown in Figure(3.3). A stop watch was also used in unsteady-state temperature measurements and flow rate measurements.

The experiments were performed in two sections as steady-state and unsteady-state cases.

3.B.1 Steay-State Experiments.

In the first set of experiments, in which only agitator speed was changed, while hot water and cold water conditions were kept constant, the following procedure was employed for the three helical coils.

1. The agitator was set at a desired speed and turned on.
2. The cold water level was maintained at the same level at a given flow rate by adjusting values at the feed to the pumps and at exit lines.
3. Hot water at a given temperature and flow rate was fed to coil.
4. After reaching steady-state, temperatures were recorded.



Figure(3.3) Experimental Arrangement

5. By adjusting agitators speed to a new values this procedure was repeated for each helical coil.

In the second set of the experiments agitator speed and cold water conditions were kept constant and hot water flow rate was changed at different hot water temperatures. The same procedure was followed also in this set for the three coils.

The variables were noted as in Table (3.4) and Table (3.5) for the two sets.

3.B.2 Unsteady State Experiments

In this set, temperatures were recorded at every thirty seconds until steady-state was reached for a given set of constant hot and cold stream conditions and at variable agitator speeds. This set was performed with a chosen helical coil to see whether heat transfer coefficient value for unsteady-state case was in a agreement with steady-state value or not.

The following procedure was followed:

1. Agitator speed was set at a given rpm and turned on.
2. Cold water at a given flow rate was pumped into vessel and liquid level was kept constant throughout the experiment.
3. Hot water at a given flow rate and temperature was fed to coil.

Table (3-4) Range of parameters for SET I. (Agitator Speed Variable)

PARAMETERS								
Fin Space (cm)	1.1	1.1	1.1	0.7	0.7	0.5	0.5	0.5
Agitator speed(rpm)	125-500	125-500	125-500	125-500	125-500	125-500	125-500	125-500
Hot Water Flow R. (ml/sec)	20 -20.25	19.9-20.5	19 -19.5	20 -20.5	19.5-20.5	17.5-18.5	19.5-20	19.5-20.25
Cold Water Flow R. (ml/sec)	19.5-20	19.8-20	10 -11	19.5-20.5	10.5-11	19.7-20	19.7-20	10 -11.5
Hot Water Inlet Temp. (°C)	69.6-70.2	78.1-79.3	77.9-79.3	68.3-69.5	78.6-82	76.7-78	68.9-70.5	71-78.5
Cold Water Inlet Temp. (°C)	22.1-22.4	17.7-18.6	19.1-19.3	22.1-22.7	17.7-21.3	17.7-18.9	22.3-22.5	23-23.3

Table (3.5) Range of parameters for Set II (Hot Water Conditions Variable)

PARAMETERES										
Fin Space (cm)	1.1	1.1	1.1	1.1	1.1	0.7	0.7	0.7	0.7	0.5
Agitator Speed (rpm)	200	200	200	200	200	200	200	200	200	200
Hot Water Flow R. (ml/sec)	10.5-28	14.5-25	11 -24	10.5-25	10 -26.5	13.5-28.5	9 -25	13 -25.5	13.5-23.5	10 -28
Cold Water Flow R. (ml/sec)	19.5-21	19.8-21	20 -21	10.75-11	10 -11.5	19.5-20	20 -22	10 -11	10.5	19.5-20.5
Cold Water Inlet Temp. (°C)	16.9-19.5	16.6-19.2	18.6-19.7	18.9-19.8	19.2-21.3	16.4-19.2	17 -20.7	18.3-19.1	17.8-18.4	22.4-22.7
Hot Water Inlet Temp. (°C)	62.2-67.1	71.5-75.3	80-84.7	64 -68.8	74.2-78.9	64.3-65.9	73.5-76.6	65.5-67.5	75 -76.6	66.2-67.5

4. After recording steady-state temperatures, hot water temperature was changed and the temperatures were recorded at regular time intervals until new steady-state values were reached.

5. Then agitator speed was changed and the same procedure was repeated for a new agitator speed.

IV. RESULTS

The experimental results and the determination of heat transfer coefficients in the stirred tank system are presented in this Chapter.

The experiments grouped in Set II were first performed in order to determine whether the H_i (inside heat transfer coefficient) was in agreement with the Sieder-Tate correlation (2.11) or not. Secondly the experiments in Set I were performed in order to find the H_o (outside heat transfer coefficient). These results were evaluated and by using least mean square analysis a correlation was obtained. Three unsteady-state experiments with high finned coil were performed to check whether the overall conductance remained constant or not.

A comparison between the H_o values for finned and those for the bare coil was also made to find the fin effect on heat transfer. All the experimental data obtained are given in Appendix (A.I.2) and (A.I.3).

4.A EVALUATION of EXPERIMENTAL DATA

4.A.1 Steady State Results.

The steady state experimental work in the present study was carried out in two sets totaling to 96 runs.

Experimental values of either U_O or U_I must be known before a plot as mentioned section 2.A can be made. The overall heat transfer coefficient based on the area of the primary surface of the finned tube was calculated directly from temperature readings and flowrate measurements of outlet streams, as follows :

$$Q_h = W.C_h.(T_1-T_2) \quad (4.1)$$

$$Q_c = M.C_w (t_1-t_o) \quad (4.2)$$

In order to check for heat loss, total heats based on cold and hot streams were calculated, and the total heat transferred based on the hot stream was used in calculations.

$$U_O = \frac{Q_h}{A_O \cdot \Delta T_{lm}} \quad (4.3)$$

ΔT_{lm} is the logarithmic mean temperature difference between vessel liquid and heating water with the assumption of proper agitation in the tank, i.e inlet temperature of cold stream.

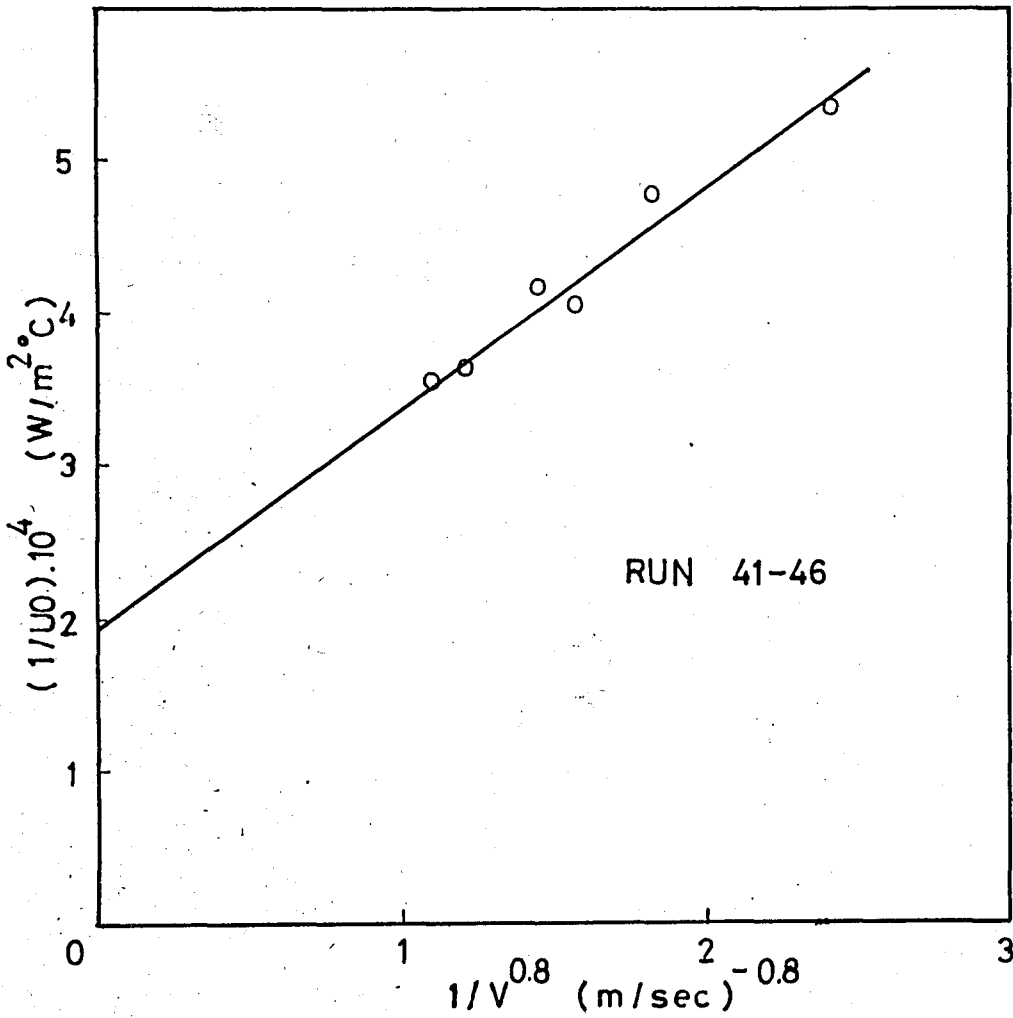
4.A.1.a Calculation of the inside film coefficient

For conditions where the flow rate and the temperature outside the coil do not change appreciably at variable fluid velocity inside the coil the overall conductance can be written using Equations 2.5 and 2.6 as follows :

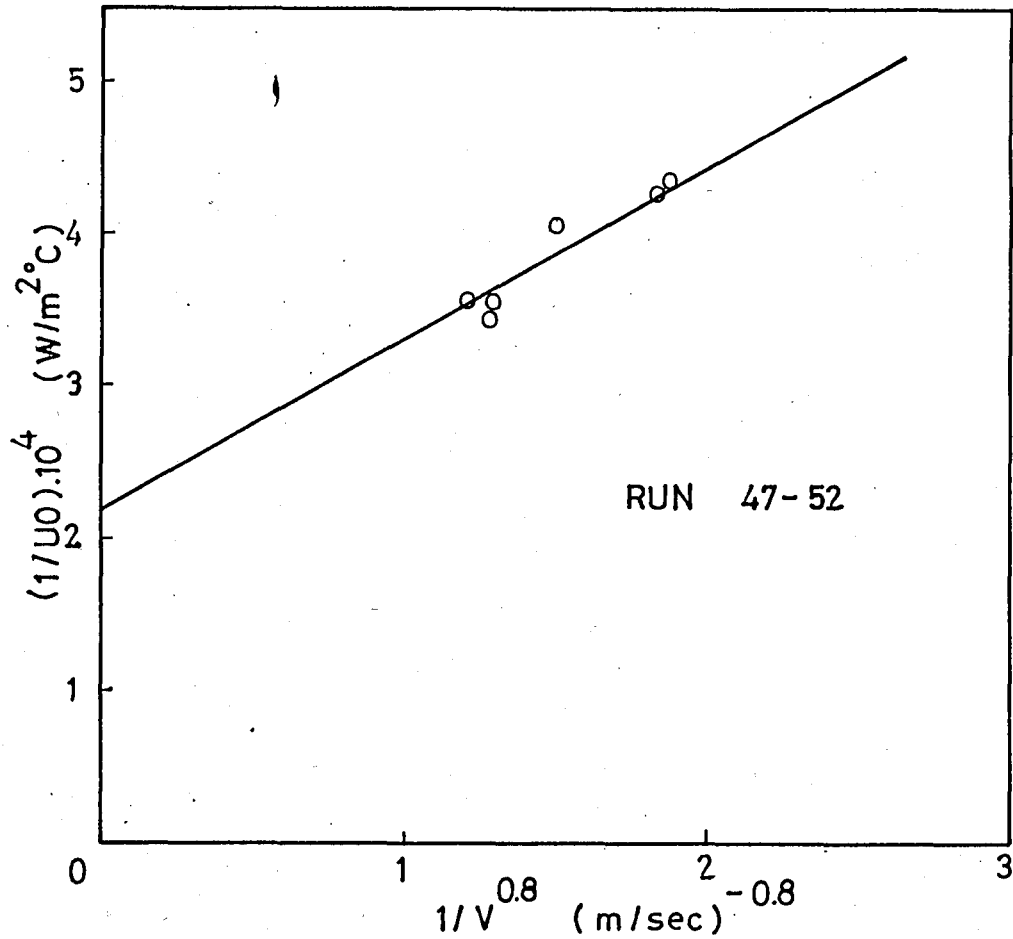
$$\frac{1}{U_o} = \gamma + \frac{1}{KV^{0.8}} \frac{A_o}{A_i} \quad (4.4)$$

When a plot $1/V^{0.8}$ versus $1/U_o$ is made, the internal film coefficient $H_i = K' \cdot V^{0.8}$ can be calculated from the slope of the straight line obtained. With this method, for different hot stream flow rates at fixed temperatures, the experiments in Set II were performed for finned coils with different fin spacing from the slopes of the curves $1/V^{0.8}$ versus $1/U_o$ internal heat transfer coefficients were calculated as shown in Figure (4.1) to (4.10) The corresponding data are presented in: Table(A.I.4).

With the Sieder-Tate correlation given in Equation(2.11), the maximum difference between the predicted and experimental values was found to be 27.97 per cent with 67 per cent of the 55 data points differing from predicted values by less than ± 15 per cent. Because this per cent error was found to be sufficiently low, in the calculations of Set II experiments Sieder-Tate correlation was used.



Figure(4.1) Wilson plot for run 41-46



Figure(4.2) Wilson plot for run 47-52 54

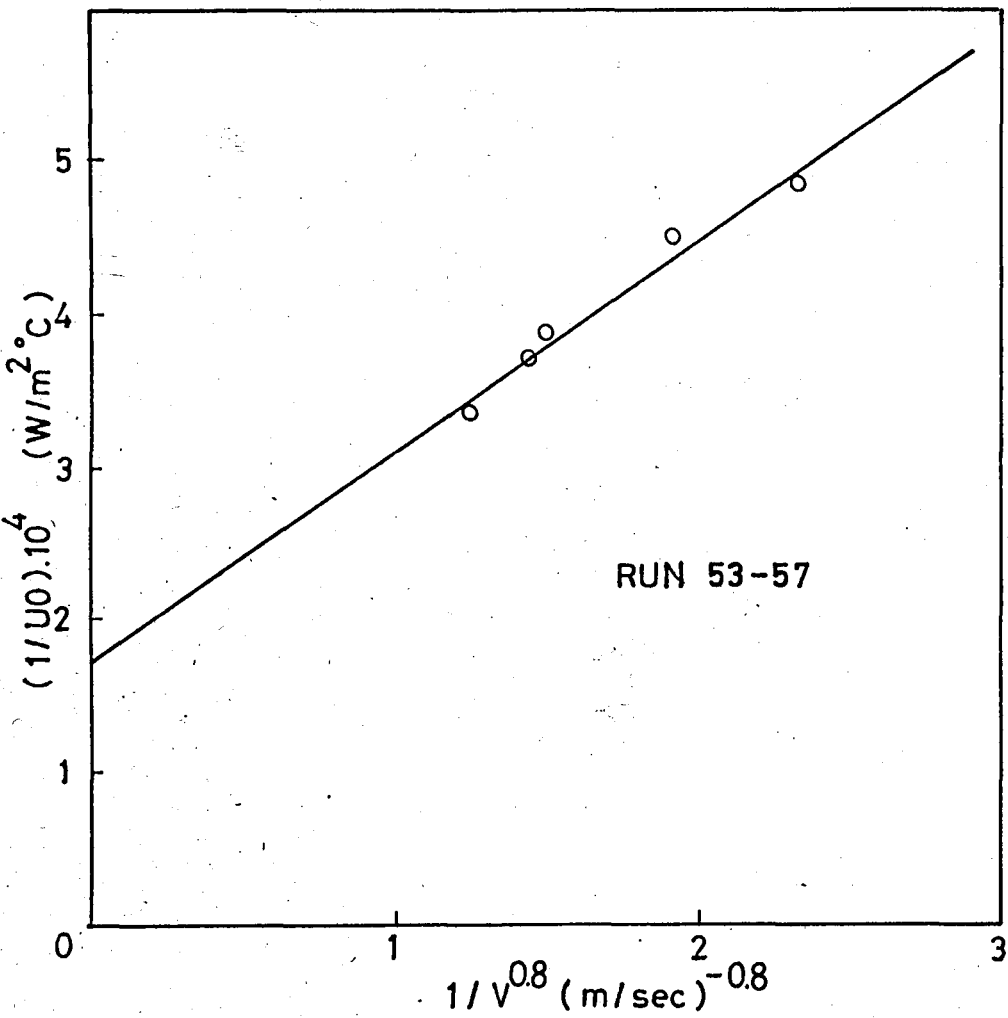


Figure (4.3) Wilson plot for run 53-57

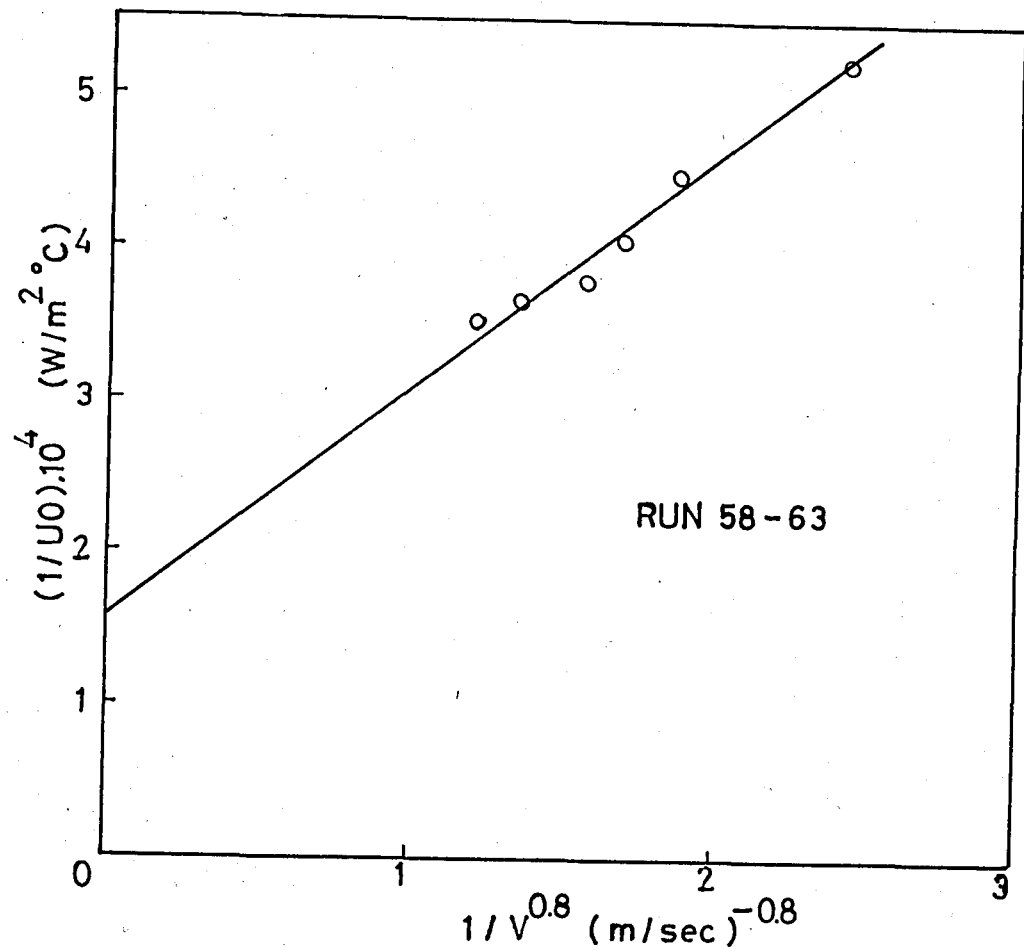


Figure (4.4) Wilson plot for run 58-63

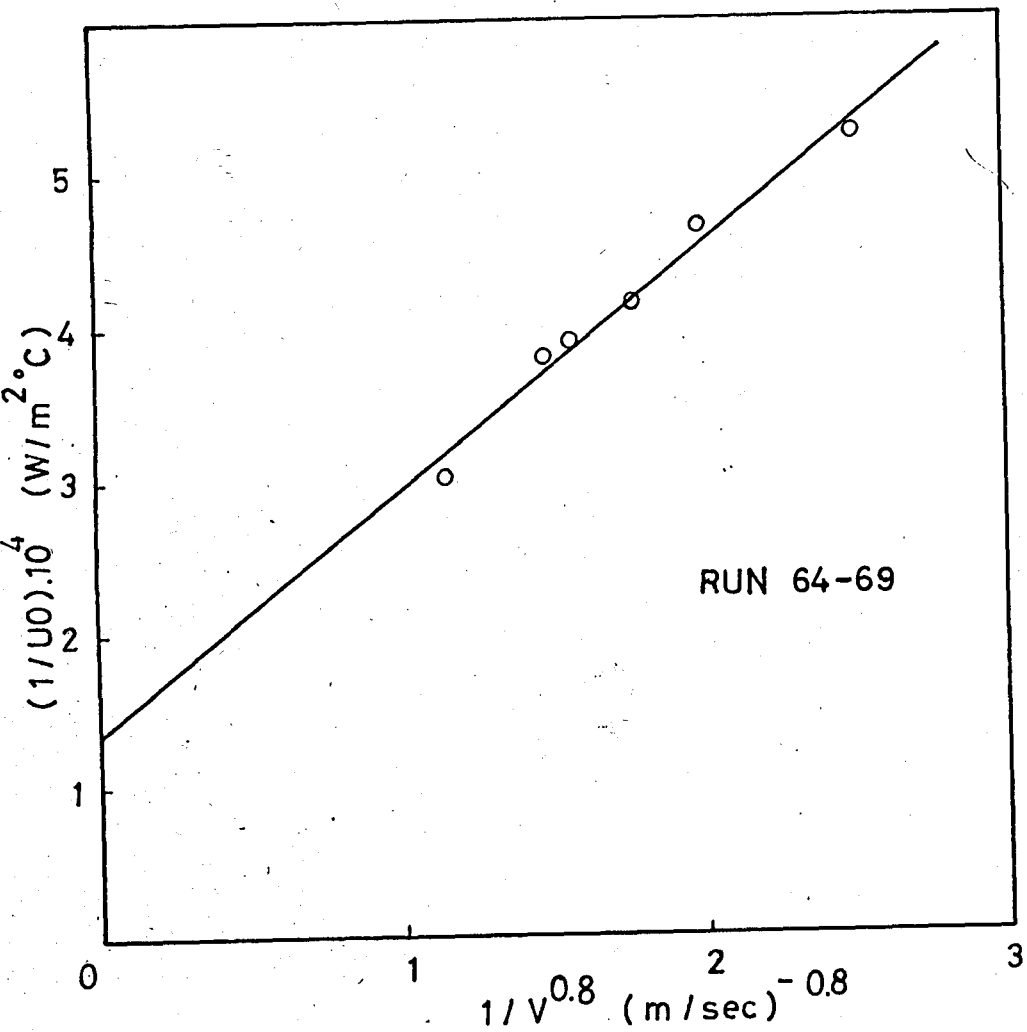


Figure (4.5) Wilson plot for run 64-69

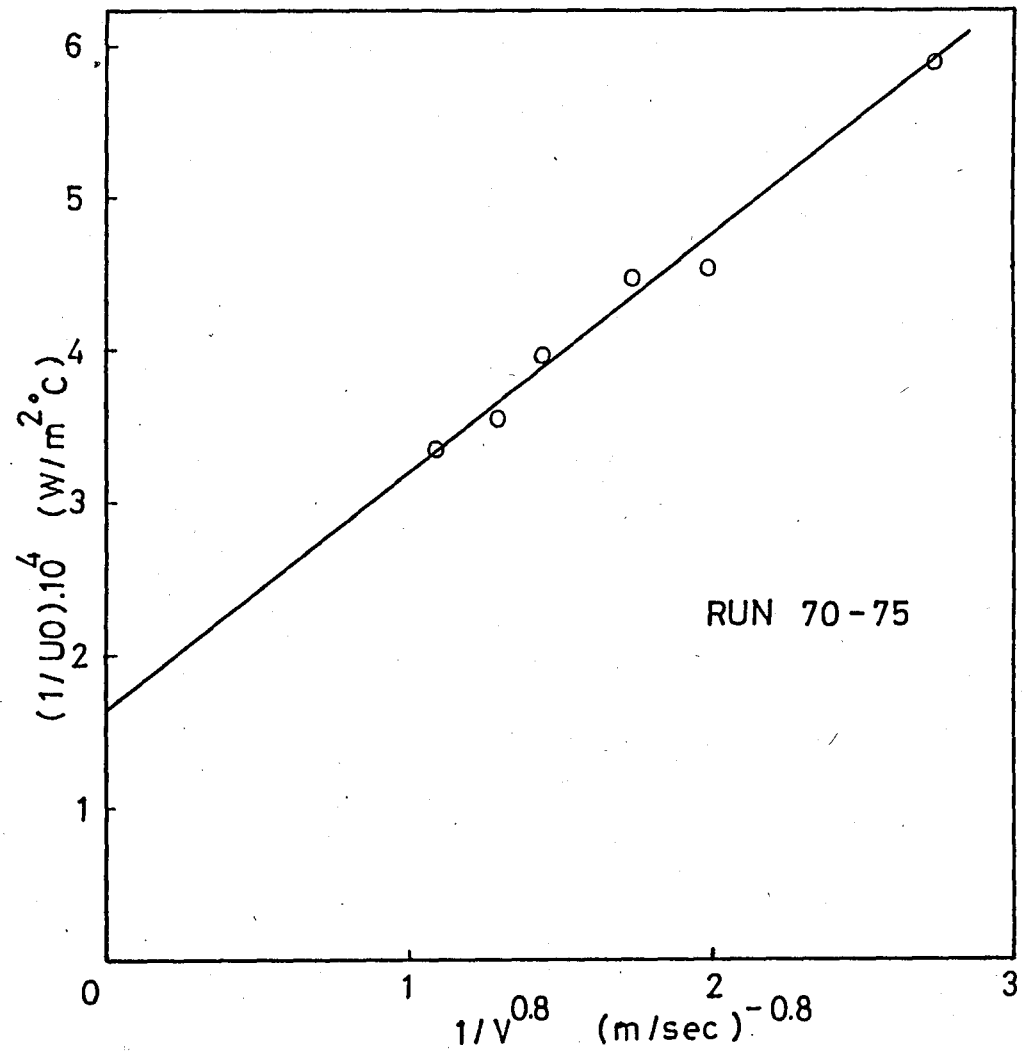


Figure (4.6) Wilson plot for run 70-75

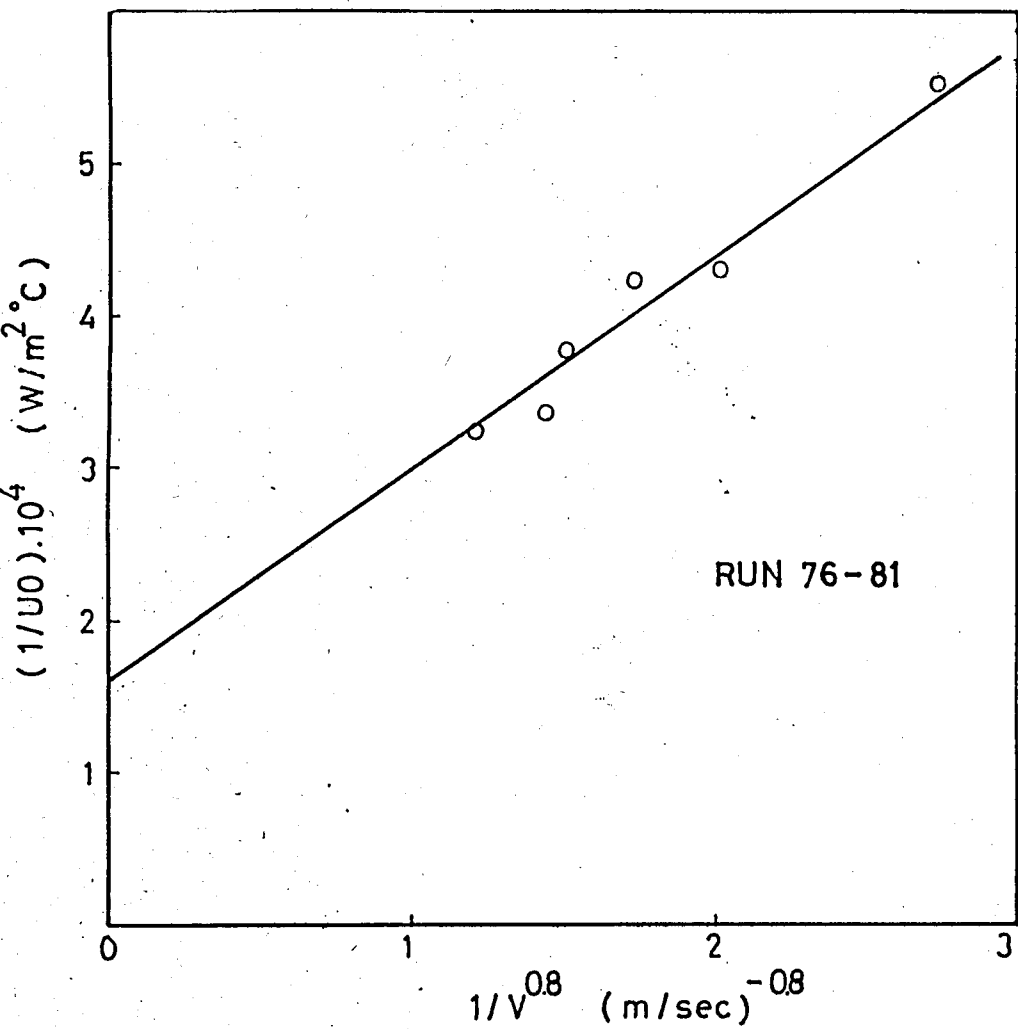


Figure (4.7) Wilson plot for run 76-81

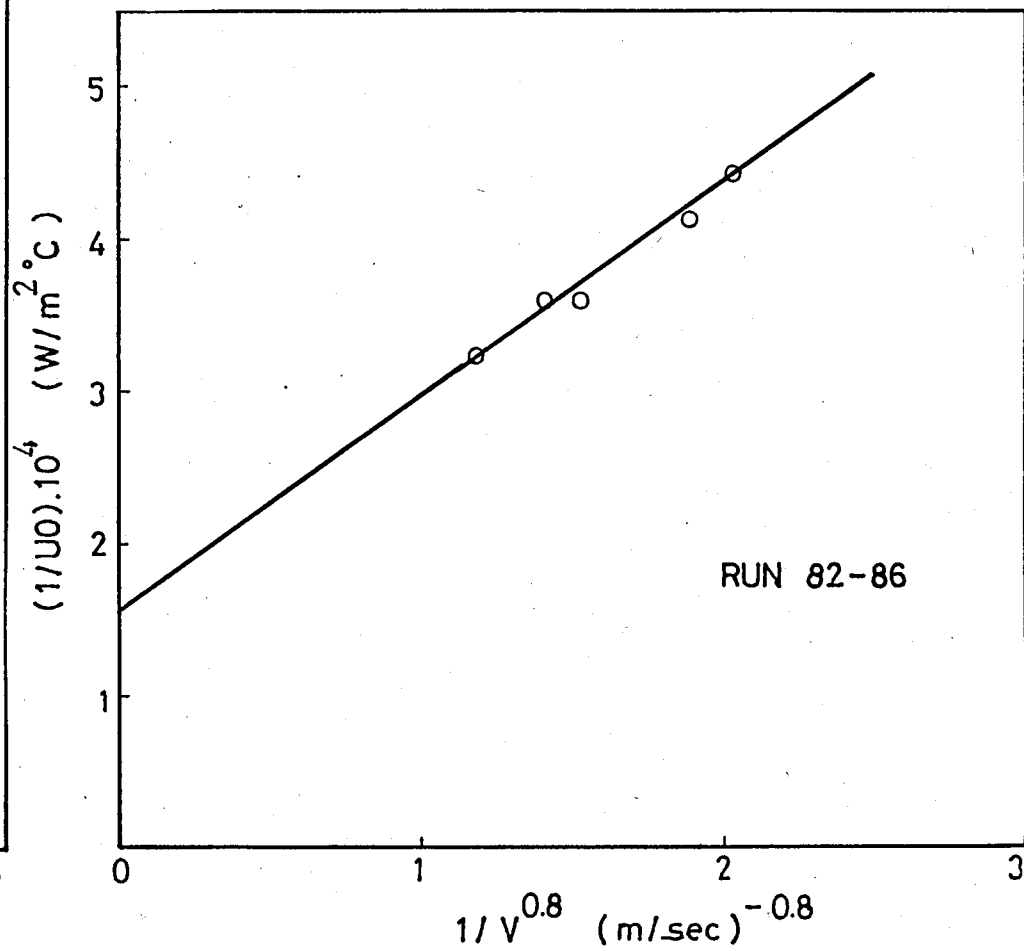


Figure (4.8) Wilson plot for run 82-86

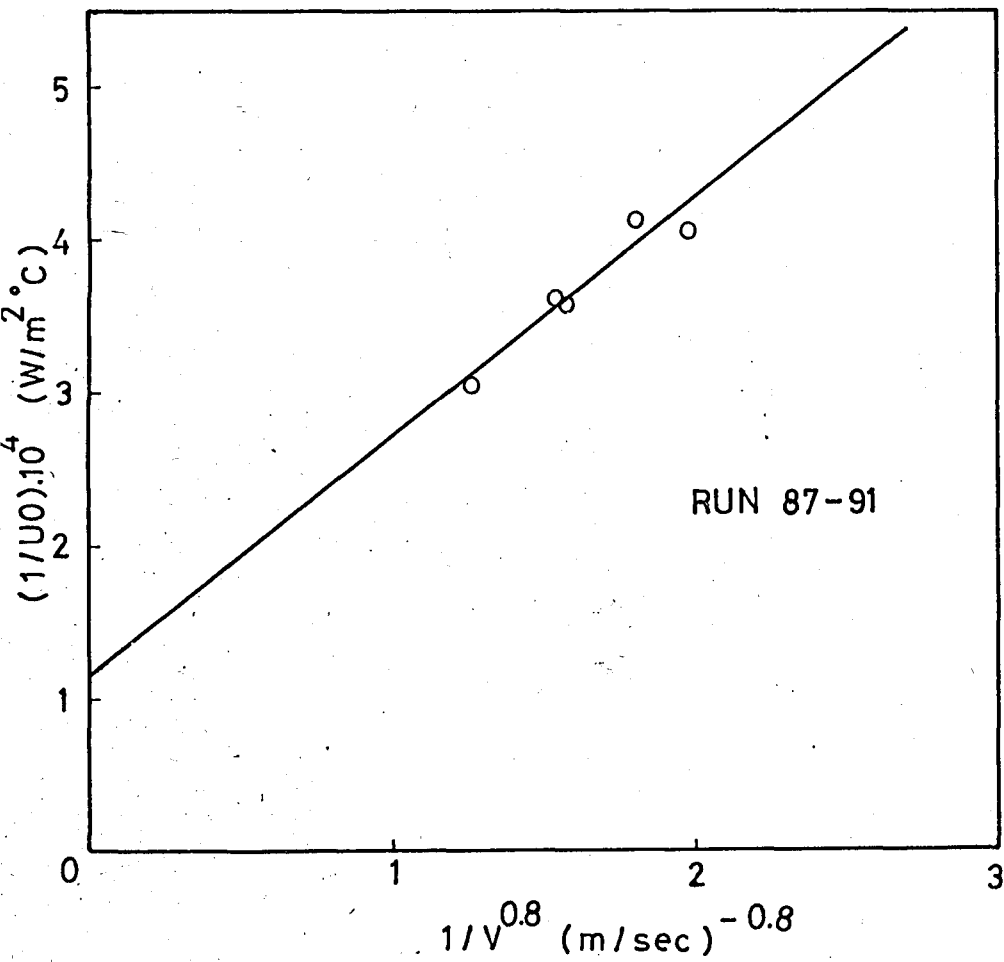


Figure (4.9) Wilson plot for run 87-91

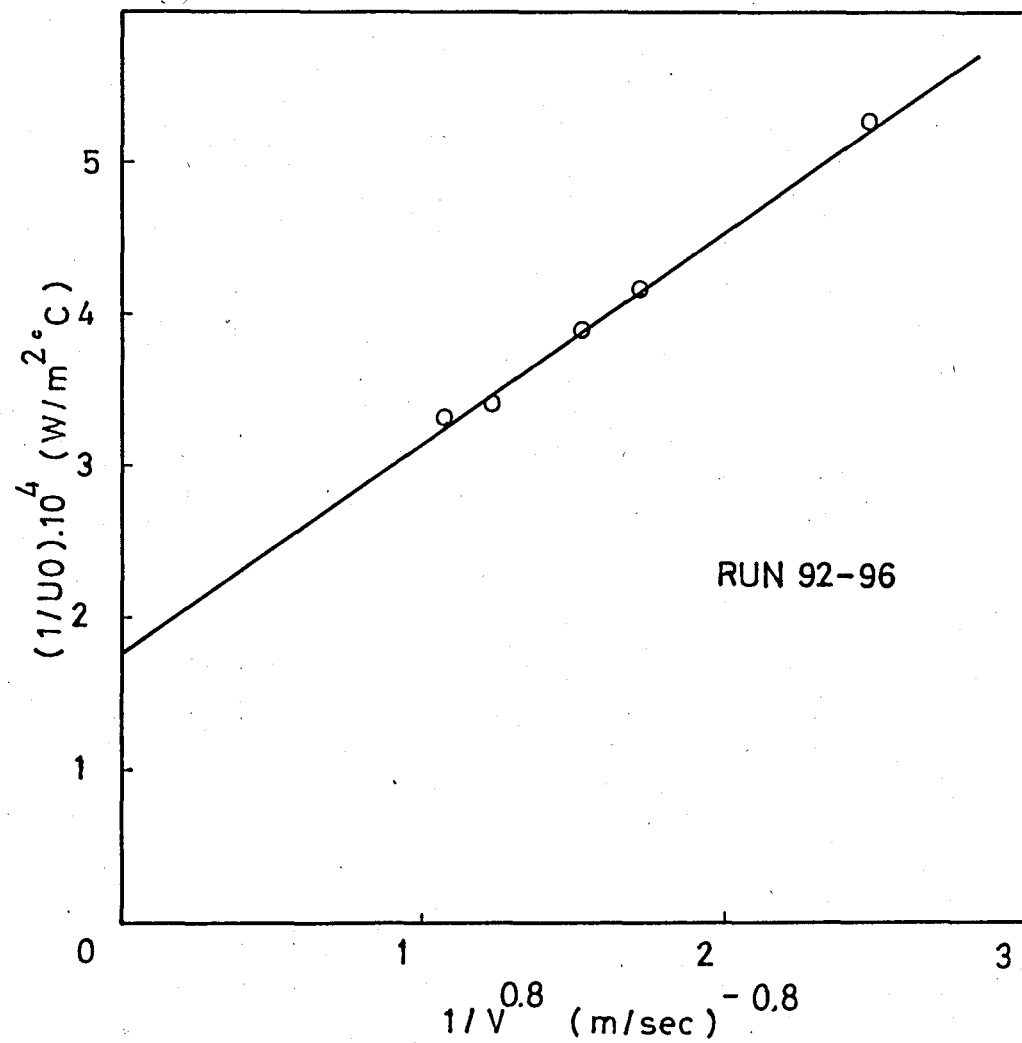


Figure (4.10) Wilson plot for run 92-96

4.A.1.b Calculation of the outside film coefficient

As discussed in section (2.A) the outside film coefficients were determined for each finned coil, by changing the agitator speed at least give times during 40 runs.

After determining the inside film coefficient from the Sieder-Tate correlation and U_o from experimental data, and using the known values of inside, outside, logarithmic mean areas as well as the thermal conductivity of copper, which was accepted to be $385 \text{ W/m}^\circ\text{C}$ [30] the H_o (outside film coefficient) was calculated from Equation (2.9).

$$H_o = \frac{1}{(A_o + \eta A_f) \left(\frac{1}{U_o A_o} - \frac{x}{k_w} - \frac{1}{A_m} - \frac{1}{H_i} - \frac{1}{A_i} \right)} \quad (2.9)$$

In the above equation, the fin efficiency (η) is directly related to the H_o term. For this reason an iterative method was used to calculate η . The outside heat transfer coefficient values for the bare tube at similar experimental conditions of flow rates and temperatures of hot and cold streams and similar agitator speed to the finned tube experiments were taken as the initial values to begin the iteration procedure. From the ϕ and Ω values cited in Table (A.I.1) fin efficiency for radial fin of constant thickness was read. By inserting this efficiency value in $A_{\text{eff}} = A_o + \eta A_f$ the effective area was calculated. Then by

using A_{eff} value, the H_o value was calculated from the above equation. This procedure was repeated until a constant H_o value was reached.

For example, for the high finned coil of run 1, the first H_o value (for bare tube) was $3603 \text{ W/m}^2 \text{ } ^\circ\text{C}$. From the Table (A.I.1), with $\phi = 0.0288 (H_o)^{1/2}$ and $\Omega = 0.53$, the fin efficiency η is found to be 0.4633. By substituting this value in the effective area equation A_{eff} was found to be $79.11.10^{-3} \text{ m}^2$. The constant value of H_o for this run was calculated to be $2694 \text{ W/m}^2 \text{ } ^\circ\text{C}$.

Then for 40 runs the calculated H_o values were used to obtain a correlation.

$$N_{\text{Nu}} = C \cdot N_{\text{Re}}^A \cdot N_{\text{Pr}}^{0.4} \cdot \left(\frac{\mu_b}{\mu_w}\right)^{0.14} \cdot \left(\frac{H_S}{H_F}\right)^D \quad (4.5)$$

In the correlation developed, the exponents of the Prandtl and viscosity correcting factors were taken from the literature and other exponents (i.e the exponent of the Reynolds number (A), the exponent of fin space to fin thickness ratio (D), geometry factor (C), were calculated according to the experimental data.

For each five runs performed for each finned coil at same conditions, $N_{\text{Nu}}/N_{\text{Pr}}^{0.4} \cdot \left(\frac{\mu_b}{\mu_w}\right)^{0.14}$ was plotted against the N_{Re} to the determine the exponents (A) and (D) and the geometry factor (C). From the slopes, Reynolds number exponent

was found. The intercept values gave the $(\frac{H_S}{H_F})^D \cdot C$. The slope and intercept values are listed in Table (4.1)

Table (4.1) Reynolds number exponents and geometry factors

Run	Reynold's Number Exponent (A) (slope)	$(H_S/H_F)^D \cdot C$ (intercept)
1-5	0.823	0.004113
6-10	0.810	0.004645
11-15	0.825	0.004006
16-20	0.801	0.004440
21-25	0.814	0.003950
26-30	0.817	0.003798
31-35	0.833	0.003260
36-40	0.813	0.003933

Another logarithmic plot of the mean intercept value for each finned coil with different fin spacing, versus (H_S/H_F) value gave the geometry factor (C) and (H_S/H_F) exponent.

In order to calculate the viscosity at the coil wall the wall temperature was calculated with the following assumption.

$$Q = H_i \cdot A_i \cdot (T_2 - t_w) \approx H_o \cdot A_{eff} \cdot (t_w - t_1) \quad (4.6)$$

$$t_w = T_2 - \frac{(T_2 - t_1)}{1 + \frac{H_i A_i}{H_o A_{eff}}} \quad (4.7)$$

Thus the heat transfer correlation for high, medium and low finned-tube coils was obtained. Final form of this equation is,

$$\frac{H_o D_H}{k_b} = 0.001883 \left(\frac{D_A^2 \rho_b N}{\mu_b} \right)^{0.817} \left(\frac{C_p \mu_b}{k_b} \right)^{0.4} \left(\frac{\mu_b}{\mu_w} \right)^{0.14} \left(\frac{H_S}{H_F} \right)^{0.207} \quad (4.8)$$

In the calculation of the physical properties of water (C_p, μ, ρ, k), the equations giving these properties as a function of temperature (A.II) were used [31].

4.A.2 Unsteady - state results

This set of experiments were carried out by using the high-finned coil. Data were taken by holding all cold and hot stream conditions constant and by changing agitator speed. Three different agitator speeds were used. The change in temperature with time was recorded every 30 seconds. 630 seconds was sufficient to reach the steady state values in all experiments All results are given in tabular form in Tables (4.2,4.3,4.4) and graphical form in Figure(4.11) and Figures (A.I.1,A.I.2,A.I.3). The Alpha values which were

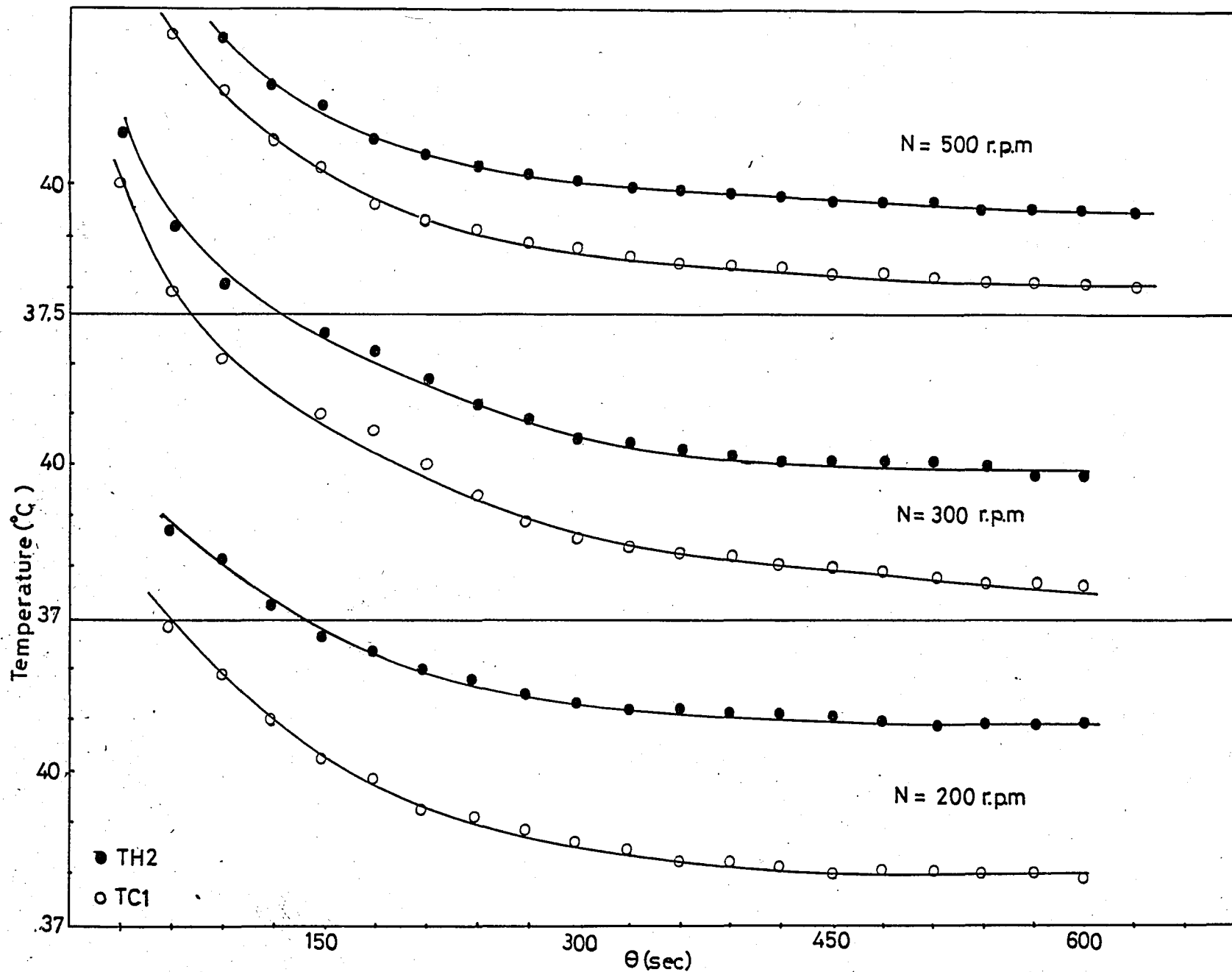


Figure (4.11) Unsteady-state results for three different agitator speed for high finned coil ⁶³

Table (4.2) Unsteady-state results of high finned coil

N = 200 rpm
 Cold water flow rate = 19ml/sec
 Hot water flow rate = 22.5 ml/sec
 Cold water inlet temperature = 24.4 °C
 Hot water inlet temperature = 68 °C
 Steady-state temperatures : TC1S = 45.9°C , TH2S = 49.8°C
 TCO(2)=24.5°C , TH1(2)=51.3°C

Time	$T_{\text{cold out}}$	$T_{\text{hot out}}$	ALPHA
60	42.9	44.8	0.226
90	42	44.2	0.237
120	41.1	43.3	0.216
150	40.3	42.8	0.227
180	39.9	42.4	0.219
210	39.3	42.1	0.233
240	39.2	41.9	0.223
270	38.9	41.6	0.218
300	38.7	41.4	0.214
330	38.5	41.3	0.219
360	38.3	41.3	0.231
390	38.3	41.2	0.223
420	38.2	41.2	0.229
450	38.1	41.2	0.235
480	38.1	41.1	0.227
510	38.1	41	0.220
540	38.1	41	0.220
570	38.1	41	0.220
600	38	41	0.226

Table (4.3) Unsteady-state results of high finned coil

N	= 300 rpm
Cold water flow rate	= 19.8 ml/sec
Hot water flow rate	= 22.5 ml/sec
Cold water inlet temperature	= 24.7 °C
Hot water inlet temperature	= 69 °C
Steady-state temperatures	: TC1S = 47.2°C, TH2S = 50°C TCO(2) = 24.9°C, TH1(2) = 50.8°C

<u>Time</u>	<u>T_{cold out}</u>	<u>T_{hot out}</u>	<u>ALPHA</u>
30	45.6	46.5	0.173
60	43.5	44.7	0.164
90	42.1	43.5	0.161
120	-	-	-
150	41	42.6	0.163
180	40.7	42.3	0.158
210	40	41.7	0.168
240	39.4	41.2	0.158
270	38.9	40.9	0.168
300	38.6	40.5	0.156
330	38.4	40.4	0.161
360	38.3	40.3	0.160
390	38.2	40.2	0.159
420	38.1	40.1	0.157
450	38	40.1	0.164
480	37.9	40.1	0.170
510	37.8	40.0	0.161
540	37.7	39.8	0.160
570	37.7	39.8	0.160
600	37.7	39.7	0.153

Table (4.4) Unsteady-state results of high finned coil

N	=	500 rpm
Cold water flow rate	=	20.5 ml/sec
Hot water flow rate	=	21.5 ml/sec
Cold water inlet temperature	=	24.7 °C
Hot water inlet temperature	=	69.8 °C
Steady-state temperature	:	TC1S = 46.4 °C , TH2S = 49 °C TCO(2) = 24.9 °C , TH1(2) = 51.7 °C

<u>Time</u>	<u>T_{cold out}</u>	<u>T_{hot out}</u>	<u>ALPHA</u>
30	44.9	45.7	0.117
60	43.0	43.9	0.103
90	41.9	42.9	0.101
120	40.9	42.0	0.095
150	40.4	41.6	0.106
180	39.7	40.9	0.100
210	39.3	40.6	0.104
240	39.2	40.4	0.096
270	38.9	40.2	0.101
300	38.8	40.1	0.101
330	38.6	40.0	0.101
360	38.5	39.9	0.106
390	38.5	39.9	0.106
420	38.4	39.8	0.105
450	38.3	39.7	0.104
480	38.3	39.7	0.104
510	38.2	39.7	0.111
540	38.1	39.6	0.110
570	38.1	39.6	0.110
600	38.1	39.6	0.110
630	38.0	39.5	0.109

$$\frac{T_2 - t_1}{T_1 - t_1} = \exp (- U_o A_o / W) = \alpha \text{ (alpha) } \text{ were approximately}$$

constant for each experiment. The Alpha values for 200, 300, 400, 500 rpm were found to be approximately 0.224, 0.162, 0.105 respectively. The decreasing in Alpha values with increasing agitator speeds were the indication of increasing heat transfer rate with agitator speed.

V. DISCUSSION

5.A DISCUSSION of the RESULTS with BARE COIL PERFORMANCE

Although values of the convective heat transfer coefficient for bare tube coils were larger than for finned-tube coils at lower Reynolds numbers, finned coils provided additional surface area which might offset these lower coefficient values. In order to reflect the surface area advantage of finned tube coils, a conductance ratio plot as a function of Reynolds number was constructed. In this plot Figure (5.1) and Table (5.1) it is evident that the ratio of high, medium and low finned tube conductance was greater than unity. Although numerical H_o values for high finned coil (less densely finned) were higher than medium and low finned coils, in the conductance ratio plot, low finned coil having the smallest fin spacing-to-thickness ratio was more heat transfer effective than other finned tube coils.

In Figures (5.2,5.3,5.4) the effect of fin spacing and agitator speed on external heat transfer coefficient are shown.

Table (5.1) Comparison of Bare and Finned Coil
Heat Transfer Performance

Run	H_o (bare) $W/m^2 \cdot ^\circ C$	H_o (finned) $W/m^2 \cdot ^\circ C$	A_{eff} $\times 10^3 m^2$	$H_o A_{eff} / H_o A_o$	N_{Re}
FIN SPACE = 1.1 cm					
1	3540.86	2640.40	81.60	1.017	21183.6
2	4725.64	3868.87	78.06	1.068	34434.99
3	6130.78	5455.68	75.06	1.116	52360
4	7336.17	6916.44	73.29	1.154	69823.2
5	8406.04	8276.93	71.98	1.184	88307.99
6	3611.87	2705.24	81.48	1.019	21773.14
7	4823.53	3965.87	77.96	1.071	35574.91
8	6240.51	5573.92	74.99	1.119	54108.94
9	7506.85	7114.93	73.19	1.159	73288.77
10	8576.35	8485.37	71.93	1.189	91468.82
11	3771.15	2882.72	80.73	1.031	26003.13
12	5054.98	4250.28	77.29	1.086	43088.34
13	6512.38	5935.43	74.32	1.132	64206.56
14	7785.17	7508.03	72.60	1.170	85688.69
15	8929.33	8998.61	71.32	1.201	106937.8
FIN SPACE = 0.7 cm					
16	3545.4	2420.42	100.2	1.143	21414.11
17	4717.19	3528.88	94.13	1.177	34434.99
18	6108.61	4962.64	88.55	1.203	52119.47
19	7345.47	6327.63	85.39	1.229	70469.31
20	8361.91	7508.38	83.13	1.247	86896.04
21	3634.31	2492.80	99.72	1.143	22233.10
22	4844.49	3646.59	93.31	1.174	36224.30
23	6345.37	5213.45	87.67	1.204	57279.60
24	7528.10	6522.22	84.50	1.223	73790.42
25	8556.38	7722.47	22.40	1.245	90364.95
26	3738.74	2605.19	98.84	1.151	25392.18

Table (5.1) Continued

27	4986.02	3809.76	92.45	1.180	41209.75
28	6434.3	5331.18	87.10	1.206	61574.37
29	7824.5	6800.45	83.92	1.219	83348.92
30	8809.5	8063.89	81.88	1.252	102211.56

FIN SPACE = 0.5 cm

31	3540.49	2257.45	109.28	1.164	21176.79
32	47712.25	3293.05	102.31	1.171	34468.08
33	6121.50	4648.36	95.01	1.205	52632.68
34	7336.69	5903.28	90.96	1.223	70527.79
35	8414.57	7071.85	86.35	1.215	88600.2
36	3779.06	2475.24	107.54	1.177	26709.93
37	5078.78	3656.60	99.08	1.192	44256.23
38	6575.00	5139.00	91.58	1.196	66450.79
39	7866.66	6503.45	89.20	1.232	88335.50
40	8995.78	7765.05	86.84	1.252	110308.32

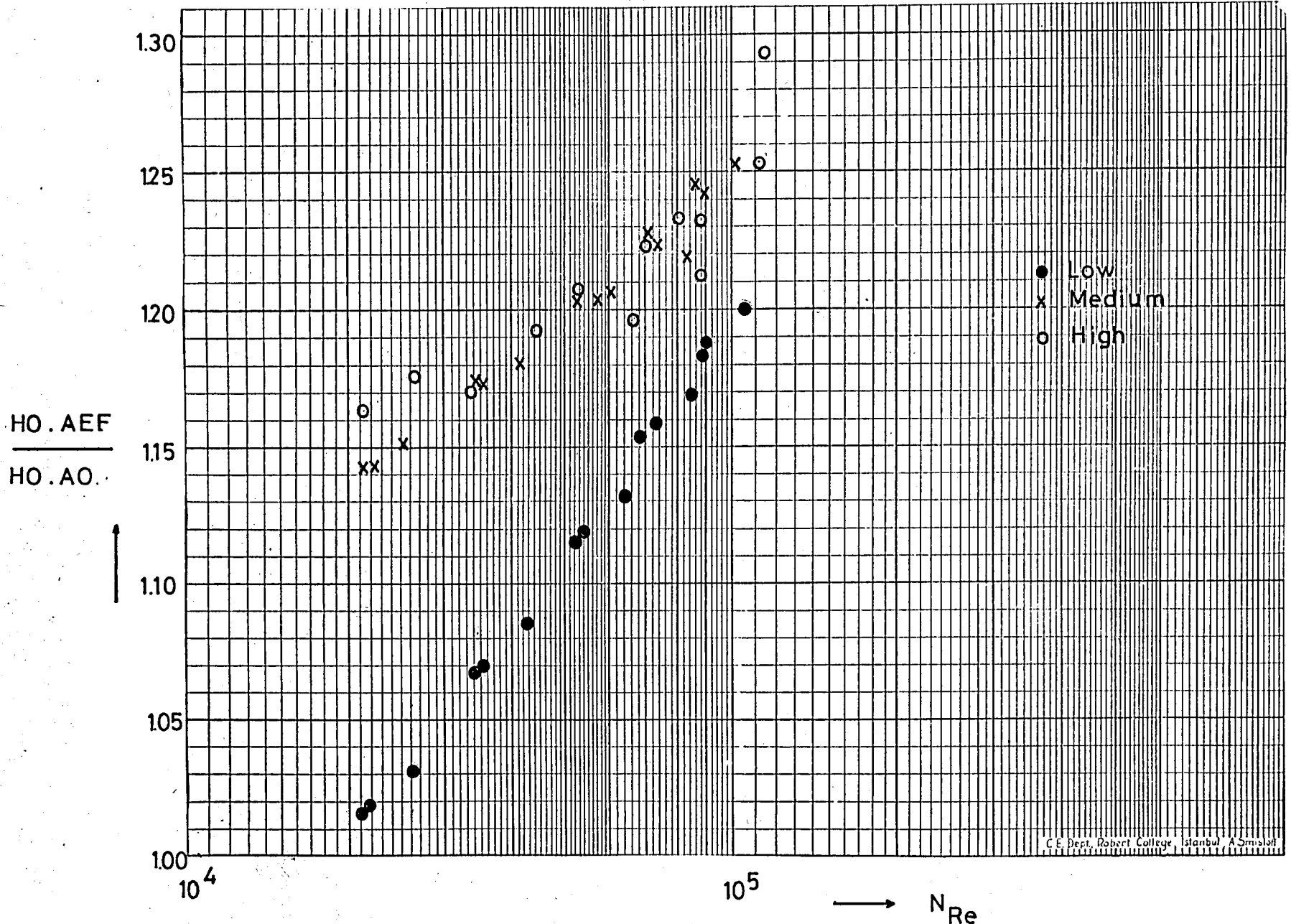


Figure (5.1) Conductance ratio of finned coil to bare coil

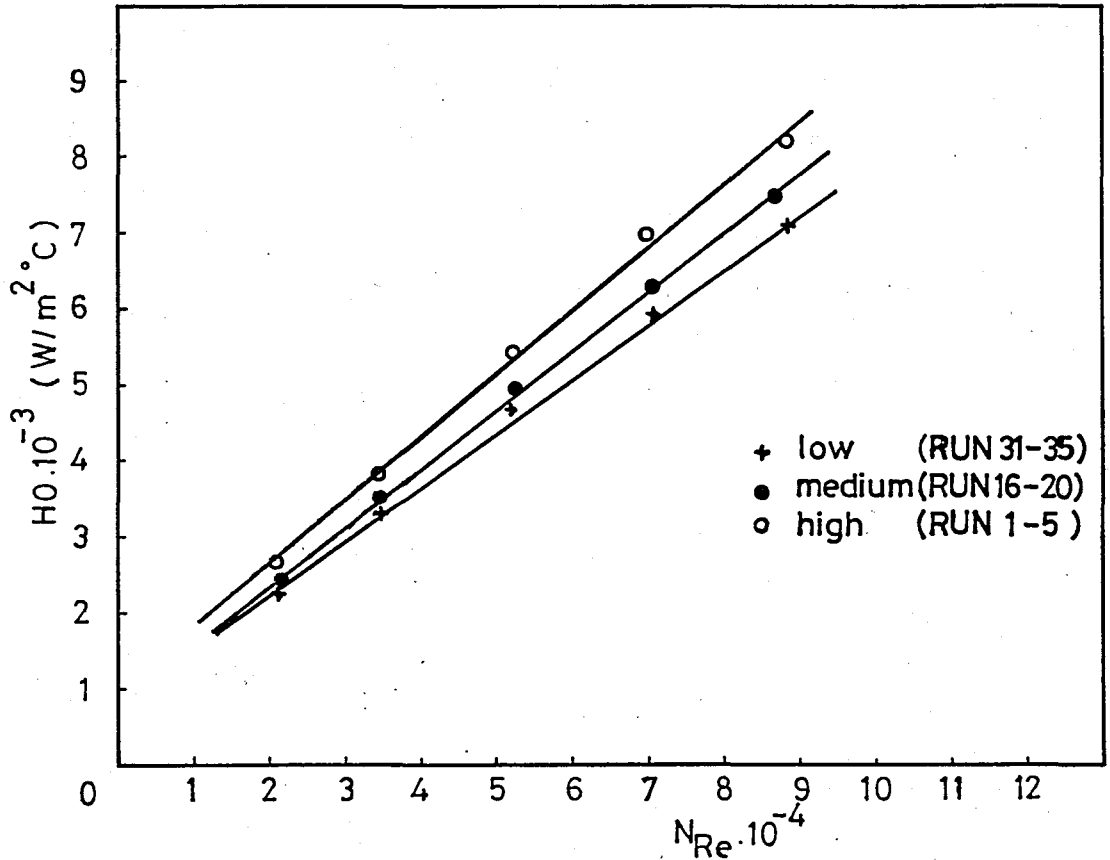


Figure (5.2) Effect of fin space and agitator speed on H_0

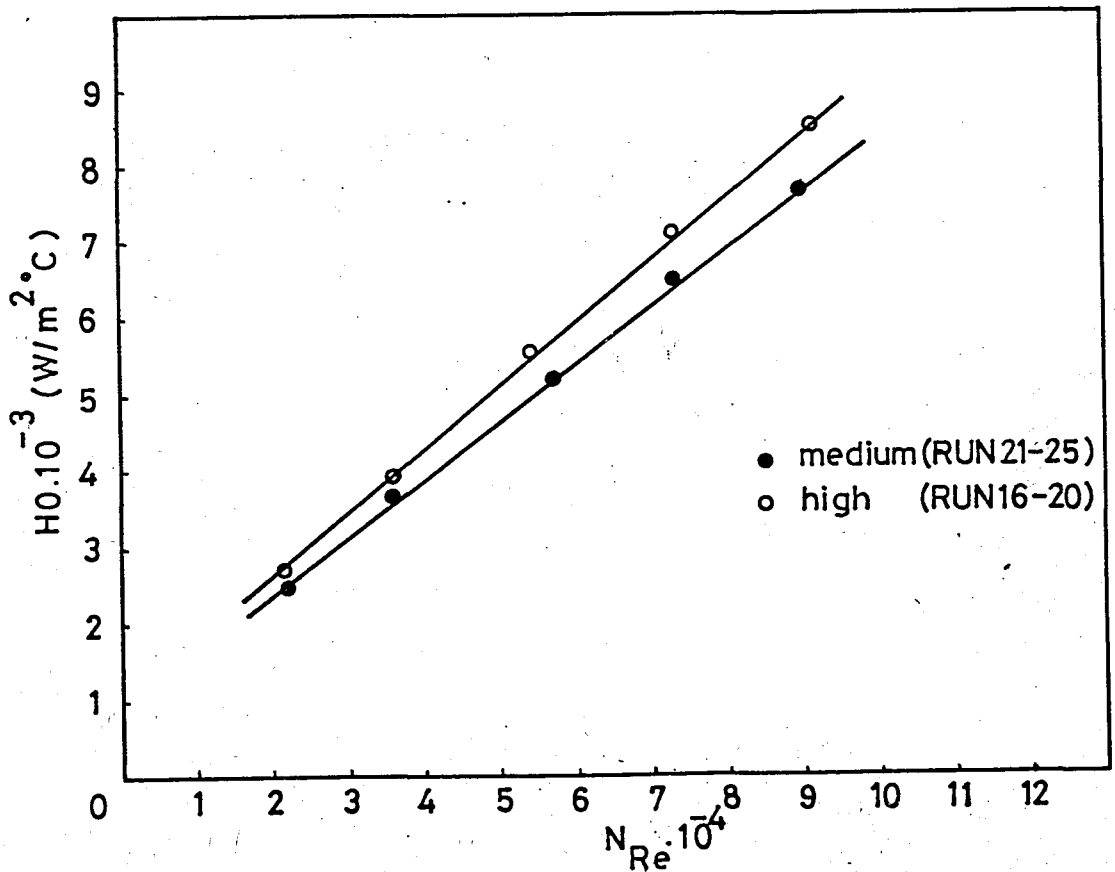


Figure (5.3) Effect of fin space and agitator speed on H_0

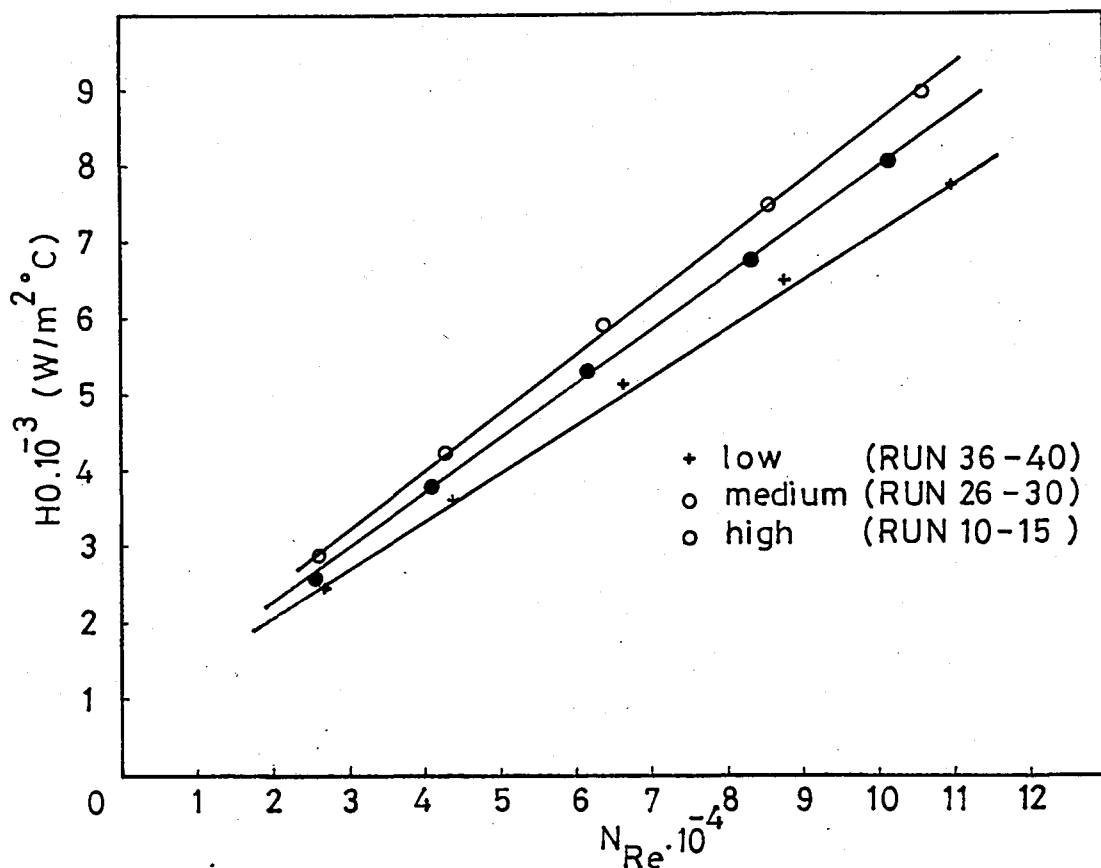


Figure (5.4) Effect of fin space and agitator speed on H_o

Final correlation

$$N_{Nu} = 0.001883 (N_{Re})^{0.817} \cdot (N_{Pr})^{0.4} \cdot \left(\frac{\mu_b}{\mu_w}\right)^{0.14} \cdot \left(\frac{H_s}{H_f}\right)^{0.207} \quad (4.8)$$

reveals that the Reynolds number exponent for finned tube coils was larger than for the bare tube coil. This same higher Reynolds number exponent value has been also reported by Appleton [10] and Gentry [29]. Also from the experiments performed with bare coils [32], in systems dimensionally similar to the present one, Reynolds number exponent has been found to be 0.62. In this investigation this value was 0.817. This higher value indicates the effect of increasing wall

turbulence.

The results appear to indicate that the feed rate of cold stream has no effect on H_o or U_o . When cold stream flow rates were decreased (Run (11-15), (26-30), (35-40)), the H_o values increased slightly by the increasing Reynolds number. So all data could be seen on the same straight line in Figure (5.5).

The Prandtl number exponent was directly taken from the literature [19,10,28]. Although this value was close to $1/3$ for smooth surfaces, for finned surface it was greater i.e about $1/2.5$ to $1/2$ [10].

In this investigation small fin thickness was chosen.

The expectation that higher agitator speeds give higher heat transfer rates was shown to be case in the range of agitator speeds used in this study.

Another conclusion obtained from unsteady state experimental results was that the convective heat transfer coefficient for unsteady-state conditions was equal to convective heat transfer coefficient calculated for steady state conditions.

5.B COMPARISON with LITERATURE

In spite of the more favorable heat transfer data of helical bare tubes immersed in tanks, results for finned helical coils are relatively scarce. Two investigations those by Appleton [10] and Gentry [23], were encountered in literature. Although Gentry's study has been carried out by using finned baffles, his data were used for comparison with the data obtained in this study. Appleton's results containing surface area terms were converted by the author into convective coefficient values and these results were used to calculate the $N_{Nu}/N_{Pr}^{0.4}$ term serving as the dependent variable. Then by using the Reynolds number as independent variable, a plot Figure (5.5) was made and the data of this study were also included in this plot. As seen from Figure (5.5), although heat transfer results by Appleton are higher by as much as 57 per cent than the results obtained in the present work and the results by Gentry are lower by 25 per cent. Difference between dimensions of systems may be the reason of this difference. In spite of this difference in heat transfer results, as is evident in Figure (5.5) the degree of agreement between also is satisfactory. This comparison also reflects the fact that fins produce larger gains in heat transfer rate with the helical coil geometry than with the baffle arrangement.

Although in Aksan's study [32], which was dimensionally similar but with bare tube coil, tank diameter has been

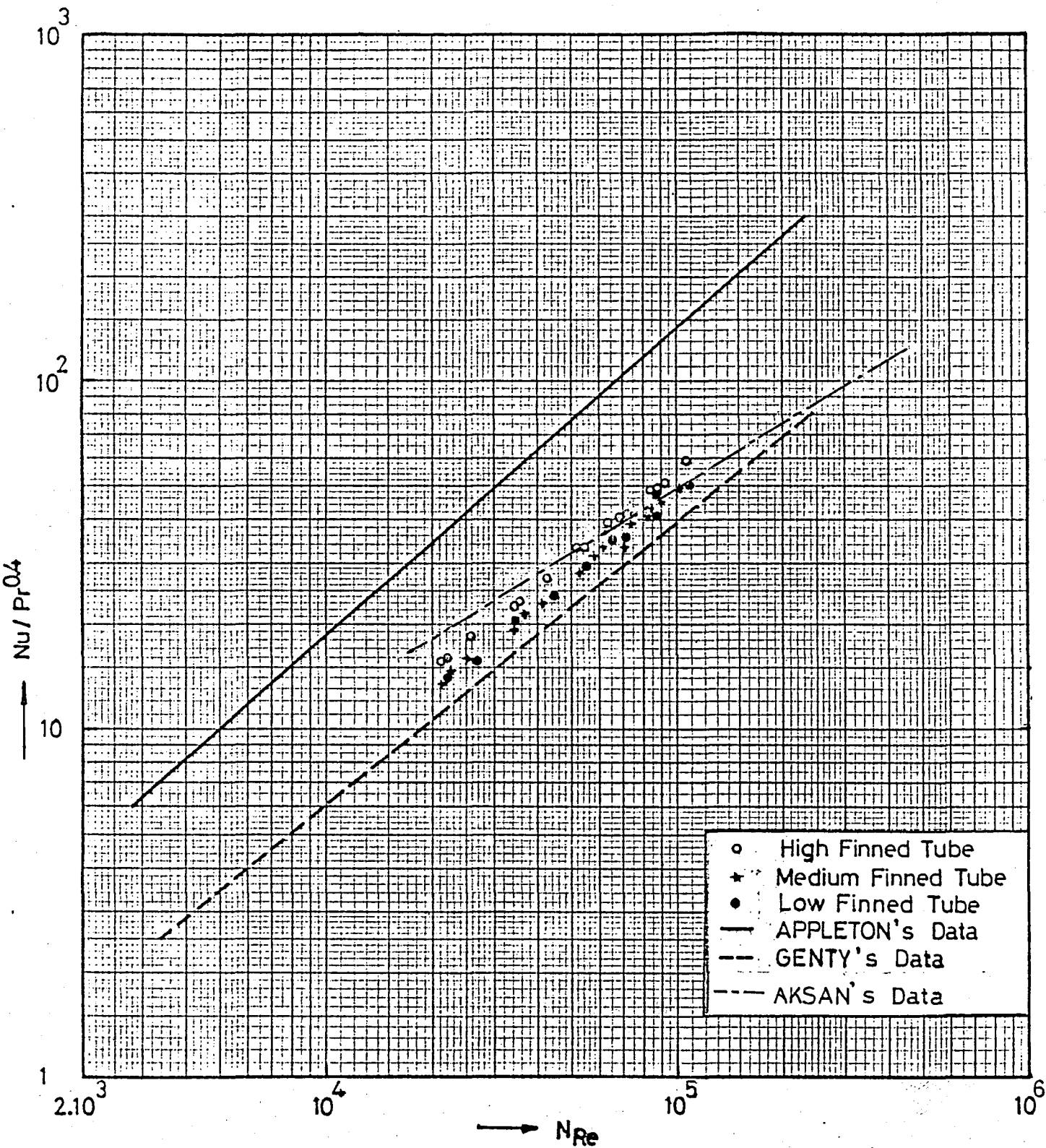


Figure (5.5) Comparison of present study with previous correlations.

utilized as characteristic length in Nusselt number definition, as in other convective heat transfer processes in this study bare tube diameter was used since heat transfer occurs from the coil surface in heating conditions.

The finned coils used in used in this study were constructed by hand, because the tube diameter of helical coils was too small to endure the tension applied to tube surface in winding the metal ribbon. So the contact point of the fin and the tube tends to minimize the influence of convection, in other words contact resistance has occurred. This matter can be solved by doing some work with a scaled up system.

Also the following work may suggested on this subject.

1. to study the effect of impeller type on the outside film coefficient
2. to carry out some experiments by using different liquids.

REFERENCES

1. Bergles, A.E., "Augmentation of Forced Convection Heat Transfer", NATO Advanced Study Institute, Istanbul, Turkey, July 20 - August 2, 1978.
2. Kern, D.Q and Kraus, A.D.. Extended Surface Heat Transfer . 1st ed., New York, Mc Graw - Hill Book Co., Inc., (1972).
3. Kern, D.Q. Process Heat Transfer . 1st ed., New York, Mc Graw - Hill Book Co., Inc, (1950).
4. Bergles, A.E., and Webb, R.L., "Augmentation of Convective Heat and Mass Transfer", New York, The American Society of Mechanical Eng., (1970).
5. Uhl, V.W., and Gray, J.B.. Mixing theory and practice. Vol.1, Chap. V, Academic Press, New York and London (1966).
6. Askew, W.S., and Beckmann, R.B., "Heat and Mass Transfer in an agitated vessel", I and EC Proc.Des.Dev.4, No.3, 311, (1965).
7. Rushton, J.H., Litcman R.S., Mahoney, L.H., Ind.Eng.Chem., 40, 1082-1087 (1948).
8. Uhl, V.W., and Voznick, H.P., Chem.Eng.Prog., March, 172, (1960)
9. Cummings, G.H., and West, A.S., "Heat Transfer Data for Kettles with Jackets and Coils", Ind.Eng.Chem., 42, 2303 (1950).
10. Appleton, W.I., and Brennan, W.C., "Some Observations on Heat Transfer to Agitated Liquids", Can.Journ.Chem.Eng., October, 276, (1966).

11. Ackley, E.J., "Film Coefficients of Heat Transfer for Agitated Process Vessels", Chem. Eng. (London), Aug. 22, p 133 (1960).
12. Stahel, E.P., and Seth, K.K., IEC, Vol. 61, No. 6, June (1969).
13. Chilton, T.H., Drew, T.B., and Jebens, R.H., "Heat Transfer Coefficient in Agitated Vessels", Ind. Chem. Eng., 36, 510 (1944).
14. Dunlop, I.R., and Rushton, J.H., "Heat Transfer Coefficients in Liquid Mixing Vertical Tube Baffles", Chem. Eng. Prog., 49, Symposium Series No. 5, 137 (1953).
15. Oldshue, J.Y., and Gretton, A.T., "Helical Coil Heat Transfer in Mixing Vessels", Chem. Eng. Prog., 50, 615 (1954).
16. Seban, R.A., and Mac Loughlin, E.F., Int. J. Heat Mass Transfer, 6, 387-95 (1963).
17. Brooks, G., and Su, G.J., "Heat Transfer in Agitated Kettles", Chem. Eng. Progr., 55, (10), 54 (1959).
18. Wilson, B., "A Basis for Rational Design of Heat Transfer Apparatus", Trans. ASME, 37, 47 (1915).
19. Mc Adams, W.H., Heat Transmition. 3rd ed., New York, Mc Graw - Hill Book Con., Inc., (1954).
20. Sieder, E.N., and Tate, G.E., "Heat Transfer and Pressure Drop of Liquids in Tubes", Ind. Eng. Chem, 28, 1429-1436 (1936).
21. Jaschke, D.Z., Ver. Deut. Ing., 69, 1526 (1925); Z. Ver. deut. Ing. Enganzungsheft, 24, 1 (1925).

22. Pratt, N.H., "The Heat Transfer in a Reaction Tank Cooled by Means of Coil", Trans. Inst.Chem.Eng. (London), 25, 163, (1947).
23. Dittus, F.W., and Boelter, L.M.K., Univ.Calif.Pubs.Eng., 2, 443 (1930).
24. Hausen, Z., Ver.,deut.,Ing., Beih., Verfahren.Tech., No.4, 9, (1943).
25. Maerteleire, E.DE., "Heat Transfer to a Helical Cooling Coil in Mechanically Agitated Gas-Liquid Dispersions.", Chem.Eng.Science, 33, 1107, (1978).
26. Skelland, A.N., and Dabrowski, J.E., J.Birmingham Univ. Chem.Eng.Soc., 14(3), 82 (1963).
27. Çakaloz, T., and Ülkü, S., "Karıştırıcılı kaplarda Isı Transferi", Türk.Bil.Teknik Ar.Kur.Bilim Kongresi, 6th, 485 (1977).
28. Gentry, C.C., and Small, W.M., "Heat Transfer and Power Expenditure for Agitated Vessels having Bare and Finned, Vertical Tube Baffles", Int., Heat, Trans., Conf., 6th, Aug. (1978).
29. Jha, R.K., and Rao, M.R., Int.J. Heat Mass Transfer, 9, 63 (1966).
30. Holman, C.P., Heat Transfer . 4th ed., (1976)
31. Borak, F., Doçentlik Tezi, Research Thesis. Boğaziçi Üniversitesi, Istanbul, September (1979).
32. Aksan, D., Master Thesis, Boğaziçi Univ., Istanbul, Aug., (1985).

References not Cited

1. Strek, F., and Masiuk, S., "Heat Transfer in Mixing Vessels with Propeller Agitator". Verfahrens Tech. 4, No.6, (1970)
2. Poggemann, R., Weinspach, P.M., "Heat Transfer in Agitated Vessels with Single-Phase Liquids.", Chem., Ing., Tech., 10, 948 (1979).
3. Ashley, C.M., "A Method of Analyzing Heat Transfer Performance", Refrigerating Eng., 6, 562, (1946).
4. Gardner, K.A., Trans. A.S.M.E., 67, 621, (1945).
5. Akse, H., Beek, W.J., Berkel, F.C.A.A., and Graauw, J., "The Local Heat Transfer at the wall of a Large Vessel Agitated by Turbine Impellers.", Chem. Eng. Science, 22, 135 (1967).

APPENDICES

APPENDIX I. EXPERIMENTAL DATA

Table (A.1.1) Efficiencies of radial fin of rectangular profile

Ω	0.40	0.41	0.42	0.43	0.44	0.45	0.46	0.47	0.48	0.49	0.50	0.51	0.52	0.53	0.54	0.55	0.56	0.57	0.58	0.59
1.02	0.6585	0.6613	0.6640	0.6667	0.6693	0.6718	0.6742	0.6766	0.6790	0.6813	0.6835	0.6857	0.6878	0.6899	0.6920	0.6940	0.6960	0.6979	0.6998	0.7016
1.04	0.6502	0.6531	0.6558	0.6585	0.6611	0.6637	0.6662	0.6686	0.6710	0.6733	0.6756	0.6778	0.6800	0.6821	0.6842	0.6862	0.6882	0.6901	0.6920	0.6939
1.06	0.6420	0.6449	0.6477	0.6504	0.6530	0.6556	0.6582	0.6606	0.6630	0.6654	0.6677	0.6699	0.6721	0.6743	0.6764	0.6784	0.6805	0.6824	0.6844	0.6863
1.08	0.6339	0.6368	0.6396	0.6424	0.6451	0.6477	0.6502	0.6527	0.6552	0.6575	0.6599	0.6621	0.6644	0.6665	0.6687	0.6708	0.6728	0.6748	0.6768	0.6787
1.10	0.6259	0.6288	0.6317	0.6344	0.6372	0.6398	0.6424	0.6449	0.6474	0.6498	0.6521	0.6544	0.6567	0.6589	0.6610	0.6632	0.6652	0.6672	0.6692	0.6712
1.12	0.6180	0.6209	0.6238	0.6266	0.6293	0.6320	0.6346	0.6372	0.6396	0.6421	0.6445	0.6468	0.6491	0.6513	0.6535	0.6556	0.6577	0.6598	0.6618	0.6637
1.14	0.6102	0.6131	0.6160	0.6189	0.6216	0.6243	0.6269	0.6295	0.6320	0.6345	0.6369	0.6392	0.6415	0.6438	0.6460	0.6481	0.6503	0.6523	0.6544	0.6564
1.16	0.6024	0.6054	0.6083	0.6112	0.6140	0.6167	0.6193	0.6219	0.6245	0.6270	0.6294	0.6318	0.6341	0.6363	0.6386	0.6408	0.6429	0.6450	0.6470	0.6491
1.18	0.5948	0.5978	0.6008	0.6036	0.6064	0.6092	0.6118	0.6145	0.6170	0.6195	0.6220	0.6244	0.6267	0.6290	0.6312	0.6334	0.6356	0.6377	0.6398	0.6418
1.20	0.5873	0.5903	0.5933	0.5962	0.5990	0.6017	0.6044	0.6071	0.6097	0.6122	0.6146	0.6170	0.6194	0.6217	0.6240	0.6262	0.6284	0.6305	0.6326	0.6347
1.22	0.5798	0.5829	0.5859	0.5888	0.5916	0.5944	0.5971	0.5998	0.6024	0.6049	0.6074	0.6098	0.6122	0.6145	0.6168	0.6191	0.6213	0.6234	0.6255	0.6276
1.24	0.5725	0.5756	0.5786	0.5815	0.5844	0.5872	0.5899	0.5926	0.5952	0.5977	0.6002	0.6027	0.6051	0.6074	0.6097	0.6120	0.6142	0.6164	0.6185	0.6206
1.26	0.5653	0.5684	0.5714	0.5743	0.5772	0.5800	0.5828	0.5855	0.5881	0.5907	0.5932	0.5956	0.5981	0.6004	0.6027	0.6050	0.6072	0.6094	0.6116	0.6137
1.28	0.5582	0.5613	0.5643	0.5673	0.5702	0.5730	0.5757	0.5784	0.5811	0.5837	0.5862	0.5887	0.5911	0.5935	0.5958	0.5981	0.6003	0.6025	0.6047	0.6068
1.30	0.5512	0.5543	0.5573	0.5603	0.5632	0.5660	0.5688	0.5715	0.5742	0.5768	0.5793	0.5818	0.5843	0.5866	0.5890	0.5913	0.5935	0.5958	0.5979	0.6001
1.32	0.5442	0.5474	0.5504	0.5534	0.5563	0.5592	0.5620	0.5647	0.5674	0.5700	0.5725	0.5750	0.5775	0.5799	0.5823	0.5846	0.5868	0.5891	0.5912	0.5934
1.34	0.5374	0.5406	0.5436	0.5466	0.5496	0.5524	0.5552	0.5580	0.5606	0.5633	0.5658	0.5683	0.5708	0.5732	0.5756	0.5779	0.5802	0.5824	0.5846	0.5868
1.36	0.5307	0.5339	0.5369	0.5400	0.5429	0.5458	0.5486	0.5513	0.5540	0.5566	0.5592	0.5618	0.5642	0.5667	0.5690	0.5714	0.5737	0.5759	0.5781	0.5803
1.38	0.5241	0.5273	0.5304	0.5334	0.5363	0.5392	0.5420	0.5448	0.5475	0.5501	0.5527	0.5552	0.5577	0.5602	0.5626	0.5649	0.5672	0.5695	0.5717	0.5739
1.40	0.5176	0.5208	0.5239	0.5269	0.5298	0.5327	0.5356	0.5383	0.5410	0.5437	0.5463	0.5488	0.5513	0.5538	0.5562	0.5585	0.5608	0.5631	0.5653	0.5675
1.42	0.5112	0.5144	0.5175	0.5205	0.5235	0.5264	0.5292	0.5320	0.5347	0.5374	0.5400	0.5425	0.5450	0.5475	0.5499	0.5522	0.5546	0.5568	0.5591	0.5613
1.44	0.5049	0.5081	0.5112	0.5142	0.5172	0.5201	0.5229	0.5257	0.5284	0.5311	0.5337	0.5363	0.5388	0.5413	0.5437	0.5460	0.5484	0.5506	0.5529	0.5551
1.46	0.4987	0.5019	0.5050	0.5081	0.5110	0.5139	0.5168	0.5196	0.5223	0.5250	0.5276	0.5301	0.5327	0.5351	0.5375	0.5399	0.5423	0.5445	0.5468	0.5490
1.48	0.4926	0.4958	0.4989	0.5020	0.5049	0.5078	0.5107	0.5135	0.5162	0.5189	0.5215	0.5241	0.5266	0.5291	0.5315	0.5339	0.5362	0.5385	0.5408	0.5430
1.50	0.4866	0.4898	0.4929	0.4960	0.4989	0.5019	0.5047	0.5075	0.5102	0.5129	0.5156	0.5181	0.5207	0.5231	0.5256	0.5280	0.5303	0.5326	0.5349	0.5371
1.52	0.4807	0.4839	0.4870	0.4901	0.4931	0.4960	0.4988	0.5016	0.5044	0.5070	0.5097	0.5123	0.5148	0.5173	0.5197	0.5221	0.5244	0.5268	0.5290	0.5312
1.54	0.4749	0.4781	0.4812	0.4843	0.4873	0.4902	0.4930	0.4958	0.4986	0.5013	0.5039	0.5065	0.5090	0.5115	0.5139	0.5163	0.5187	0.5210	0.5233	0.5255
1.56	0.4692	0.4724	0.4755	0.4786	0.4816	0.4845	0.4873	0.4901	0.4929	0.4956	0.4982	0.5008	0.5033	0.5058	0.5082	0.5106	0.5130	0.5153	0.5176	0.5198
1.58	0.4636	0.4668	0.4699	0.4730	0.4759	0.4789	0.4817	0.4845	0.4873	0.4899	0.4926	0.4952	0.4977	0.5002	0.5026	0.5050	0.5074	0.5097	0.5120	0.5142
1.60	0.4581	0.4613	0.4644	0.4674	0.4704	0.4733	0.4762	0.4790	0.4817	0.4844	0.4871	0.4897	0.4922	0.4947	0.4971	0.4995	0.5019	0.5042	0.5065	0.5087
1.62	0.4527	0.4559	0.4590	0.4620	0.4650	0.4679	0.4708	0.4736	0.4763	0.4790	0.4816	0.4842	0.4868	0.4893	0.4917	0.4941	0.4965	0.4988	0.5011	0.5033
1.64	0.4473	0.4505	0.4536	0.4567	0.4596	0.4625	0.4654	0.4682	0.4709	0.4736	0.4763	0.4789	0.4814	0.4839	0.4863	0.4888	0.4911	0.4934	0.4957	0.4980
1.66	0.4421	0.4453	0.4484	0.4514	0.4544	0.4573	0.4601	0.4629	0.4657	0.4684	0.4710	0.4736	0.4761	0.4786	0.4811	0.4835	0.4858	0.4882	0.4904	0.4927
1.68	0.4369	0.4401	0.4432	0.4462	0.4492	0.4521	0.4550	0.4578	0.4605	0.4632	0.4658	0.4684	0.4710	0.4734	0.4759	0.4783	0.4807	0.4830	0.4853	0.4875
1.70	0.4319	0.4350	0.4381	0.4412	0.4441	0.4470	0.4499	0.4527	0.4554	0.4581	0.4607	0.4633	0.4658	0.4683	0.4708	0.4732	0.4756	0.4779	0.4801	0.4824
1.72	0.4269	0.4300	0.4331	0.4362	0.4391	0.4420	0.4449	0.4477	0.4504	0.4531	0.4557	0.4583	0.4608	0.4633	0.4658	0.4682	0.4705	0.4728	0.4751	0.4774
1.74	0.4220	0.4251	0.4282	0.4312	0.4342	0.4371	0.4399	0.4427	0.4455	0.4481	0.4508	0.4533	0.4559	0.4584	0.4608	0.4632	0.4656	0.4679	0.4702	0.4724
1.76	0.4172	0.4203	0.4234	0.4264	0.4294	0.4323	0.4351	0.4379	0.4406	0.4433	0.4459	0.4485	0.4510	0.4535	0.4559	0.4583	0.4607	0.4630	0.4653	0.4675
1.78	0.4125	0.4156	0.4187	0.4217	0.4246	0.4275	0.4303	0.4331	0.4358	0.4385	0.4411	0.4437	0.4462	0.4487	0.4511	0.4535	0.4559	0.4582	0.4605	0.4627
1.80	0.4078	0.4109	0.4140	0.4170	0.4199	0.4228	0.4256	0.4284	0.4311	0.4338	0.4364	0.4390	0.4415	0.4440	0.4464	0.4488	0.4512	0.4535	0.4558	0.4580
1.82	0.4032	0.4063	0.4094	0.4124	0.4153	0.4182	0.4210	0.4238	0.4265	0.4292	0.4318	0.4343	0.4369	0.4393	0.4418	0.4442	0.4465	0.4488	0.4511	0.4533
1.84	0.3987	0.4018	0.4049	0.4079	0.4108	0.4137	0.4165	0.4192	0.4220	0.4246	0.4272	0.4298	0.4323	0.4348	0.4372	0.4396	0.4419	0.4442	0.4465	0.4487
1.86	0.3943	0.3974	0.4005	0.4034	0.4064	0.4092	0.4120	0.4148	0.4175	0.4201	0.4227	0.4253	0.4278	0.4303	0.4327	0.4351	0.4374	0.4397	0.4420	0.4442
1.88	0.3900	0.3931	0.3961	0.3991	0.4020	0.4048	0.4076	0.4104	0.4131	0.4157	0.4183	0.4209	0.4234	0.4259	0.4283	0.4307	0.4330	0.4353	0.4375	0.4398
1.90	0.3857	0.3888	0.3918	0.3948	0.3977	0.4005	0.4033	0.4061	0.4088	0.4114	0.4140	0.4165	0.4190	0.4215	0.4239	0.4263	0.4286	0.4309	0.4332	0.4354
1.92	0.3815	0.3846	0.3876	0.3906	0.3935	0.3963	0.3991	0.4018	0.4045	0.4071	0.4097	0.4123	0.4148	0.4172	0.4196	0.4220	0.4243	0.4266	0.4289	0.4311
1.94	0.3774	0.3805	0.3835	0.3864	0.3893	0.3921	0.3949	0.3976	0.4003	0.4029	0.4055	0.4081	0.4105	0.4130	0.4154	0.4178	0.4201	0.4224	0.4246	0.4268
1.96	0.3733	0.3764	0.3794	0.3823	0.3852	0.3880	0.3908	0.3935	0.3962	0.3988	0.4014	0.4039	0.4064	0.4088	0.4112	0.4136	0.4159	0.4182	0.4204	0.4227
1.98	0.3694	0.3724	0.3754	0.3783	0.3812	0.3840	0.3868	0.3895	0.3921	0.3948	0.3973	0.3998	0.4023	0.4048	0.4072	0.4095	0.4118	0.4141	0.4163	0.4185
2.00	0.3654	0.3685	0.3715	0.3744	0.3772	0.3800	0.3828	0.3855	0.3882	0.3908	0.3933	0.3958	0.3983	0.4007	0.4031	0.4055	0.4078	0.4101	0.4123	0.4145

Table (A. I. 1). Continued

2.02	0.3616	0.3646	0.3676	0.3705	0.3733	0.3761	0.3789	0.3816	0.3842	0.3868	0.3894	0.3919	0.3944	0.3968	0.3992	0.4015	0.4038	0.4061	0.4083	0.4105
2.04	0.3578	0.3608	0.3638	0.3667	0.3695	0.3723	0.3750	0.3777	0.3804	0.3830	0.3855	0.3880	0.3905	0.3929	0.3953	0.3976	0.3999	0.4022	0.4044	0.4066
2.06	0.3541	0.3571	0.3600	0.3629	0.3658	0.3685	0.3713	0.3739	0.3766	0.3792	0.3817	0.3842	0.3866	0.3891	0.3914	0.3938	0.3960	0.3983	0.4005	0.4027
2.08	0.3504	0.3534	0.3564	0.3592	0.3621	0.3648	0.3675	0.3702	0.3728	0.3754	0.3780	0.3804	0.3829	0.3853	0.3876	0.3900	0.3923	0.3945	0.3967	0.3989
2.10	0.3468	0.3498	0.3527	0.3556	0.3584	0.3612	0.3639	0.3666	0.3692	0.3717	0.3743	0.3767	0.3792	0.3816	0.3839	0.3862	0.3885	0.3908	0.3930	0.3951
2.12	0.3433	0.3463	0.3492	0.3520	0.3548	0.3576	0.3603	0.3629	0.3656	0.3681	0.3706	0.3731	0.3755	0.3779	0.3803	0.3826	0.3849	0.3871	0.3893	0.3915
2.14	0.3398	0.3428	0.3457	0.3485	0.3513	0.3541	0.3568	0.3594	0.3620	0.3645	0.3671	0.3695	0.3719	0.3743	0.3767	0.3790	0.3812	0.3835	0.3857	0.3878
2.16	0.3364	0.3393	0.3422	0.3451	0.3479	0.3506	0.3533	0.3559	0.3585	0.3610	0.3635	0.3660	0.3684	0.3708	0.3731	0.3754	0.3777	0.3799	0.3821	0.3842
2.18	0.3330	0.3360	0.3389	0.3417	0.3445	0.3472	0.3498	0.3525	0.3551	0.3576	0.3601	0.3625	0.3649	0.3673	0.3696	0.3719	0.3742	0.3764	0.3785	0.3807
2.20	0.3297	0.3327	0.3355	0.3383	0.3411	0.3438	0.3465	0.3491	0.3517	0.3542	0.3567	0.3591	0.3615	0.3639	0.3662	0.3685	0.3707	0.3729	0.3751	0.3772
2.22	0.3265	0.3294	0.3322	0.3351	0.3378	0.3405	0.3432	0.3458	0.3483	0.3508	0.3533	0.3558	0.3581	0.3605	0.3628	0.3651	0.3673	0.3695	0.3717	0.3738
2.24	0.3233	0.3262	0.3290	0.3318	0.3346	0.3373	0.3399	0.3425	0.3450	0.3476	0.3500	0.3524	0.3548	0.3572	0.3595	0.3617	0.3640	0.3662	0.3683	0.3704
2.26	0.3201	0.3230	0.3259	0.3286	0.3314	0.3341	0.3367	0.3393	0.3418	0.3443	0.3468	0.3492	0.3516	0.3539	0.3562	0.3585	0.3607	0.3629	0.3650	0.3671
2.28	0.3170	0.3199	0.3227	0.3255	0.3282	0.3309	0.3335	0.3361	0.3386	0.3411	0.3436	0.3460	0.3484	0.3507	0.3530	0.3552	0.3574	0.3596	0.3617	0.3639
2.30	0.3140	0.3169	0.3197	0.3224	0.3251	0.3278	0.3304	0.3330	0.3355	0.3380	0.3404	0.3428	0.3452	0.3475	0.3498	0.3520	0.3542	0.3564	0.3586	0.3607
2.32	0.3110	0.3139	0.3167	0.3194	0.3221	0.3248	0.3274	0.3299	0.3324	0.3349	0.3373	0.3397	0.3421	0.3444	0.3467	0.3489	0.3511	0.3533	0.3554	0.3575
2.34	0.3081	0.3109	0.3137	0.3164	0.3191	0.3218	0.3243	0.3269	0.3294	0.3319	0.3343	0.3367	0.3390	0.3413	0.3436	0.3458	0.3480	0.3502	0.3523	0.3544
2.36	0.3052	0.3080	0.3108	0.3135	0.3162	0.3188	0.3214	0.3239	0.3264	0.3289	0.3313	0.3337	0.3360	0.3383	0.3405	0.3428	0.3449	0.3471	0.3492	0.3513
2.38	0.3023	0.3051	0.3079	0.3106	0.3133	0.3159	0.3185	0.3210	0.3235	0.3259	0.3283	0.3307	0.3330	0.3353	0.3375	0.3398	0.3419	0.3441	0.3462	0.3483
2.40	0.2995	0.3023	0.3051	0.3078	0.3104	0.3130	0.3156	0.3181	0.3206	0.3230	0.3254	0.3278	0.3301	0.3324	0.3346	0.3368	0.3390	0.3411	0.3432	0.3453
2.42	0.2967	0.2995	0.3023	0.3050	0.3076	0.3102	0.3128	0.3153	0.3177	0.3202	0.3226	0.3249	0.3272	0.3295	0.3317	0.3339	0.3361	0.3382	0.3403	0.3424
2.44	0.2940	0.2968	0.2995	0.3022	0.3049	0.3074	0.3100	0.3125	0.3149	0.3174	0.3197	0.3221	0.3244	0.3266	0.3288	0.3310	0.3332	0.3353	0.3374	0.3395
2.46	0.2914	0.2941	0.2968	0.2995	0.3021	0.3047	0.3072	0.3097	0.3122	0.3146	0.3169	0.3193	0.3216	0.3238	0.3260	0.3282	0.3304	0.3325	0.3346	0.3366
2.48	0.2887	0.2915	0.2942	0.2968	0.2995	0.3020	0.3045	0.3070	0.3095	0.3119	0.3142	0.3165	0.3188	0.3211	0.3233	0.3254	0.3276	0.3297	0.3318	0.3338
2.50	0.2861	0.2889	0.2916	0.2942	0.2968	0.2994	0.3019	0.3044	0.3068	0.3092	0.3115	0.3138	0.3161	0.3183	0.3205	0.3227	0.3248	0.3269	0.3290	0.3310
2.52	0.2836	0.2863	0.2890	0.2916	0.2942	0.2968	0.2993	0.3017	0.3041	0.3065	0.3089	0.3112	0.3134	0.3157	0.3178	0.3200	0.3221	0.3242	0.3263	0.3283
2.54	0.2811	0.2838	0.2865	0.2891	0.2917	0.2942	0.2967	0.2991	0.3016	0.3039	0.3062	0.3085	0.3108	0.3130	0.3152	0.3173	0.3195	0.3215	0.3236	0.3256
2.56	0.2786	0.2813	0.2840	0.2866	0.2892	0.2917	0.2942	0.2966	0.2990	0.3014	0.3037	0.3060	0.3082	0.3104	0.3126	0.3147	0.3168	0.3189	0.3210	0.3230
2.58	0.2762	0.2789	0.2815	0.2841	0.2867	0.2892	0.2917	0.2941	0.2965	0.2988	0.3011	0.3034	0.3056	0.3078	0.3100	0.3121	0.3142	0.3163	0.3184	0.3204
2.60	0.2738	0.2765	0.2791	0.2817	0.2842	0.2867	0.2892	0.2916	0.2940	0.2963	0.2986	0.3009	0.3031	0.3053	0.3075	0.3096	0.3117	0.3138	0.3158	0.3178
2.62	0.2714	0.2741	0.2767	0.2793	0.2818	0.2843	0.2868	0.2892	0.2915	0.2939	0.2962	0.2984	0.3006	0.3028	0.3050	0.3071	0.3092	0.3112	0.3133	0.3152
2.64	0.2691	0.2718	0.2744	0.2769	0.2795	0.2819	0.2844	0.2868	0.2891	0.2915	0.2937	0.2960	0.2982	0.3004	0.3025	0.3046	0.3067	0.3087	0.3108	0.3127
2.66	0.2668	0.2695	0.2721	0.2746	0.2771	0.2796	0.2820	0.2844	0.2868	0.2891	0.2914	0.2936	0.2958	0.2980	0.3001	0.3022	0.3043	0.3063	0.3083	0.3103
2.68	0.2645	0.2672	0.2698	0.2723	0.2748	0.2773	0.2797	0.2821	0.2844	0.2867	0.2890	0.2912	0.2934	0.2956	0.2977	0.2998	0.3019	0.3039	0.3059	0.3079
2.70	0.2623	0.2650	0.2675	0.2701	0.2726	0.2750	0.2774	0.2798	0.2821	0.2844	0.2867	0.2889	0.2911	0.2932	0.2953	0.2974	0.2995	0.3015	0.3035	0.3055
2.72	0.2601	0.2628	0.2653	0.2679	0.2703	0.2728	0.2752	0.2775	0.2799	0.2821	0.2844	0.2866	0.2888	0.2909	0.2930	0.2951	0.2971	0.2992	0.3011	0.3031
2.74	0.2580	0.2606	0.2632	0.2657	0.2681	0.2706	0.2730	0.2753	0.2776	0.2799	0.2821	0.2843	0.2865	0.2886	0.2907	0.2928	0.2948	0.2968	0.2988	0.3008
2.76	0.2559	0.2585	0.2610	0.2635	0.2660	0.2684	0.2708	0.2731	0.2754	0.2777	0.2799	0.2821	0.2843	0.2864	0.2885	0.2905	0.2926	0.2946	0.2965	0.2985
2.78	0.2538	0.2564	0.2589	0.2614	0.2638	0.2662	0.2686	0.2709	0.2732	0.2755	0.2777	0.2799	0.2820	0.2842	0.2862	0.2883	0.2903	0.2923	0.2943	0.2962
2.80	0.2517	0.2543	0.2568	0.2593	0.2617	0.2641	0.2665	0.2688	0.2711	0.2733	0.2756	0.2777	0.2799	0.2820	0.2840	0.2861	0.2881	0.2901	0.2920	0.2940
2.82	0.2497	0.2523	0.2548	0.2572	0.2597	0.2621	0.2644	0.2667	0.2690	0.2712	0.2734	0.2756	0.2777	0.2798	0.2819	0.2839	0.2859	0.2879	0.2898	0.2918
2.84	0.2477	0.2502	0.2527	0.2552	0.2576	0.2600	0.2623	0.2646	0.2669	0.2691	0.2713	0.2735	0.2756	0.2777	0.2797	0.2818	0.2838	0.2857	0.2877	0.2896
2.86	0.2457	0.2483	0.2508	0.2532	0.2556	0.2580	0.2603	0.2626	0.2648	0.2671	0.2692	0.2714	0.2735	0.2756	0.2776	0.2797	0.2817	0.2836	0.2855	0.2874
2.88	0.2438	0.2463	0.2488	0.2512	0.2536	0.2560	0.2583	0.2606	0.2628	0.2650	0.2672	0.2693	0.2715	0.2735	0.2756	0.2776	0.2796	0.2815	0.2834	0.2853
2.90	0.2419	0.2444	0.2469	0.2493	0.2517	0.2540	0.2563	0.2585	0.2608	0.2630	0.2652	0.2673	0.2694	0.2715	0.2735	0.2755	0.2775	0.2794	0.2814	0.2833
2.92	0.2400	0.2425	0.2449	0.2474	0.2497	0.2521	0.2544	0.2566	0.2589	0.2611	0.2632	0.2653	0.2674	0.2695	0.2715	0.2735	0.2755	0.2774	0.2793	0.2812
2.94	0.2381	0.2406	0.2431	0.2455	0.2478	0.2502	0.2525	0.2547	0.2569	0.2591	0.2612	0.2634	0.2654	0.2675	0.2695	0.2715	0.2735	0.2754	0.2773	0.2792
2.96	0.2363	0.2388	0.2412	0.2436	0.2460	0.2483	0.2506	0.2528	0.2550	0.2572	0.2593	0.2614	0.2635	0.2655	0.2675	0.2695	0.2715	0.2734	0.2753	0.2772
2.98	0.2345	0.2369	0.2394	0.2418	0.2441	0.2464	0.2487	0.2509	0.2531	0.2553	0.2574	0.2595	0.2616	0.2636	0.2656	0.2676	0.2695	0.2714	0.2733	0.2752
3.00	0.2327	0.2352	0.2376	0.2399	0.2423	0.2446	0.2468	0.2491	0.2513	0.2534	0.2555	0.2576	0.2597	0.2617	0.2637	0.2657	0.2676	0.2695	0.2714	0.2733

Table (A.I.2) Experimental Data of Set I (Agitator Speed as Variable)

Run	Fin Space (cm)	Agitator (rpm)	Cold Stream			Hot Stream			ΔT_{lm} °C	Q_h Cal/hr
			ml/sec	in °C	out °C	ml/sec	in °C	out °C		
1	1.1	125	20	22.3	43	20	69.8	48.8	13.72	1739.70
2	1.1	200	19.5	22.2	44.2	20	69.6	48.3	11.68	1763.40
3	1.1	300	20	22.2	44.8	20.25	70.2	47.7	10.37	1885.60
4	1.1	400	20	22.1	44.6	20	69.7	47	9.67	1879.04
5	1.1	500	19.5	22.4	45.3	20.25	69.7	47.4	9.09	1868.50
6	1.1	125	20	18.5	45.6	20	78.3	50.7	14.85	2307.47
7	1.1	200	20	17.7	46.2	20	79.3	50.7	14.33	2365.96
8	1.1	300	20	17.8	46.3	20	78.8	50.1	13.37	2374.20
9	1.1	400	20	18.2	47.3	20	79.1	49.8	11.52	2422.80
10	1.1	500	20	18.6	47.5	20.5	78.3	49.8	10.98	2415.60
11	1.1	125	11	19.1	54.9	19.5	79.3	58.9	11.28	1990.13
12	1.1	200	10	19.2	56.6	19.5	78.9	59.5	9.51	1791.32
13	1.1	300	10.5	19.3	55.8	19.5	78.1	58.2	8.93	1604.04
14	1.1	400	10.75	19.2	55.4	19	77.9	56.9	7.75	1656.70
15	1.1	500	10.75	19.3	56.6	19.5	78.5	57.9	7.29	1654.76
16	0.7	125	19.5	22.7	43.7	20.4	69.2	49.1	12.95	1697.68
17	0.7	200	19.5	22.3	44.2	20.5	68.7	48	11.11	1756.58
18	0.7	300	19.5	22.1	44.5	20.5	68.7	47.4	10.04	1807.20
19	0.7	400	19.5	22.3	44.8	20	69.5	47.3	9.69	1837.50

Table (A.I.2) Continued

Run	Fin Space (cm)	Agitator (rpm)	Cold Stream			Hot Stream			ΔT_{lm} °C	Q_h Cal/hr
			ml/sec	in °C	out °C	ml/sec	in °C	out °C		
20	0.7	500	19.5	22.1	44.6	20.5	68.3	46.7	8.91	1832.69
21	0.7	125	20.5	17.7	46	19.5	82	52.1	16.80	2411.66
22	0.7	200	20	18.8	46.4	19.5	80.2	50.7	14.31	2379.41
23	0.7	300	19.5	21.3	49.9	20	80.5	52.9	11.88	2279.76
24	0.7	400	20.5	17.9	47.1	20.5	80.2	50.3	12.80	2534.20
25	0.7	500	20.5	18.6	47.2	20	78.6	49.4	10.98	2414.60
26	0.7	125	10.5	17.7	53.4	18	78	57	10.93	1559.11
27	0.7	200	10.5	18.9	53	18	77.3	56.5	10.73	1544.50
28	0.7	300	11	18.7	53.8	18.5	76.7	55.6	8.30	1609.87
29	0.7	400	10.5	18.6	54.7	18	77	56.5	8.15	1521.08
30	0.7	500	10.5	17.7	54.1	17.5	76.9	55.4	7.51	1551.46
31	0.5	125	20	22.4	43.5	20	69.7	48.3	12.61	1772.80
32	0.5	200	19.7	22.3	44.1	20	68.9	47.5	10.76	1772.04
33	0.5	300	20	22.5	44.8	19.5	70.1	47.4	9.98	1832.30
34	0.5	400	20	22.4	44.8	20	69.5	47.1	9.44	1854.21
35	0.5	500	20	22.5	45.6	20	70.5	45.6	8.94	1903.40
36	0.5	125	20	23	56	10.5	77	59.4	9.67	1455.03
37	0.5	200	19.5	23.1	58.2	10	78.5	60.4	8.15	1452.82
38	0.5	300	20	23.3	58.4	10	77.9	60	7.16	1473.61
39	0.5	400	20.25	23.1	57.8	11.5	79.1	59.4	7.61	1642.53
40	0.5	500	20	23	58.4	10.5	78.2	59.7	6.79	1523.00

Table (A.I.3) Experimental Data of Set II (hot stream conditions as variable) N= 200 rpm.

Run	Cold Stream			Hot Stream			ΔT_{lm} °C	Q_h Cal/hr
	ml/sec	in °C	out °C	ml/sec	in °C	out °C		
FIN SPACE = 1.1 cm								
41	19.5	19.1	34.4	10.5	65.2	36.9	11.27	1234.90
42	20	19.5	36.4	15	63	40.1	11.61	1426.10
43	20	19.3	40.6	18	67.1	44.4	11.69	1693.70
44	21	16.9	38	20	64.9	42.9	12.92	1825.9
45	19.8	17	39.4	25	62.2	44.2	11.55	1865.96
46	20	17.4	41.9	28	65.6	47.6	12.63	2089.09
47	21	19.2	39.5	14.5	75.3	43.3	14.27	1924.2
48	20	18.5	40.9	15	74	44.5	13.29	1833.90
49	20	17	41.1	19	71.5	46	13.97	2007.90
50	20	18.5	45.8	23	74.6	50.9	13.69	2255.20
51	21	18.9	45.9	23.5	74.9	50.9	13.65	2333.42
52	20	16.6	45.8	25	75.3	51.8	14.76	2430.65
53	21	19.6	40.6	11	80	43.4	13.84	1668.50
54	20	19.2	43.4	14	82.8	47.6	15.72	2041.20
55	21	19.7	46.7	19	82.2	51.9	15.77	2381.30
56	21	19.5	47	20	80.7	52	15.04	2373.2
57	20	18.6	51.7	24	84.7	57.4	15.55	2702.9
58	10.75	19.7	42.9	10.5	68.8	44.9	9.33	1040.2
59	11	19.4	44.7	14.5	66.4	47.2	8.88	1152.6
60	10.75	19.4	47.4	16.5	67.9	49.9	8.55	1228
61	11	18.9	45.2	18	64	47.6	7.97	1221.7
62	11	19	47.4	21.5	64.9	50.3	8.12	1298.03
63	10.75	19.8	50.3	25	66.4	53.5	7.98	1331.82
64	11	21.3	45.4	10	74.2	47.3	9.90	1113.72
65	10	19.7	51.1	13.5	78	53.9	10.65	1343.50
66	11.5	19.5	50	15.5	75.8	52.8	10.36	1472.58
67	10.5	20	53.6	18	76.1	56.5	9.57	1454.99
68	10	19.2	56.6	19.5	78.9	59.8	9.84	1534.25
69	10	21	57.9	26.5	75.3	60.9	8.19	1570.75

Table (A.I.3) Continued

Run	Cold Stream			Hot Stream			ΔT_{lm} °C	Q_h Cal/hr
	ml/sec	in °C	out °C	ml/sec	in °C	out °C		
FIN SPACE = 0.7 cm								
70	20	19.2	33.1	9	66.6	35.5	11.80	1163.20
71	19.5	19.1	36.7	13.5	65.9	39.5	11.57	1479.70
72	20	16.4	36.3	16	65.1	40.4	12.67	1640.80
73	20	16.8	38.2	20	64.3	42.7	12.28	1793.6
74	20	17.5	41.4	23	65.9	45.8	11.70	1915.6
75	20	17.3	41.9	28.5	64.2	47	11.66	2031.89
76	22	17	32.6	9	73.5	35.1	13.74	1439.16
77	20.5	18.5	39.9	13	76.5	42.9	13.43	1811.40
78	22	17	39.9	16	76.5	44.5	15.43	2122.3
79	20	18.7	44.8	18.5	76.5	48.8	13.38	2121.5
80	21	20.7	46.5	22	75.9	50.9	13.16	2274.97
81	20.5	18.8	48.1	25	76.6	52.9	13.3	2450
82	10	18.6	44	13	65.5	45.9	8.08	1054.90
83	10	19.1	46.4	14.5	67.5	48.4	8.11	1145.60
84	11	18.9	46.7	18.5	66	49	7.99	1300.90
85	11	18.7	48.1	20.5	67.1	50.9	8.46	1373.10
86	11	18.3	50.1	25.5	67.1	53.2	8.17	1463.76
87	10.5	18.2	49.2	13.5	76.1	51.5	9.68	1371.5
88	10.5	18.4	50.1	15	75	52.7	9.87	1381.38
89	10.5	17.9	53.4	18	77	56.1	9.64	1551.5
90	10.5	18.3	53.5	18.5	76.4	56.3	9.57	1533.6
91	10.5	17.8	56.5	23.5	76.6	59.5	8.72	1655.4
FIN SPACE = 0.5 cm								
92	20	22.5	36.7	10	67.5	38.9	10.84	1187.39
93	20.5	22.6	41	16	68	44.4	11.39	1564.91
94	20	22.4	41.9	18.5	66.8	45.5	11.01	1633.34
95	19.5	22.5	44.7	24	67.1	48.8	10.78	1817.63
96	20	22.7	45.3	28	66.2	50	10.86	1878.00

Table (A.I.4) Experimental results of Set II from Wilson Plot

Run	U_o	H_i^*	H_i	% Error	H_o
41	1863.04	2848	2853.5	+ 0.19	3778
42	2088.3	3825.94	3793.12	- 0.86	3778
43	2463.2	4586.98	4401.12	- 4.05	3778
44	2402.64	4906.6	4760.40	- 2.98	3778
45	2746.6	5869.8	5706.95	- 2.77	3778
46	2812.09	6619.73	6338.45	- 4.25	3778
47	2292.00	3966.5	4670.40	+ 17.7	3581.8
48	2344.75	4061.88	4798.7	+ 18.14	3581.8
49	2443.50	4000.63	5822.40	+ 18.81	3581.8
50	2800.60	5918.4	6770.20	+ 14.39	3581.8
51	2906.30	6026.31	6876.85	+ 14.13	3581.8
52	2799.70	6359.45	7217.85	+ 13.50	3581.8
53	1668.5	3194.68	3036.7	- 4.95	4547.7
54	2041.20	4012.58	3685.2	- 8.16	4547.7
55	2381.3	5219.87	4701.33	- 9.93	4547.7
56	2373.2	5414.17	4913.5	- 9.25	4547.7
57	2702.9	6494.44	5660.4	- 12.84	4547.7
58	1895.4	3028.57	2225.66	- 26.51	4664.5
59	2206.7	3937.37	2880.27	- 26.85	4664.5
60	2441.79	4450.74	3206.01	- 27.97	4664.5
61	2606	4662.61	3430.6	- 26.42	4664.5
62	2717.71	5462.89	3960.37	- 27.50	4664.5
63	2835.96	6293.2	5386.10	- 14.41	4664.5
64	1913.5	3004.31	2470.8	- 17.76	5573
65	2144.3	3999.15	3119.7	- 21.99	5573
66	2417.24	4407.13	3489.8	- 20.81	5573
67	2584.8	5062.41	3934.4	- 22.28	5573
68	2651.33	5523.87	4202.	- 23.93	5573
69	3529.81	7047.98	5371.3	- 29.79	5573
70	1697.8	2508.82	2306.2	- 8.08	3987.8

* H_i calculated from Sieder-Tate correlation

Table (A.I.4). Continued

71	2202.4	3552.71	3179.74	- 10.50	3987.8
72	2230.1	4053.36	3639.2	- 10.22	3987.8
73	2515.2	4901.67	4372.14	- 10.80	3987.8
74	2819.9	5599.52	4880.5	- 12.84	3987.8
75	3000.89	6659.74	5776	- 13.27	3987.8
76	1803.73	2560.56	2566	+ 0.21	4136.5
77	2322.66	3624.4	3446.	- 4.91	4136.5
78	2368.6	4304.59	4064.08	- 5.59	4136.5
79	2649.2	4950.04	4565.5	- 7.77	4136.5
80	2976.9	5750.45	4882.5	- 15.09	4136.5
81	3078	6432.18	5810.6	- 9.66	4136.5
82	2248.4	3577.09	3421.7	- 4.34	4272.2
83	2433.3	3987.13	3732.8	- 6.38	4272.2
84	2804	4839.09	4532.7	- 6.33	4272.2
85	2794.99	5321.63	4915.7	- 7.63	4272.2
86	3085.3	6408.87	5865.8	- 8.45	4272.2
87	2441.1	3928.35	3146.6	- 19.90	5418.5
88	2410.15	4280.58	3423.2	- 20.03	5418.5
89	2771.6	5070.2	3968.3	- 21.73	5418.5
90	2761.0	5177.48	4045.65	- 21.86	5418.5
91	3269.15	6365.82	4905.7	- 22.94	5418.5
92	1899.39	2797.88	2759.6	- 1.37	3210
93	2382.4	4202.01	3987.8	- 5.10	3210
94	2572.4	4732.54	4479.8	- 15.34	3210
95	2923.73	5940.26	5519.12	- 7.04	3210
96	2998.58	6733.35	6329.3	- 6.00	3210

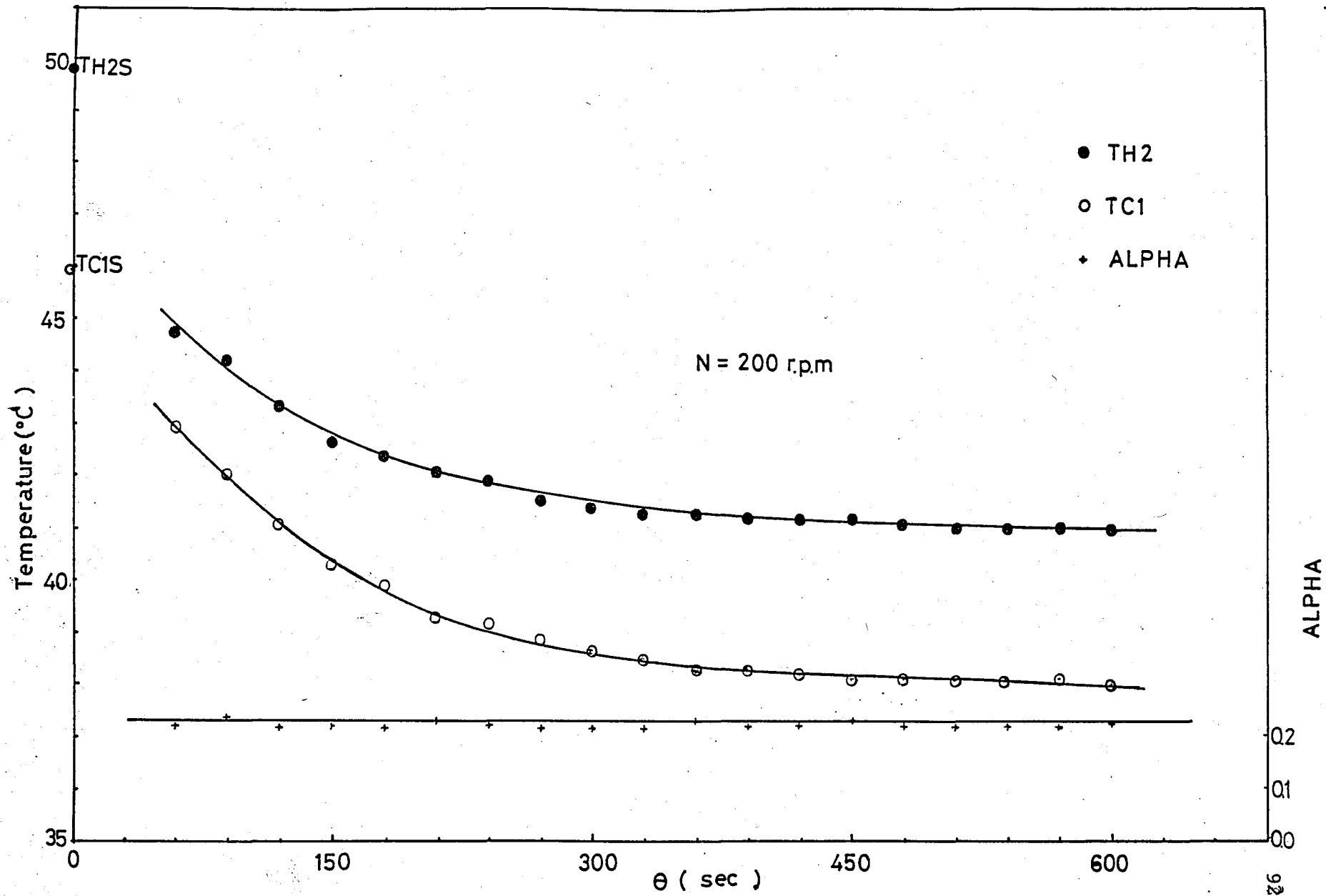


Figure A.I.1 Temperature time data (for high finned coil)

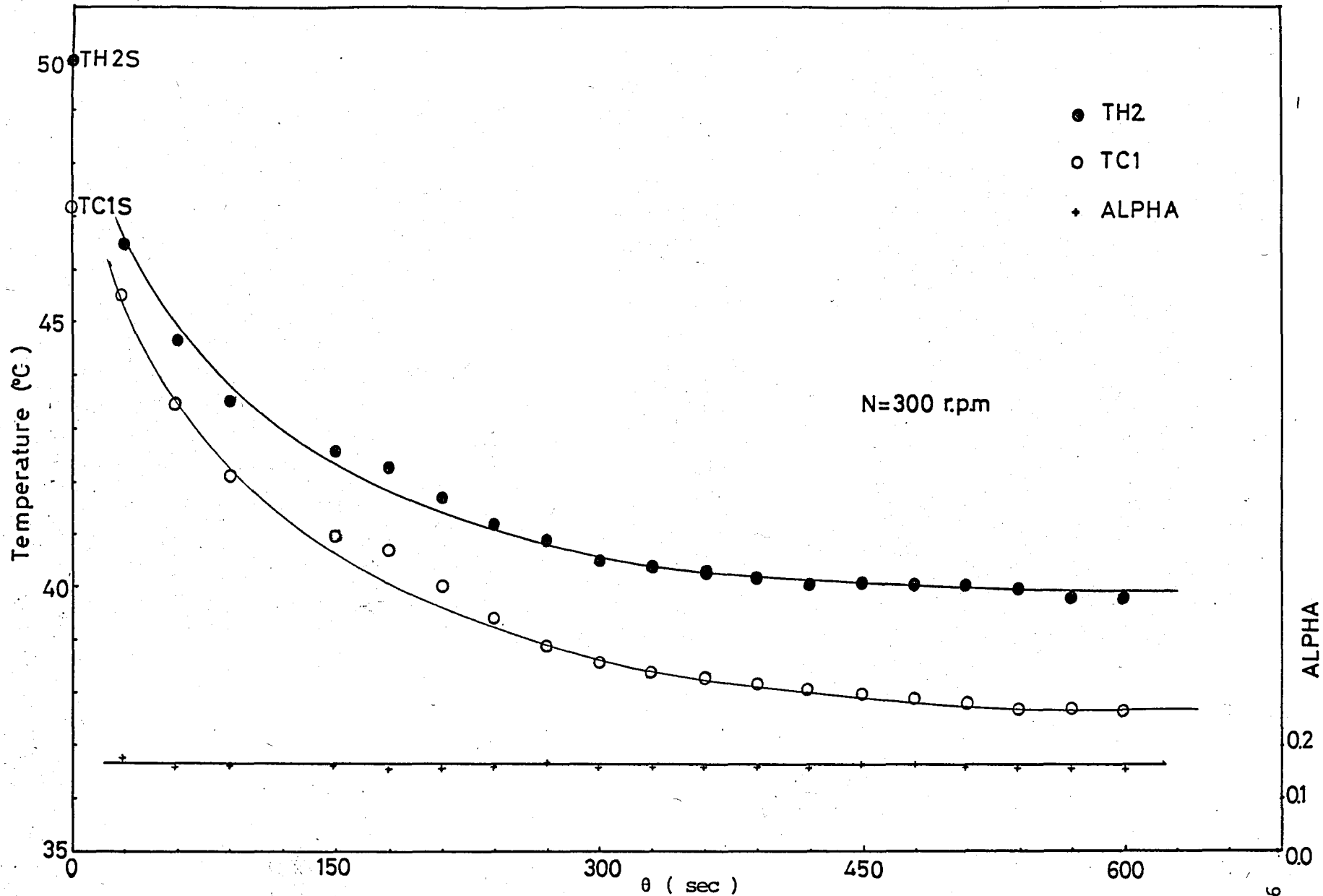


Figure A.I.2 Temperature time data (for high finned coil)

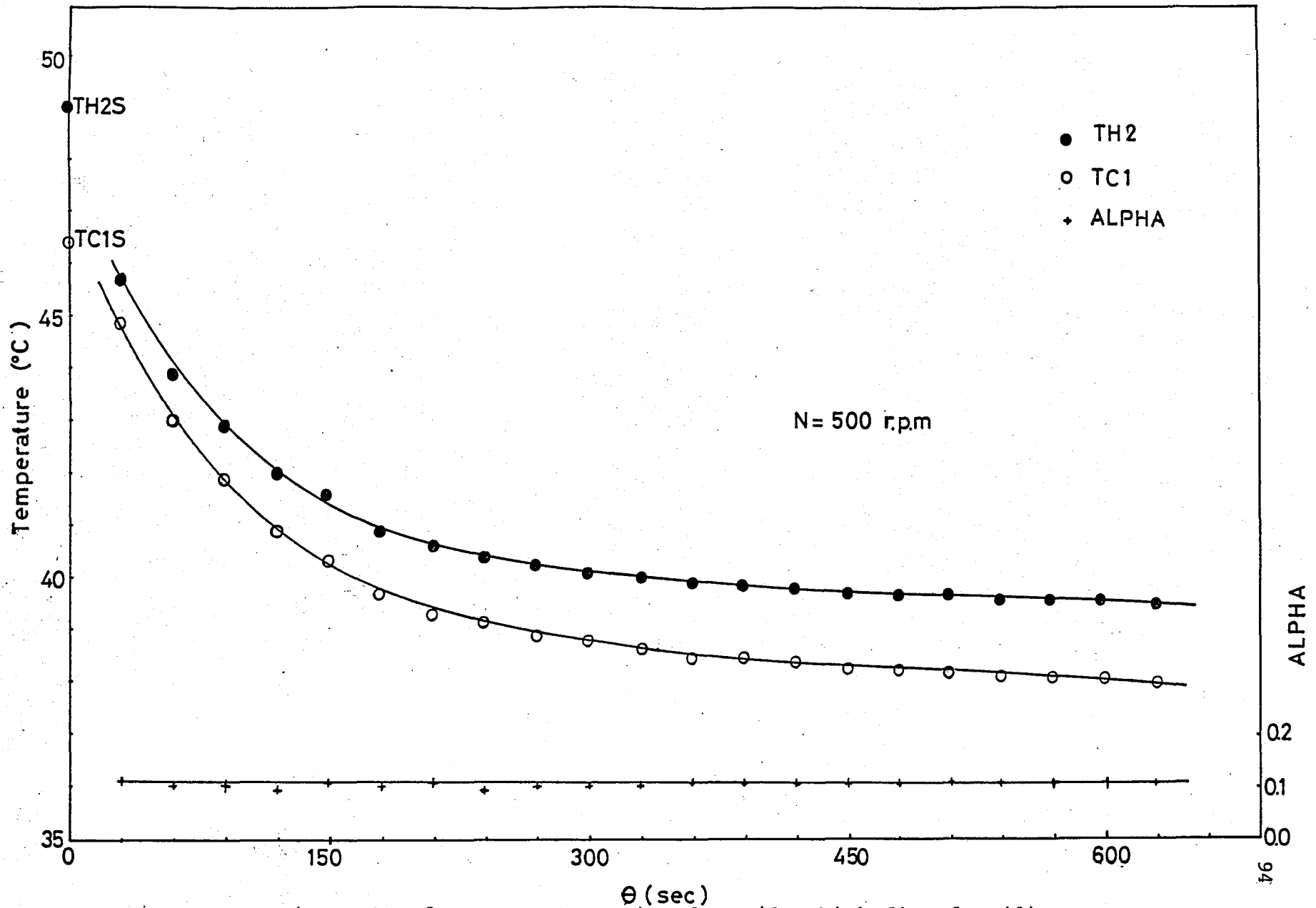


Figure A.I.3 Temperature time data (for high finned coil)

APPENDIX II

PHYSICAL PROPERTIES OF WATER

This section describes the physical properties of water as a function of temperatures [32].

A.4.A Thermal conductivity of water

$$k = 0.570671 + 0.178690 \cdot 10^{-2} T - 0.684359 \cdot 10^{-5} T^2$$

A.4.B Viscosity of water

$$\mu = 0.148237 \cdot 10^{-2} - 0.295743 \cdot 10^{-4} T + 0.258156 \cdot 10^{-6} T^2 - 0.822939 \cdot 10^{-9} T^3$$

A.4.C Specific heat of water

$$C_p = 0.419318 \cdot 10^4 - 0.744678 T + 0.100875 \cdot 10^{-1} T^2$$

A.4.D Density of water

$$\rho = 1 / (0.997426 \cdot 10^{-3} + 0.135802 \cdot 10^{-6} T + 0.32518 \cdot 10^{-8} T^2)$$